R. & M. No. 2112
(8597)
A.R.C. Technical Report

MINISTRY OF SUPPLY

AERONAUTICAL RESEARCH COUNCIL
REPORTS AND MEMORANDA

A New Method of Two-dimensional Aerodynamic Design

By

M. J. LIGHTHILL, B.A.,
of the Aerodynamics Division, N.P.L.

LONDON: HIS MAJESTY'S STATIONERY OFFICE
Price 10*s.* 0*d.* net

A New Method of Two-dimensional Aerodynamic Design

By

M. J. Lighthill, B.A.,
of the Aerodynamics Division, N.P.L.

Reports and Memoranda No. 2112
April, 1945

Summary.—The main object of this report is to describe and illustrate a fairly simple exact method by which aerofoils and other surfaces may be constructed to have desired velocity distributions. Its subsidiary interest is as a progress report on shapes already constructed, which are described in the Appendices and Figures, but should not be regarded as the best which, after further development, the method may be capable of producing.

CONTENTS

	Page
1. Introduction	2
2. Symmetrical Aerofoils	3
3. Cambered Aerofoils	7
4. Evaluation of the Moment Coefficient	9
5. Symmetrical Channels	10
6. Cascades	12
References	13
Introduction to Appendices	14
Appendix I.—Joukowsky Aerofoil modified to give " Low-drag " Section	15
,, II.—Joukowsky Aerofoil modified to give Very Thick Suction Aerofoil	18
,, III.—Calculations for " Direct Design at Incidence "	20
,, IV.—" Direct Design at Incidence " used to produce Fairly Thick Suction Aerofoil	23
,, V.—" Direct Design at Incidence " used to produce Thicker Suction Aerofoil	25
,, VI.—Low-drag Wing with Upper Surface Velocity (at Incidence) Quite Flat up to Half Chord	25
,, VII.—Thicker Version of the Aerofoil of Appendix VI	26
,, VIII.—Thin Aerofoil with High Maximum Lift, obtained by Forward Suction	27
,, IX.—The Obtaining of a Leading-edge Radius of Curvature	30
,, X.—As in Appendix VI, but with Leading-edge Radius of Curvature	32
,, XI.—Cambered Suction Aerofoil with Incidence Range 0 to 20 deg.	34
,, XII.—Calculations for Cambered Aerofoils	36
,, XIII.—Cambered Suction Aerofoil with Slots Approximately Opposite	38
,, XIV.—Contraction Cone with Wall Velocity Always Increasing	40
,, XV.—Finite Contraction Cone	42
,, XVI.—Short Contraction Cone with Small Adverse Velocity Gradient	43
Summary of Appendices	44

1. *Introduction.*—It is well known that many requirements for the flow of air past a surface, *e.g.* deferment of transition or separation of the boundary layer, may be met by imposing certain conditions on the velocity distribution along the surface, as calculated from the classical potential theory. Control of velocity distribution is therefore essential in aerodynamic design.

Goldstein's theory of thin aerofoils[1] achieves this, but is approximate at best. The exact theory of Theodorsen on which it is based is prohibitively long even for the calculation of velocity distribution from profile shape, and does not afford a method of design. The theory of this paper is the outcome of a search for an exact method not too long in application.

Consider first an aerofoil in a uniform infinite two-dimensional stream of " perfect " fluid. By Riemann's theorem the space outside the aerofoil can be conformally represented on the outside of a circle by a unique analytic function $z(\zeta)$, where z and ζ are complex variables in the planes of the aerofoil and the circle respectively, so that the trailing edge corresponds to $\zeta = 1$, and $| dz/d\zeta | \to 1$ as $| \zeta | \to \infty$. If the complex potential for the flow past the aerofoil is $w(z)$, then in the circle plane we must have

$$w = w_\alpha = \zeta e^{-i\alpha} + 1/\zeta e^{-i\alpha} + i\varkappa \log \zeta \,, \qquad (1)$$

for some α and $\varkappa$, the radius of the circle and the velocity at infinity being taken as unity. Its derivative is

$$\frac{dw_\alpha}{d\zeta} = e^{-i\alpha} - \frac{e^{i\alpha}}{\zeta^2} + \frac{i\varkappa}{\zeta} \,, \qquad (2)$$

and the Kutta-Joukowsky condition demands that this shall vanish at $\zeta = 1$, *i.e.* that $\varkappa = 2 \sin \alpha$. Hence

$$\frac{dw_\alpha}{d\zeta} = (e^{-i\alpha}\,\zeta^{-1} + e^{i\alpha}\,\zeta^{-2})\,(\zeta - 1) = 4ie^{-i\theta} \cos\left(\frac{\theta}{2} - \alpha\right) \sin \frac{\theta}{2} \,, \qquad (3)$$

if $\zeta = e^{i\theta}$. But the velocity q in the aerofoil plane is $\left|\frac{dw_\alpha}{dz}\right| = \left|\frac{dw_\alpha}{d\zeta}\right| \left|\frac{d\zeta}{dz}\right|$. In particular the velocity at zero lift at a point on the surface of the aerofoil is

$$q_0 = \left|\frac{dw_0}{dz}\right| = 2 \sin \theta \left|\frac{d\zeta}{dz}\right| = 2 \sin \theta \left|\frac{d\theta}{ds}\right| = \frac{2}{\left|\dfrac{ds}{d \cos \theta}\right|} \,, \qquad (4)$$

if $dz = ds\, e^{i\chi}$; and at incidence α, the velocity is

$$q_\alpha = q_0 \frac{\cos\left(\frac{1}{2}\theta - \alpha\right)}{\cos \frac{1}{2}\theta} \,. \qquad (5)$$

Now $dw_0/dz = q_0 e^{-i\chi}$, where χ is the direction of motion at any point (on the aerofoil it is along the tangent, so that the two definitions of χ are consistent). Hence $\log q_0 - i\chi$ is an analytic function in the domain outside the circle, and $\log q_0$ *and* χ *can be expanded in conjugate Fourier series in* θ *on the circle.*

Now $\oint \frac{dz}{d\zeta}\, d\zeta$ round the circle is zero. By (2), with $\alpha = 0$, this can be written

$$\oint \frac{dz}{dw_0}\left(1 - \frac{1}{\zeta^2}\right) d\zeta = 0 \,. \qquad (6)$$

Hence, if $\dfrac{dz}{dw_0} = 1 + \dfrac{a_1}{\zeta} + \dfrac{a_2}{\zeta^2} + \ldots$ (it must take this form since $q_0 = 1$ at infinity), we have $a_1 = 0$. Hence $\log \dfrac{dz}{dw_0} = \dfrac{a_2}{\zeta^2} + \ldots$ But this is $-\log \dfrac{dw_0}{dz} = -\log q_0 + i\chi$. Thus $\log q_0$ can be expanded in a Fourier series in θ, containing terms in $\cos n\theta$ and $\sin n\theta$ *only for* $n \geqslant 2$. This fact can be written

$$\left.\begin{aligned} \int_{-\pi}^{\pi} \log q_0 \, d\theta &= 0, \\ \int_{-\pi}^{\pi} \log q_0 \cos \theta \, d\theta &= 0, \\ \int_{-\pi}^{\pi} \log q_0 \sin \theta \, d\theta &= 0. \end{aligned}\right\} \qquad (7)$$

Of these three very important conditions, the first amounts to requiring unit velocity at infinity, and the latter two to requiring that the aerofoil defined by the function $\log q_0(\theta)$ shall close up.

The method of this report is to select the relation between $\log q_0$ and θ so that it satisfies (7); and then to construct the corresponding aerofoil by finding χ as the conjugate Fourier series of $\log q_0$, and using (4) to give for the ordinates and abscissae of points on the aerofoil

$$x = \int \frac{2}{q_0} \cos \chi d\,(\cos \theta),\; y = \int \frac{2}{q_0} \sin \chi d\,(\cos \theta)\,. \qquad (8)$$

After some experience it is possible, for almost all types of velocity distribution which are desired in practice, to decide upon the corresponding relation between $\log q_0$ and θ. The whole art in the application of the method is to choose this relation, (i) to fulfil well the purposes for which the aerofoil is to be designed, (ii) simply enough for the purposes of the subsequent computation.

When the aerofoil has been constructed and the chord found, we know the lift curve slope. For the circulation is $4\pi \sin \alpha$ and so

$$C_L = \frac{4\pi \sin \alpha \,.\, \rho \,.\, 1}{\frac{1}{2}\rho \,.\, 1^2 \,.\, \text{chord}} = \frac{8\pi}{\text{chord}} \sin \alpha\,. \qquad (9)$$

For very thin aerofoils the chord is asymptotically 4; for thicker ones it is rather less.

Poisson's integral relating conjugate functions is

$$\chi(\theta) = \frac{1}{2\pi} \int_{-\pi}^{\pi} \log q_0(t) \cot \tfrac{1}{2}(\theta - t)\, dt\,, \qquad (10)$$

being taken as a Cauchy principal value at the singularity $\theta = t$.

2. *Symmetrical Aerofoils.*—For symmetrical aerofoils q_0 is an even function, χ an odd function, of θ. (10) then takes the simpler form

$$\left.\begin{aligned} \chi(\theta) &= -\frac{\sin \theta}{\pi} \int_0^{\pi} \frac{\log q_0(t)}{\cos \theta - \cos t}\, dt, \\ \log q_0(\theta) &= \frac{1}{\pi} \int_0^{\pi} \frac{\chi(t) \sin t}{\cos \theta - \cos t}\, dt. \end{aligned}\right\} \qquad (11)$$

Also the third condition of (7) is automatically satisfied.

A fairly simple method of application of the ideas of § 1, which was used at first, is the modification of a known shape. In Appendices I and II there have been obtained two aerofoils by modifying a 13 per cent. thick symmetrical Joukowsky aerofoil. Shapes obtainable by this method are seen to be most varied. If q_{J0} and χ_J are the velocity and direction of flow round the Joukowsky aerofoil at zero lift, then we take

$$\left.\begin{aligned} \log q_0 &= \log q_{J0} + \log q_M \,, \\ \chi &= \chi_J + \chi_M \,, \end{aligned}\right\} \qquad \ldots \qquad (12)$$

where χ_M is the conjugate of $\log q_M$. q_M is chosen to give a specific type of velocity distribution at some positive incidence α; this is quite possible since in virtue of (5) we have also

$$\log q_\alpha = \log q_{J\alpha} + \log q_M \,. \qquad \ldots \qquad (12a)$$

However a more efficient method is that of *direct design at incidence.* This enables us to obtain aerofoils whose upper surface velocity distribution at a given incidence is, for example, quite flat for the forward portion of the chord and then either (say) falls off fairly evenly or jumps down suddenly to another quite flat portion.

Suppose in fact we want q_α to be such a simple function S. Then by (5) we must have

$$\log q_0 = \log \frac{\cos \frac{1}{2}\theta}{\cos (\frac{1}{2}\theta - \alpha)} + \log S. \qquad \ldots \qquad (13)$$

Hence the conjugate and first two Fourier constants of the function $\log \dfrac{\cos \frac{1}{2}\theta}{\cos (\frac{1}{2}\theta - \alpha)}$ are important. In Appendix III it is shown that the conjugate is

$$\frac{2}{\pi} \int_0^T \frac{\log x}{x^2 - 1}\, dx \,, \qquad \ldots \qquad (14)$$

where $T = \tan \alpha \tan \dfrac{\theta}{2}$; and the function $F(T) = \dfrac{360}{\pi^2} \displaystyle\int_0^T \frac{\log x}{x^2 - 1}\, dx,$ which is the corresponding value of χ in degrees, is tabulated there. $F(T) = 0$ deg. at $T = 0$ (*i.e.* $\theta = 0$) and $= 90$ deg. at $T = \infty$ (*i.e.* $\theta = \pi$); these are the values for an ordinary cusped aerofoil. The Fourier constants are also shown to be

$$\left.\begin{aligned} K(\alpha) &= \int_0^\pi \left[\log \frac{\cos \frac{1}{2}\theta}{\cos (\frac{1}{2}\theta - \alpha)}\right] \cos \theta \, d\theta = \pi \sin^2\alpha + \sin 2\alpha \log \cot \alpha \,, \\ -L(\alpha) &= \int_0^\pi \left[\log \frac{\cos \frac{1}{2}\theta}{\cos (\frac{1}{2}\theta - \alpha)}\right] d\theta = 2 \int_0^{\tan \alpha} \frac{\log x}{1 + x^2}\, dx \,. \end{aligned}\right\} \qquad \ldots \qquad (15)$$

The simplest aerofoil of this type is one for which S is a step-function. If

$$\left.\begin{aligned} \log S &= l \text{ for } \beta < \theta < \pi \\ \text{and } & l - k \text{ for } 0 < \theta < \beta , \end{aligned}\right\} \quad \ldots \quad (16)$$

then the conditions (7) become

$$\left.\begin{aligned} l\pi - \beta k - L(\alpha) &= 0 , \\ - k \sin \beta + K(\alpha) &= 0 , \end{aligned}\right\} \quad \ldots \quad (17)$$

which determine l and k. Thus such an aerofoil is completely determined by the values of α and β. At β, the discontinuity, there is a slot where the boundary layer is sucked away. The doubly infinite series of suction aerofoils produced by (16) and (17) may be expected to have thickness very near the minimum for low drag at the C_L and point of suction obtained.

χ for this aerofoil is

$$F(T) + k \frac{1}{\pi} \log \frac{\sin \frac{1}{2} | \theta - \beta |}{\sin \frac{1}{2} (\theta + \beta)} . \quad \ldots \quad (18)$$

Examples are discussed in Appendices IV and V.

Another simple case is

$$\left.\begin{aligned} \log S &= l \text{ for } \beta < \theta < \pi \\ \text{and } & l - k (\cos \theta - \cos \beta) \text{ for } 0 < \theta < \beta . \end{aligned}\right\} \quad \ldots \quad (19)$$

Since it is found that x varies rather like $\cos \theta$, this gives a velocity distribution flat from $\theta = \pi$ to β, and thereafter falling off fairly evenly. Conditions (7) become

$$\left.\begin{aligned} l\pi - k (\sin \beta - \beta \cos \beta) - L(\alpha) &= 0 , \\ - k (\tfrac{1}{2} \beta - \tfrac{1}{4} \sin 2\beta) + K(\alpha) &= 0 , \end{aligned}\right\} \quad \ldots \quad (20)$$

and the conjugate of (19) is $- k$ times

$$\begin{aligned} - \frac{\sin \theta}{\pi} \int_0^\beta \frac{\cos t - \cos \beta}{\cos \theta - \cos t} dt &= - \frac{\sin \theta}{\pi} \int_0^\beta \left(- 1 + \frac{\cos \theta - \cos \beta}{\cos \theta - \cos t} \right) dt \\ &= \frac{\beta}{\pi} \sin \theta - \frac{\cos \theta - \cos \beta}{\pi} \log \frac{\sin \frac{1}{2} | \theta - \beta |}{\sin \frac{1}{2} (\theta + \beta)} , \end{aligned} \quad (21)$$

$$\text{giving } \chi = F(T) - k \frac{\beta}{\pi} \sin \theta + k \frac{\cos \theta - \cos \beta}{\pi} \log \frac{\sin \frac{1}{2} | \theta - \beta |}{\sin \frac{1}{2} (\theta + \beta)} . \quad \ldots \quad (22)$$

Examples of this method are given in Appendices VI and VII.

The above two types are special cases of the following :—

$$\left.\begin{aligned} \log S &= a \text{ for } \beta < \theta < \pi \\ \text{and } & b - c \cos \theta \text{ for } 0 < \theta < \beta , \end{aligned}\right\} \quad \ldots \quad (23)$$

for which conditions (7) are

$$\left.\begin{aligned} a (\pi - \beta) + b\beta - c \sin \beta - L(\alpha) &= 0 , \\ (b - a) \sin \beta - \tfrac{1}{2} c (\beta + \tfrac{1}{2} \sin 2\beta) + K(\alpha) &= 0 , \end{aligned}\right\} \quad \ldots \quad (24)$$

$$\text{and } \chi = F(T) + (a - b + c \cos \theta) \frac{1}{\pi} \log \frac{\sin \frac{1}{2} | \theta - \beta |}{\sin \frac{1}{2} (\theta + \beta)} - c \frac{\beta}{\pi} \sin \theta . \quad \ldots \quad (25)$$

This case is interesting when β is near to π. Dr. Goldstein suggested that, with this type of velocity distribution, a thin aerofoil with high maximum lift might be obtained, with suction near the nose. Appendix VIII shows how far this is achieved.

Other more complicated velocity distributions present little more difficulty. The only drawback of the method of "direct design at incidence" based on the function (14) is the shape of the nose, which depends on the behaviour of the function at infinity. In fact for $\theta = \pi - \delta$,

$\chi \simeq \frac{\pi}{2} - \frac{\cot \alpha}{\pi} \delta \log \frac{1}{\delta}$. But $s \simeq A\delta$, so

$$x = \int ds \cos \chi \simeq A \int \delta \log \frac{1}{\delta} d\delta \simeq A\delta^2 \log \frac{1}{\delta},$$

while $y \simeq s \simeq A\delta$. Hence

$$x \simeq Ay^2 \log \frac{1}{y}. \qquad \ldots \qquad (26)$$

(A stands for any positive number, possibly different in each occurrence.)

Thus the radius of curvature is zero at the nose: for finite radius of curvature we have $x \simeq Ay^2$.

For thinner aerofoils this is a drawback as it leads to large adverse velocity gradients at the leading edge for the higher incidences, and hence to low maximum lifts. For thicker ones such as that of Appendix IV it is not serious.

It is due to the fact that near the nose q_0 has been taken as

$$A \frac{\cos \frac{1}{2}\theta}{\cos (\frac{1}{2}\theta - \alpha)} = A \frac{\frac{\delta}{2} - \frac{1}{6}\left(\frac{\delta}{2}\right)^3 + \ldots}{\left(\frac{\delta}{2} - \frac{1}{6}\left(\frac{\delta}{2}\right)^3 + \ldots\right) \cos \alpha + \left(1 - \frac{1}{2}\left(\frac{\delta}{2}\right)^2 + \ldots\right) \sin \alpha}$$

$$= A \frac{\delta}{2 \sin \alpha} (1 - \tfrac{1}{2}\delta \cot \alpha + \ldots), \qquad \ldots \qquad (27)$$

if $\theta = \pi - \delta$. For a finite leading-edge radius of curvature it is necessary to have

$$q_0 = a_1\delta + a_3\delta^3 + a_4\delta^4 + \ldots \qquad \ldots \qquad (28)$$

To obtain this we must multiply (27) by something of the form $1 + \frac{1}{2}\delta \cot \alpha + \ldots$. A simple choice is the function

$$\left.\begin{array}{ll} e^{\frac{\sin n(\pi - \theta) - 1}{2n \tan \alpha}} & \left(\theta = \pi - \frac{\pi}{2n} \text{ to } \pi\right), \\ 1 & \left(\theta = 0 \text{ to } \pi - \frac{\pi}{2n}\right), \end{array}\right\} \qquad \ldots \qquad (29)$$

for some value of n. Appendix IX shows how far this achieves the desired object and how the number n must be chosen. In Appendix X the method is used to produce an aerofoil.

3. *Cambered Aerofoils.*—For cambered aerofoils $\log q_0$ must be given over the whole circle. The natural thing is to design the *upper* surface for high lift, and the *lower* surface for C_L zero or small and negative.

A simple way of obtaining this (for a suction aerofoil) is to take $\log q_0$ as

$$\left\{\begin{array}{ll} \log\left|\dfrac{\cos\frac{1}{2}\theta}{\cos(\frac{1}{2}\theta-\alpha)}\right| & (\alpha<\theta<\pi+\alpha) \\ 0 & (\alpha<\theta<-\pi+\alpha) \end{array}\right\} \text{ plus } \left\{\begin{array}{l} l\ (\beta_1<\theta<2\pi-\beta_2) \\ l-k\,(-\beta_2<\theta<\beta_1) \end{array}\right\} \quad \ldots \quad \ldots \qquad (30)$$

The left-hand portion is continuous at α and $\pi+\alpha$ (though its derivative is not). If $\beta_1<\alpha$, the velocity at incidence α is flat on the upper surface right up to the slot, while the same thing is true on the lower surface at zero lift. (Here the leading edge, which divides the two surfaces, must be taken as $\theta=\pi+\alpha$: it is the stagnation point for the *middle* of the C_L range).

As always we must satisfy conditions (7). Put $\vartheta=\theta-\alpha$. Then conditions (7) are equivalent to those obtained by writing ϑ for θ. Now

$$\int_0^\pi \log\frac{\cos\frac{1}{2}(\vartheta+\alpha)}{\cos\frac{1}{2}(\vartheta+\alpha)}\cos\vartheta\,d\vartheta=\int_0^\pi\sin\vartheta\frac{\sin\alpha}{\cos\vartheta+\cos\alpha}\,d\vartheta=2\sin\alpha\log\cot\frac{\alpha}{2}, \quad \ldots \qquad (31)$$

while

$$\int_0^\pi \log\frac{\cos\frac{1}{2}(\vartheta+\alpha)}{\cos\frac{1}{2}(\vartheta-\alpha)}\sin\vartheta\,d\vartheta=-\int_0^\pi\cos\vartheta\frac{\sin\alpha}{\cos\vartheta+\cos\alpha}\,d\vartheta=-\pi\sin\alpha.\ \ldots \quad \ldots \qquad (32)$$

Hence the latter two of conditions (7) become

$$\left.\begin{array}{l} k\{\sin(\beta_1-\alpha)+\sin(\beta_2+\alpha)\}=2\sin\alpha\log\cot\dfrac{\alpha}{2}, \\ k\{\cos(\beta_1-\alpha)-\cos(\beta_2+\alpha)\}=\pi\sin\alpha. \end{array}\right\} \quad \ldots \quad \ldots \quad \ldots \quad \ldots \quad \ldots \qquad (33)$$

Dividing, we obtain

$$\cot\left(\frac{\beta_2-\beta_1}{2}+\alpha\right)=\frac{2}{\pi}\log\cot\frac{\alpha}{2} \quad \ldots \quad \ldots \quad \ldots \quad \ldots \quad \ldots \quad \ldots \qquad (34)$$

The function $\beta_2-\beta_1=2\left[\cot^{-1}\left(\dfrac{2}{\pi}\log\cot\dfrac{\alpha}{2}\right)-\alpha\right]$ is tabulated in Table 1. The result is rather surprising. For all values of α, β_2 must exceed β_1 by quite a considerable amount. This means that the distance of the slot from the trailing edge is much greater on the lower surface than on the upper surface—in fact the ratio is $(1-\cos\beta_2)/(1-\cos\beta_1)$. In Appendix XI the case $\alpha=20$ deg., $\beta_1=\alpha$, is worked out and Fig. 9 shows how marked the above-mentioned effect is. But the C_L range (from 0 to 2·69) obtained with an aerofoil only 30 per cent. thick is a heavy counterbalancing advantage.

TABLE 1

α deg.	$(\beta_2-\beta_1)$ deg.
0·1	24·94
0·5	31·24
1	34·66
5	43·28
10	45·62
15	45·53
20	44·30
25	42·40
30	40·05
35	37·38

When k has been obtained from (33) we calculate l by the first of conditions (7):—

$$2\,l\pi-k\,(\beta_1+\beta_2)-2L\left(\frac{\alpha}{2}\right)=0\ . \quad \ldots \quad \ldots \quad \ldots \quad \ldots \quad \ldots \quad \ldots \quad \ldots \qquad (35)$$

Thus if β_1 is taken equal to α, there is one aerofoil of this type defined by each value of α. They are all qualitatively like that of Fig. 9.

The conjugate of (30) is

$$\chi = F\left(|\tan\tfrac{1}{2}\vartheta\,|\tan\tfrac{1}{2}\alpha\right) + k\left(\frac{1}{\pi}\right)\log\frac{\sin\frac{1}{2}(\theta-\beta_1)}{\sin\frac{1}{2}(\theta+\beta_2)} + \text{const.} \qquad \ldots \quad \ldots \qquad (36)$$

This is demonstrated in Appendix XII.

To avoid the asymmetry of the aerofoil of Fig. 9, for which the large concave portion on the lower surface will probably possess a turbulent boundary layer, it is necessary to have the maximum velocities at the two ends of the C_L range different, that at the upper end being greater.

This can be achieved by the velocity distribution

$$\log q_0 = \left\{\begin{array}{ll} \log\left|\dfrac{\cos\frac{1}{2}\theta}{\cos(\frac{1}{2}\theta-\alpha)}\right| & (\alpha < \theta < \pi + \alpha - \delta\alpha) \\ 0 & (\text{elsewhere}) \end{array}\right\}.$$

$$\text{plus}\left\{\begin{array}{l} l_1 + k\ (\pi + \alpha - \delta\alpha < \theta < \beta) \\ l_2 + k\ (\pi + \alpha - \delta\alpha < \theta < 2\pi - \beta) \\ k\ (-\beta < \theta < \beta) \end{array}\right\}, \qquad \ldots \qquad (37)$$

where δ is a small positive number and $l_1 - l_2 = \log\dfrac{\sin\frac{1}{2}(\alpha+\delta\alpha)}{\sin\frac{1}{2}(\alpha-\delta\alpha)}$, so that there is no discontinuity at $\pi + \alpha - \delta\alpha$. Conditions (7) are derived and exhibited in Appendix XII. To obtain the conjugate (10) of (37) the only new thing required is the integral

$$\frac{1}{2\pi}\int_0^{\delta\alpha}\log\left|\frac{\sin\frac{1}{2}(\phi-\alpha)}{\sin\frac{1}{2}(\phi+\alpha)}\right|\cot\tfrac{1}{2}(\vartheta+\phi-\pi)\,d\phi, \qquad \ldots \quad \ldots \quad \ldots \quad \ldots \quad \ldots \qquad (38)$$

to which we approximate by

$$\frac{1}{2\pi}\int_0^{\delta\alpha}\left(-\frac{2\phi}{\alpha}\right)\cot\tfrac{1}{2}(\vartheta+\phi-\pi)\,d\phi$$

$$= -\frac{2\delta}{\pi}\log\sin\tfrac{1}{2}(\vartheta+\delta\alpha-\pi) + \frac{2}{\alpha\pi}\int_{\theta-\pi}^{\theta-\pi+\delta\alpha}\log\sin\tfrac{1}{2}\vartheta\,d\vartheta. \qquad \ldots \quad \ldots \qquad (39)$$

Hence

$$\chi = F(T) + \frac{2\delta}{\pi}\log\sin\tfrac{1}{2}(\vartheta+\delta\alpha-\pi) - \frac{2}{\alpha\pi}\int_{\theta-\pi}^{\theta-\pi+\delta\alpha}\log\sin\tfrac{1}{2}\vartheta\,d\vartheta$$

$$-\frac{l_1}{\pi}\log\sin\tfrac{1}{2}(\theta-(\pi+\alpha-\delta\alpha)) + \frac{l_1}{\pi}\log\sin\tfrac{1}{2}(\theta-\beta)$$

$$+\frac{l_2}{\pi}\log\sin\tfrac{1}{2}(\theta-(\pi+\alpha-\delta\alpha)) - \frac{l_2}{\pi}\log\sin\tfrac{1}{2}(\theta+\beta). \qquad \ldots \quad \ldots \qquad (40)$$

To the same order of approximation $l_1 - l_2 = 2\delta$ and we obtain

$$\chi = F(T) - \frac{2}{\alpha\pi}\int_{\theta-\pi}^{\theta-\pi+\delta\alpha}\log\sin\tfrac{1}{2}\vartheta\,d\vartheta + \frac{l_1}{\pi}\log\sin\tfrac{1}{2}(\theta-\beta) - \frac{l_2}{\pi}\log\sin\tfrac{1}{2}(\theta+\beta), \quad \ldots \qquad (41)$$

which is a convenient form. The integral can be replaced by $\delta\alpha\log\sin\frac{1}{2}(\vartheta-\pi+\frac{1}{2}\delta\alpha)$, except near $\vartheta = \pi$ where we use the table of $\int_0^\theta\log\sin\frac{1}{2}\vartheta\,d\vartheta$ given in Appendix XII (extracted from a fuller seven-place table of this function by E. J. Watson).

In Appendix XIII the case $\alpha = 20$ deg., $\beta = 40$ deg. is computed, and the result shown in Fig. 10. This aerofoil is much thicker than that of Fig. 9; yet its drag is almost certainly less since both slots are well to the rear. In choosing between the two we have then to weigh thickness against low drag.

Cambered low-drag aerofoils without suction can be constructed just as easily by this method. For them it is essential to use the $\delta\alpha$ technique exemplified in (37).

Finally it may be remarked that considerations of pitching moment will often make it desirable to have negative loading over the rear end of aerofoil. This is of course not hard to achieve.

4. *Evaluation of the Moment Coefficient.*—By Blasius' Theorem the nose-up moment at zero lift is the real part of

$$\tfrac{1}{2}\rho \oint \left(\frac{dw_0}{dz}\right)^2 z\,dz, \qquad (42)$$

the integral being taken round the aerofoil in the positive direction. Choose the axes in the aerofoil plane so that dw_0/dz (itself, not merely its modulus) is unity at infinity. Then it follows from §1 that

$$\log \frac{dw_0}{dz} = \frac{a_2}{\zeta^2} + \frac{a_3}{\zeta^3} + \ldots \text{ at } \zeta = \infty. \qquad (43)$$

But $$\frac{d\zeta}{dz} = \frac{dw_0/dz}{dw_0/d\zeta} \rightarrow 1 \text{ as } \zeta \rightarrow \infty. \quad \text{Hence}$$

$$\log \frac{dw_0}{dz} \simeq \frac{a_2}{z^2} \text{ as } z \rightarrow \infty. \qquad (44)$$

Hence (42) becomes

$$\tfrac{1}{2}\rho \oint \left(1 + \frac{a_2}{z_2} + O\left(\frac{1}{z^3}\right)\right)^2 z\,dz = \tfrac{1}{2}\rho \,.\, 2\pi i \,.\, 2a_2. \qquad (45)$$

Hence if $a_2 = b_2 + ic_2$, the moment at zero lift is $-\,2\pi\rho c_2$. But (43) can be written

$$\log q_0 - i\chi = (b_2 + ic_2)(\cos 2\theta - i \sin 2\theta) + \ldots \qquad (46)$$

Hence $$c_2 = \frac{1}{\pi}\int_{-\pi}^{\pi} \log q_0 \,.\, \sin 2\theta \, d\theta \qquad (47)$$

Hence finally $$C_{M0} = \frac{\text{nose-up moment at zero lift}}{\tfrac{1}{2}\rho \,.\, 1^2 \,.\, (\text{chord})^2}$$

$$= -\,\frac{4}{(\text{chord})^2}\int_{-\pi}^{\pi} \log q_0 \,.\, \sin 2\theta \, d\theta \,. \qquad (48)$$

(The reader is reminded that the word "chord" here, and throughout this report, stands for a non-dimensional quantity rather less than four, and is the ratio of the actual chord (as measured) to the radius of the circle into which the aerofoil can be transformed conformally with no magnification at infinity.)

(48) makes it possible to determine beforehand the moment coefficient at zero lift of an aerofoil about to be designed. If $C_{M0} = 0$ is required, a $\log q_0$ must be chosen with (48) zero: if some other value for C_{M0} is stipulated, the problem is hardly more difficult, as the chord can generally be guessed to 2 or 3 per cent. accuracy before the design calculations are carried out.

For the moment coefficient at incidences other than zero, the exact expressions afforded by this theory are more complicated, but we give them for the sake of completeness. By (3) we have

$$\frac{dw_a/d\zeta}{dw_0/d\zeta} = \frac{e^{-i\alpha}\,\zeta^{-1} + e^{i\alpha}\,\zeta^{-2}}{\zeta^{-1} + \zeta^{-2}} = e^{-i\alpha}\left[1 + \frac{e^{2i\alpha} - 1}{\zeta} - \frac{e^{2i\alpha} - 1}{\zeta^2} + O\left(\frac{1}{\zeta^3}\right)\right] . \quad \ldots \quad (49)$$

If we choose the origin O in the aerofoil plane so that $z - \zeta \to 0$ as $\zeta \to \infty$, then we have also

$$\frac{dw_a/dz}{dw_0/dz} = e^{-i\alpha}\left[1 + \frac{e^{2i\alpha} - 1}{z} - \frac{e^{2i\alpha} - 1}{z^2} + O\left(\frac{1}{z^3}\right)\right] . \quad \ldots \quad \ldots \quad \ldots \quad \ldots \quad (50)$$

Hence $\frac{1}{2}\rho\oint\left(\frac{dw_a}{dz}\right)^2 z\,dz$ can be written as

$$\tfrac{1}{2}\rho\oint\left(1 + \frac{2a^2}{z^2} + O\left(\frac{1}{z^3}\right)\right)\left[1 + 2\,\frac{e^{2i\alpha} - 1}{z} + \frac{(e^{2i\alpha} - 1)^2 - 2\,(e^{2i\alpha} - 1)}{z^2} + O\left(\frac{1}{z^3}\right)\right] e^{-2i\alpha}\,z\,dz$$

$$= \tfrac{1}{2}\rho \,.\, 2\pi i\,(2a_2 + e^{4i\alpha} - 4e^{2i\alpha} + 3)\,e^{-2i\alpha}\,, \quad \ldots \quad \ldots \quad \ldots \quad \ldots \quad (51)$$

and its real part is $2\pi\rho((1 + b_2)\sin 2\alpha - c_2\cos 2\alpha)$.

Thus the moment coefficient at incidence α about the point O defined above is

$$\frac{4}{(\text{chord})^2}\left[-\cos 2\alpha\int_{-\pi}^{\pi}\log q_0\sin 2\theta\,d\theta + \sin 2\alpha\left(\pi + \int_{-\pi}^{\pi}\log q_0\cos 2\theta\,d\theta\right)\right] . \quad \ldots \quad (52)$$

Now $\lim_{\zeta\to\infty}(z - \zeta) = \frac{1}{2\pi}\int_{-\pi}^{\pi} z\,d\theta$, and after the ordinates and abscissae of the aerofoil have been found it is a fairly easy matter to calculate where the origin O must be chosen to render this integral zero—and hence to find the moment coefficient about the usual point of reference. Clearly O will lie, generally speaking, just on the forward side of the mid-chord position.

The aerodynamic centre will be at a distance of

$$\lim_{\alpha\to 0}\frac{C_{M\alpha} - C_{M0}}{C_{L\alpha}} = \frac{1 + \frac{1}{\pi}\int_{-\pi}^{\pi}\log q_0 \,.\, \cos 2\theta\,d\theta}{\text{chord}} \quad \ldots \quad \ldots \quad \ldots \quad \ldots \quad \ldots \quad \ldots \quad (53)$$

aerofoil chords forward from the point O. For thin aerofoils (with chord $\simeq$ 4, and O approximately at mid-chord) this is of course the quarter-chord point.

5. *Symmetrical Channels.*—With a few alterations the method of this report can be applied just as easily to the design of symmetrical channels, indeed more easily owing to the absence of circulation.

If the flux through a channel is $2h$, so that we may assume that the stream function ψ is $+h$ on the upper wall and $-h$ on the lower one; and if the channel is transformed symmetrically into a circle (the points $\pm\infty$ becoming ± 1 respectively), then on the circle $\psi = +h$ for $0 < \theta < \pi$ and $\psi = -h$ for $-\pi < \theta < 0$. The velocity potential ϕ is the conjugate of this, *i.e.*

$$\phi = \frac{1}{\pi}\int_0^{\pi}\frac{h\sin t}{\cos\theta - \cos t}\,dt = \frac{1}{\pi}\Big[h\log|\cos\theta - \cos t|\Big]_0^{\pi} = \frac{2h}{\pi}\log\cot\frac{\theta}{2} \quad \ldots \quad (54)$$

Hence

$$q\frac{ds}{d\theta} = \frac{d\phi}{d\theta} = -\frac{2h}{\pi}\operatorname{cosec}\theta \,. \quad \ldots \quad \ldots \quad \ldots \quad \ldots \quad \ldots \quad \ldots \quad \ldots \quad (55)$$

Here ds is an element of length on the channel and q the speed at any point. If χ is the direction of motion then $\log q - i\chi$ is an analytic function in the physical plane and hence in the plane of the circle. Hence $\log q$ and χ are conjugates of one another in the circle. When they are chosen we have by (55)

$$x = -\int \frac{\cos \chi}{q} \frac{2h}{\pi} \operatorname{cosec} \theta \, d\theta, \quad y = -\int \frac{\sin \chi}{q} \frac{2h}{\pi} \operatorname{cosec} \theta \, d\theta . \qquad (56)$$

This " cosec θ " corresponds to $\sin \theta$ in (8). There are no *a priori* conditions on the choice of $\log q$, as channels do not " close up ".

The simplest requirement for $\log q$ is that it should not decrease as θ goes from π to 0. (This has application in the design of contraction cones for low-turbulence wind tunnels). If $a > 0$, $\log q = a \cos \theta$ does this, and its conjugate is $a \sin \theta$. a is chosen as $\frac{1}{2} \log (V/U)$, if it is desired to make q increase from U to V.

But contraction cones should also be short, that is, χ must tend to zero as rapidly as possible at the two ends. Thus, given $\log (V/U)$, we want

$$\alpha = \left(\frac{d\chi}{d\theta}\right)_{\theta=0} - \left(\frac{d\chi}{d\theta}\right)_{\theta=\pi} \qquad (57)$$

to be as small as possible. Now $f(\theta) = -\dfrac{d}{d\theta} \log q$ is a positive function, and $\int_0^\pi f(t)\, dt = \log (V/U)$.

Its conjugate is $\dfrac{d\chi}{d\theta} = \dfrac{1}{\pi} \displaystyle\int_0^\pi \frac{f(t) \sin t}{\cos \theta - \cos t} dt$. Hence

$$\alpha = \frac{1}{\pi} \int_0^\pi \frac{f(t) \sin t}{1 - \cos t} dt - \frac{1}{\pi} \int_0^\pi \frac{f(t) \sin t}{-1 - \cos t} dt = \frac{2}{\pi} \int_0^\pi f(t) \operatorname{cosec} t \, dt. \qquad (58)$$

The minimum of $\dfrac{\alpha}{\log (V/U)}$ occurs (since cosec t is a minimum at $t = \frac{1}{2}\pi$) when $f(t)$ is concentrated near $t = \frac{1}{2}\pi$, or in the notation of Dirac, when $f(t) = \log (V/U) \,.\, \delta (t - \frac{1}{2}\pi)$. This means that $\log q$ is constant on the wall up to the point corresponding to $\theta = \frac{1}{2}\pi$ and then jumps up to another constant value. For this case, $\dfrac{\alpha}{(\log V/U)} = \dfrac{2}{\pi} = 0{\cdot}64$. For the previously mentioned case $\log q = \text{const.} + \frac{1}{2} \log (V/U) \,.\, \cos \theta$, we have $\dfrac{\alpha}{\log (V/U)} = 1{\cdot}00$. For an intermediate case $\log q = \text{const.} + \frac{9}{16} \log (V/U) \,.\, (\cos \theta - \frac{1}{9} \cos 3\theta)$, which is a non-decreasing function also, we have $\dfrac{\alpha}{\log (V/U)} = 0{\cdot}75$. This case possibly has merits over the discontinuous case, as it allows a margin of safety. It is chosen as an example in Appendix XIV, and the shape is drawn in Fig. 11.

Another problem in the design of contraction cones is this ; if a certain amount of adverse velocity gradient is allowed, but not too much, how much more favourable are the shapes obtained ? In Appendix XV, a *finite* contraction cone (*i.e.* one whose walls from some point onwards on both sides are straight and parallel to the axis) is constructed, using a value of χ as follows :—

$$\left.\begin{aligned} \chi &= 0 \text{ for } 0 < \theta < \beta \\ &\quad \text{and } a\,[1 - \cos (\theta - \beta)] \text{ for } \beta < \theta < \frac{\pi}{2}, \end{aligned}\right\} \qquad (59)$$

where β is small and $\chi(\theta) = \chi(\pi - \theta)$. The maximum adverse velocity gradient obtained is found to be $0{\cdot}75$ working section velocities per working section diameter—rather a high value, though it occurs very close to the working section.

In Appendix XVI a short cone is obtained with a very much smaller adverse gradient. For this cone

$$\left.\begin{aligned} \log q &= \tfrac{1}{4}\log (V/U)\,.\,(1 + 2\cos\theta - \cos 2\theta), \\ \chi &= \tfrac{1}{4}\log (V/U)\,.\,(2\sin\theta - \sin 2\theta). \end{aligned}\right\} \quad \ldots \quad (60)$$

At $\theta = 0$ (the wide end) $\chi \to 0$ very rapidly; but not nearly so rapidly at $\theta = \pi$ (the narrow end). This was taken because in most contraction cones the wide end is far longer than the narrow end, while the large value of $d\chi/d\theta$ at $\theta = \pi$ hardly increases the length and yet eliminates altogether the (large) adverse velocity gradient over the narrow end visible in Fig. 12. With a four to one ratio the maximum adverse gradient is $0{\cdot}025$ working section velocities per working section diameter.

6. *Cascades.*—The method is also applicable to the design of a cascade of aerofoils. If congruent aerofoils are arranged in the complex z-plane, periodically in $2\pi i$, and $w(z)$ is the complex potential of flow past them, then dw/dz is periodic in $2\pi i$. Let it have the value $u_1 - iv_1$ at infinity on the left and $u_2 - iv_2$ at infinity on the right. The transformation $Z = e^z$ gives us a plane in which there is just one aerofoil, $x = -\infty$ gives $Z = 0$, $x = +\infty$ gives $Z = \infty$. Hence, since $\dfrac{dw}{dZ} = \dfrac{dw}{dz}\cdot\dfrac{1}{z}$, we have

$$\frac{dw}{dZ} \simeq \frac{u_1 - iv_1}{Z} \text{ at } Z = 0 \text{ and } \simeq \frac{u_2 - iv_2}{Z} \text{ at } Z = \infty\,. \quad \ldots \quad (61)$$

These are the only singularities outside the aerofoil in the Z-plane. The aerofoil can be transformed into the unit circle in the ζ-plane with the trailing edge corresponding to $\zeta = 1$, and ∞ to ∞. Let $Z = 0$ become $\zeta = a$. Then

$$\frac{dw}{d\zeta} \simeq \frac{u_1 - iv_1}{\zeta - a} \text{ at } \zeta = a \text{ and } \simeq \frac{u_2 - iv_2}{\zeta} \text{ at } \zeta = \infty\,. \quad \ldots \quad (62)$$

Hence

$$W = w - u_1 \log\frac{(\zeta - a)\,(1 - \bar{a}\zeta)}{\zeta} + iv_1 \log\frac{\zeta - a}{1 - \bar{a}\zeta} + iv_2 \log\zeta \quad \ldots \quad (63)$$

has no singularity outside or on the circle, has imaginary part constant on the circle, and behaves like $(u_2 - u_1)\log\zeta$ at infinity. Hence $u_1 = u_2$ and W is constant everywhere. Hence (dropping the suffices on u)

$$\begin{aligned} \frac{dw}{d\zeta} &= u\left(\frac{1}{\zeta - a} - \frac{\bar{a}}{1 - \bar{a}\zeta} - \frac{1}{\zeta}\right) - iv_1\left(\frac{1}{\zeta - a} + \frac{\bar{a}}{1 - \bar{a}\zeta}\right) - \frac{iv_2}{\zeta} \\ &= \frac{u\,(a - \bar{a}\zeta^2) - iv_1\zeta\,(1 - a\bar{a}) - iv_2\,(\zeta - a)\,(1 - \bar{a}\zeta)}{\zeta\,(\zeta - a)\,(1 - \bar{a}\zeta)}\,. \quad \ldots \quad (64) \end{aligned}$$

By the Kutta-Joukowsky condition this must vanish at $\zeta = 1$. Hence it can be factorised as

$$\frac{dw}{d\zeta} = \frac{(1 - \zeta)\,(a\,(u + iv_2) + \bar{a}\,(u - iv_2)\,\zeta)}{\zeta\,(\zeta - a)\,(1 - \bar{a}\zeta)}\,. \quad \ldots \quad (65)$$

If $a = Ae^{i\alpha}$, $u + iv_1 = B_1e^{i\beta_1}$, $u_2 + iv_2 = B_2e^{i\beta_2}$, and $\zeta = e^{i\theta}$, then this becomes

$$\begin{aligned} \frac{dw}{d\zeta} &= \frac{-\,2ie^{i\theta/2}\sin\tfrac{1}{2}\theta\,.\,2AB_2\cos(\alpha + \beta_2 - \tfrac{1}{2}\theta)\,e^{i\theta/2}}{e^{2i\theta}\,(1 - 2A\cos(\alpha - \theta) + A^2)} \\ &= 4AB_2\frac{\sin\tfrac{1}{2}\theta\cos(\alpha + \beta_2 - \tfrac{1}{2}\theta)}{1 - 2A\cos(\alpha - \theta) + A^2}\cdot\frac{e^{-i\theta}}{i}\,. \quad \ldots \quad (66) \end{aligned}$$

The relation between v_1 and v_2 is

$$u\,(a - \bar{a}) - iv_1\,(1 - a\bar{a}) - iv_2\,(1 - a)\,(1 - \bar{a}) = 0. \quad \ldots \quad \ldots \quad \ldots \quad (67)$$

or

$$2Au \sin\alpha + v_1\,(A^2 - 1) - v_2\,(A^2 - 2A\cos\alpha + 1) = 0\,. \quad \ldots \quad \ldots \quad (68)$$

It gives $v_1 = v_2$ when $v_1 = \dfrac{A\sin\alpha}{1 - A\cos\alpha}\,u$. The angle $T = -\tan^{-1}\dfrac{A\sin\alpha}{1 - A\cos\alpha}$ between the *angle of zero deflection* and the real axis (in the z-plane) is a measure of the *stagger* of the cascade. α will generally be nearer π than 0. A is large if the pitch-chord ratio is large, and near unity if the latter is small. The second stagnation point on the circle is seen from (66) to be $\theta = \pi + 2\,(\alpha + \beta)$.

The method of design is to choose $\log q$ on the circle so that the resulting values of $\log\,(dw/dz)$ at a and ∞ are correct. By Poisson's integral,

$$\log\frac{dw}{dz} = \frac{1}{2\pi i}\oint \log q\,\frac{\zeta + t}{\zeta - t}\,\frac{dt}{t} + \text{imaginary constant}, \quad \ldots \quad \ldots \quad \ldots \quad \ldots \quad (69)$$

the integral being taken round the circle and q standing for its value at t. Hence

$$\log\frac{u - iv_1}{u - iv_2} = \left[\log\frac{dw}{dz}\right]_{\zeta=a} - \left[\log\frac{dw}{dz}\right]_{\zeta=\infty} = \frac{1}{\pi i}\oint \log q\,\frac{dt}{a - t}\,, \quad \ldots \quad \ldots \quad \ldots \quad (70)$$

which, together with

$$\frac{1}{2\pi}\int_{-\pi}^{\pi} \log q\,d\theta = \log B_2\,, \quad \ldots \quad \ldots \quad \ldots \quad \ldots \quad \ldots \quad \ldots \quad (71)$$

is sufficient.

χ is, as usual, the conjugate of $\log q$ on the circle, and since, by (66), we have

$$q\,\frac{ds}{d\theta} = 4AB_2\,\frac{\sin\frac{1}{2}\theta\,\cos\,(\alpha + \beta_2 - \frac{1}{2}\theta)}{1 - 2A\cos\,(\alpha - \theta) + A^2}\,, \quad \ldots \quad \ldots \quad \ldots \quad \ldots \quad \ldots \quad (72)$$

the expressions for the ordinates and abscissae of a typical aerofoil of the cascade are

$$\left.\begin{aligned} x^{\delta} &= \int \frac{4AB_2}{q}\,\frac{\sin\frac{1}{2}\theta\,\cos\,(\alpha + \beta_2 - \frac{1}{2}\theta)}{1 - 2A\cos\,(\alpha - \theta) + A^2}\cos\chi\,d\theta\,, \\ y &= \int \frac{4AB_2}{q}\,\frac{\sin\frac{1}{2}\theta\,\cos\,(\alpha + \beta_2 - \frac{1}{2}\theta)}{1 - 2A\cos\,(\alpha - \theta) + A^2}\sin\chi\,d\theta\,. \end{aligned}\right\} \quad \ldots \quad \ldots \quad \ldots \quad (73)$$

A full discussion of cascade design with a worked example is to be found in R. & M. 2104[2].

REFERENCES

No.	*Author*	*Title, etc.*
1	Goldstein, S.	A Theory of Aerofoils of Small Thickness. Part I—Velocity Distributions for Symmetrical Aerofoils. A.R.C. 5804. May, 1942. (To be published.) Part II—Velocity Distributions for Cambered Aerofoils. A.R.C. 6156. September, 1942. (To be published.) Part III—Approximate Designs of Symmetrical Aerofoils for Specified Pressure Distributions. A.R.C. 6225. October, 1942. (To be published.) Part IV—The Design of Centre Lines. A.R.C. 8548. March, 1945. (To be published.) Part V—The Positions of Maximum Velocity and Theoretical C_L-ranges. A.R.C. 8549. March, 1945. (To be published.)
2	Lighthill, M. J.	A Mathematical Method of Cascade Design. R. & M. 2104. June, 1945.

Introduction to Appendices.—As first essays in a method of design the results of whose application could not possibly be known beforehand, the majority of the computations in the following Appendices were done only to fairly low accuracy. Dale's five-place tables were used and in the final shape four, and in certain cases three, significant figures only were obtained with any confidence of accuracy. This was sufficient to give such fundamental properties as thickness-ratio, C_L range, points of maximum suction and thickness, and general shape, and hence to show how useful the different variations of the method would be, But a rough design once decided upon for use as an actual wing should, for the purposes of construction, be computed to greater exactitude. Appendix IV shows how this can be done, using seven figure tables, a multitude of points, and the most accurate methods of integration available. For the low accuracy computations, $1\frac{1}{2}$ days was the usual time for the construction of an areofoil. For the high accuracy of Appendix IV, 4 or 5 days were needed.

In some of the Appendices cos θ is used as an independent variable. This has the advantage that a great many tables of the trigonometric functions $\left(\text{including those of the type } \frac{1}{\pi}\log\frac{\sin\frac{1}{2}(\theta+\beta)}{\sin\frac{1}{2}|\theta-\beta|}\right)$ have been tabulated against cos θ by computors working under Dr. Goldstein on the method of Ref. 1. But experience has shown that it is wiser to use θ itself. This gives the extra points near the leading and trailing edges which are so desirable and greatly facilitates the integration near the leading edge.

A method of integration which has been frequently used and found satisfactory is shown in the Table 2 following :—

TABLE 2

x	0	a	$2a$	$3a$	$4a$	$5a$	$6a$	$7a$	....
y	y_0	y_1	y_2	y_3	y_4	y_5	y_6	y_7	....
$\frac{3}{a}\int_0 y\,dx$	0	$Z-(y_1+4y_2+y_3)$	$y_0+4y_1+y_2$	$\frac{9}{8}(y_0+3y_1+3y_2+y_3)=Z$	$y_0+4y_1+2y_2+4y_3+y_4$	$Z+(y_3+4y_4+y_5)$	$y_0+4y_1+2y_2+4y_3+2y_4+4y_5+y_6$	$Z+(y_3+4y_4+2y_5+4y_6+y_7)$	....

It is a combination of Simpson's Rule and the cubic (1:3:3:1) rule, and can be carried out very speedily on an adding machine. More accurate (but more laborious) procedures are indicated in Appendix IV.

For suction aerofoils integration breaks down near the slot but can be supplemented by our knowledge of the theory of the logarithmic spiral. This is explained in Appendix II.

APPENDIX I

Joukowsky Aerofoil modified to give "Low-drag" Section

A symmetrical Joukowsky aerofoil is obtained from the unit circle by the transformation

$$z = \zeta - b + \frac{(1-b)^2}{\zeta - b} \quad \ldots \quad (I.1)$$

and

$$\frac{dz}{d\zeta} = \frac{(\zeta - 1)(\zeta + 1 - 2b)}{(\zeta - b)^2} \quad \ldots \quad (I.2)$$

These give

$$q_{J0} = \frac{2 \cos \frac{1}{2}\theta \, (1 - 2b \cos \theta + b^2)}{\sqrt{[(1-2b)^2 + 2(1-2b)\cos\theta + 1]}}$$

and

$$\chi_J = \frac{3\theta}{2} + \tan^{-1}\frac{\sin\theta}{\cos\theta + (1-2b)} - 2\tan^{-1}\frac{\sin\theta}{\cos\theta - b} \,. \quad \ldots \quad (I.3)$$

We take $b = 0 \cdot 1$, giving thickness ratio approximately 13 per cent. We then plot $\log_{10} (\frac{1}{2}q_{J\alpha})$ against $\cos\theta$ for a given incidence α, which we have taken as 2 deg. 30 min. (corresponding to $C_L \simeq 0 \cdot 3$), in Table 3, column 1. In column 2 is plotted χ_J, and, in column 3, $\log_{10} (\sin\theta / q_J)$.

Now we observe from column 1 that the maximum value of $-\dfrac{d \log_{10} (\frac{1}{2}q_{J\alpha})}{d \cos\theta}$ on the upper surface for $\pi \geqslant \theta \geqslant \dfrac{\pi}{2}$ is $0 \cdot 1005$ as far as the table indicates. If therefore we add to $\log_{10} q_J$ a function $\log_{10} q_M$, whose derivative with respect to $\cos\theta$ is everywhere $> 0 \cdot 1005$ in this range, an aerofoil will be obtained with increasing velocity (at 2 deg. 30 min. incidence) over all points corresponding to $\pi \geqslant \theta \geqslant \pi/2$. The function chosen was

$$\left.\begin{aligned} \log_{10} q_M &= 0 \cdot 1012\left(\cos\theta + \frac{2}{\pi}\right), \quad \left(\pi \geqslant \theta \geqslant \frac{\pi}{2}\right), \\ &= 0 \cdot 1012\left(-\cos\theta + \frac{2}{\pi}\right), \quad \left(\frac{\pi}{2} \geqslant \theta \geqslant 0\right). \end{aligned}\right\} \quad \ldots \quad (I.4)$$

This satisfies conditions (7). Its conjugate is $0 \cdot 1012 . \dfrac{2}{\pi} \cos\theta \log \left|\tan\dfrac{\pi}{4} - \dfrac{\theta}{2}\right|$. The addition to χ, which we call χ_M, is conjugate to $\log_e q_M$, and so in degrees

$$\chi_M = \frac{180}{\pi} . \log_e 10 . \frac{2}{\pi} . 0 \cdot 1012 \cos\theta \log \left|\tan\left(\frac{\pi}{4} - \frac{\theta}{2}\right)\right|$$

$$= 8 \cdot 500 \cos\theta . \log \left|\tan\left(\frac{\pi}{4} - \frac{\theta}{2}\right)\right| . \quad \ldots \quad (I.5)$$

The new $\chi = \chi_J + \chi_M$ is given in column 4. Now in order to get x and y from (8) we need $2/q_0$.

But we have

$$\log_{10}\left(\frac{2}{q_0}\right) = \log_{10}\left(\frac{2}{q_{J0}}\right) - 0\cdot 1012\ (\pm \cos\theta) - 0\cdot 1012\,\frac{2}{\pi} \quad \ldots \quad (\text{I.6})$$

But $10^{0\cdot 1012\delta}\ \dfrac{2}{\pi} = 1\cdot 1600$. Column 5 gives $1\cdot 16/q_0$ obtained from column 3 and (I.6). Columns 6 and 7 give $\dfrac{1\cdot 16}{q_0}\cos\chi\left(\text{that is } 0\cdot 58\,\dfrac{dx}{d\cos\theta}\right)$ and $\dfrac{1\cdot 16}{q_0}\sin\chi\left(\text{that is } 0\cdot 58\,\dfrac{dy}{d\cos\theta}\right)$; and in columns 8 and 9 these are integrated up from the trailing edge by Simpson's rule (or other rules as found convenient) to give $0\cdot 58\ (c - x)$ and $0\cdot 58y$. It is found that the chord is $2\cdot 02852/0\cdot 58 = 3\cdot 497$.

The expressions $X = x/c$, $Y = y/c$ are tabulated in columns 10 and 11. The thickness-ratio is found to be $19\cdot 6$ per cent., and

$$C_L = \frac{8\pi \sin 2 \text{ deg. } 30 \text{ min.}}{3\cdot 497} = 0\cdot 3135.$$

The velocity distribution at incidence, q_α, is given in column 12 and in Fig. 1, where the profile shape is also shown.

L.E.R. = ~~0.2207~~ 0.0227 chord
(See p. 44)

(77090)

TABLE 3

$\cos\theta$	1 $\log_{10}(\frac{1}{2}q_{Ja})$	2 χ_J (deg.)	3 $\log_{10}\left(\frac{\sin\theta}{q_J}\right)$	4 χ (deg.)	5 $\frac{1\cdot16}{q_0}$	6 $\frac{1\cdot16}{q_0}\cos\chi$	7 $\frac{1\cdot16}{q_0}\sin\chi$	8 $0\cdot58\,(c\text{-}x)$	9 $0\cdot58y$	10 X	11 Y	12 q_a
−1	$\bar{1}$·42144	90	$\bar{1}$·21824	90	(0·20866 cosec θ)	0·9463	∞	2·0285	0	0	0	0·4850
−0·9	$\bar{1}$·84974	21·26	$\bar{1}$·56383	24·83	1·03641	0·9406	0·43517	1·9342	0·0892	0·0465	0·0440	1·3310
−0·8	$\bar{1}$·84308	12·08	$\bar{1}$·68708	16·79	0·97698	0·9353	0·28221	1·8404	0·1244	0·0927	0·0613	1·3415
−0·7	$\bar{1}$·83333	7·18	$\bar{1}$·76201	12·51	0·95293	0·9303	0·20641	1·9471	0·1482	0·1387	0·0731	1·3427
−0·6	$\bar{1}$·82328	3·89	$\bar{1}$·81472	9·49	0·93831	0·9255	0·15471	1·6543	0·1665	0·1845	0·0821	1·3429
−0·5	$\bar{1}$·81340	+ 1·47	$\bar{1}$·85435	7·07	0·92771	0·9207	0·11419	1·5620	0·1795	0·2300	0·0885	1·3437
−0·4	$\bar{1}$·80361	− 0·44	$\bar{1}$·88512	4·89	0·91931	0·9160	0·07837	1·4702	0·1895	0·2753	0·0934	1·3447
−0·3	$\bar{1}$·79386	− 1·97	$\bar{1}$·90931	2·81	0·91232	0·9112	0·04472	1·3788	0·1953	0·3203	0·0963	1·3458
−0·2	$\bar{1}$·78404	− 3·21	$\bar{1}$·92816	+ 0·69	0·90629	0·9062	+0·01092	1·2879	0·1984	0·3651	0·0978	1·3468
−0·1	$\bar{1}$·77437	− 4·25	$\bar{1}$·94247	− 1·71	0·90112	0·9007	−0·02689	1·1976	0·1973	0·4096	0·0973	1·3481
0	$\bar{1}$·76453	− 5·08	$\bar{1}$·95258	− 5·08	0·89658	0·8931	−0·07938	1·1079	0·1926	0·4538	0·0949	1·3489
+0·1	$\bar{1}$·75459	− 5·74	$\bar{1}$·95858	− 8·28	0·93517	0·9254	−0·13467	1·0169	0·1814	0·4987	0·0894	1·2882
0·2	$\bar{1}$·74452	− 6·23	$\bar{1}$·96039	−11·13	0·97610	0·9609	−0·17168	0·9227	0·1662	0·5452	0·0820	1·2296
0·3	$\bar{1}$·73430	− 6·58	$\bar{1}$·95748	−11·36	1·01933	0·9994	−0·20078	0·8246	0·1473	0·5935	0·0726	1·1733
0·4	$\bar{1}$·72389	− 6·75	$\bar{1}$·94905	−12·08	1·06510	1·0415	−0·22289	0·7226	0·1263	0·6438	0·0623	1·1191
0·5	$\bar{1}$·71327	− 6·75	$\bar{1}$·93362	−12·35	1·11348	1·0877	−0·23815	0·6161	0·1030	0·6963	0·0508	1·0670
0·6	$\bar{1}$·70241	− 6·65	$\bar{1}$·90860	−12·25	1·16472	1·1382	−0·24713	0·5048	0·0789	0·7511	0·0389	1·0166
0·7	$\bar{1}$·69124	− 6·11	$\bar{1}$·86898	−11·44	1·21908	1·1949	−0·24184	0·3882	0·0540	0·8086	0·0266	0·9680
0·8	$\bar{1}$·67971	− 5·34	$\bar{1}$·80327	−10·05	1·27667	1·2571	−0·22279	0·2656	0·0310	0·8791	0·0153	0·9209
0·9	$\bar{1}$·66758	− 4·02	$\bar{1}$·67469	− 7·59	1·33781	1·3261	−0·17671	0·1364	0·0103	0·9327	0·0051	0·8750
1	$\bar{1}$·65280	0	$-\infty$	0	1·40267	1·4027	0	0	0	1	0	0·8261

APPENDIX II

Thin Joukowsky Aerofoil modified to give Very Thick Suction Aerofoil

In order to show the flexibility of the method we now choose an incidence about 10 times as great as that of Appendix I, in fact, $\sin \alpha = 0 \cdot 3$. The corresponding value of $\log_{10} (\frac{1}{2} q_{Ja})$ is shown in Table 4, column 1. To make a suction aerofoil with slot at $\cos \theta = 0 \cdot 8$, and increasing velocity up to the slot in the upper surface at this incidence we add to $\log_{10} q_{Ja}$ the function

$$\left.\begin{aligned} \log_{10} q_M &= 0 \cdot 25 \cos \theta \; (0 < \theta < \pi) \\ &\text{plus} \quad 0 \cdot 057 \, (\cos 3\theta - 1) \qquad \left(\frac{2\pi}{3} < \theta + \pi\right) \\ &\text{plus} \quad 0 \cdot 065 \, (\cos 5\theta - 1) \qquad \left(\frac{4\pi}{5} < \theta < \pi\right) \\ &\text{plus} \begin{cases} 0 \cdot 20184 & (\cos^{-1} 0 \cdot 8 < \theta < \pi) \\ -0 \cdot 62731 & (0 < \theta < \cos^{-1} 0 \cdot 8) \end{cases} \end{aligned}\right\} \quad \ldots \quad \ldots \quad \ldots \quad \ldots \quad (\text{II.1})$$

The last two numbers are determined by the necessity that the first two Fourier (cosine) constants of $\log q_M$ should be zero. The value of $q_a = q_{Ja} \, q_M$ obtained from this is shown in column 10. There is a discontinuity in velocity at $\theta = \cos^{-1} 0 \cdot 8$. Boundary-layer suction must be applied here. It will be seen that the exact configuration at the point is a "logarithmic" spiral—in construction this would be smoothed out.

The corresponding value of χ_M in degrees will be $\frac{180}{\pi} \log_e 10$ times the conjugate of (II.1). This latter is

$$0 \cdot 25 \sin \theta + 0 \cdot 057 \left[\tfrac{1}{3} \sin 3\theta + (1 - \cos 3\theta) f\left(\theta, \frac{2\pi}{3}\right) + \frac{\sqrt{3}}{2\pi} \sin \theta - \frac{\sqrt{3}}{\pi} \sin 2\theta\right]$$
$$+ 0 \cdot 065 \left[\tfrac{1}{5} \sin 5\theta + (1 - \cos 5\theta) f\left(\theta, \frac{4\pi}{5}\right) + \frac{1}{2\pi} \sin \frac{\pi}{5} \sin \theta - \frac{2}{3\pi} \sin \frac{2\pi}{5} \sin 2\theta + \frac{1}{\pi} \sin \frac{2\pi}{5} \sin 3\theta\right.$$
$$\left. - \frac{2}{\pi} \sin \frac{\pi}{5} \sin 4\theta\right] - 0 \cdot 82915 f(\theta, \cos^{-1} 0 \cdot 8), \quad \ldots \quad \ldots \quad \ldots \quad \ldots \quad \ldots \quad \ldots \quad \ldots \quad (\text{II.2})$$

where

$$f(\theta, \theta_0) = \frac{1}{\pi} \log \frac{\sin \frac{1}{2}(\theta + \theta_0)}{\sin \frac{1}{2}(\theta - \theta_0)},$$

giving

$$\begin{aligned} \chi = \chi_0 &+ 35 \cdot 8574 \sin \theta - 5 \cdot 8766 \sin 2\theta + 5 \cdot 1027 \sin 3\theta - 3 \cdot 2081 \sin 4\theta \\ &+ 1 \cdot 7151 \sin 5\theta + 7 \cdot 5199 \, (1 - \cos 3\theta) f\left(\theta, \frac{2\pi}{3}\right) \\ &+ 8 \cdot 5753 \, (1 - \cos 5\theta) f\left(\theta, \frac{4\pi}{5}\right) - 109 \cdot 3884 f(\theta, \cos^{-1} 0 \cdot 8). \quad \ldots \quad (\text{II.3}) \end{aligned}$$

This is tabulated in column 2. In column 3 is shown $\log_{10} 1/q_0$, whose antilogarithm is multiplied in columns 4 and 5 by $\cos \chi$ and $\sin \chi$ respectively, and integrated in columns 6 and 7 to give $\frac{1}{2}x$ and $\frac{1}{2}y$.

The integration is harder than before owing to the indeterminacy at the slot. It is advisable to use the following considerations from the theory of the logarithmic spiral.

The curve whose tangent makes a constant angle ϕ with the radius vector must, in polar co-ordinates r, ϑ, satisfy

$$r\frac{d\vartheta}{dr} = \tan\phi, \text{ or } \vartheta = \tan\phi \log r. \qquad \text{(II.4)}$$

Then $s = r \sec\phi$ and $\chi = \vartheta + \phi = \phi + \tan\phi \log (s \cos\phi)$. For us therefore $\tan\phi = 0{\cdot}82915 \log_e 10$; $\phi = 62{\cdot}21$. It is also true that for two values of θ at equal distances from $\cos^{-1} 0{\cdot}8$ χ is approximately the same, and hence ϑ is. Hence, the points on the aerofoil corresponding to $\cos\theta = 0{\cdot}75$, $0{\cdot}8$, $0{\cdot}85$ are approximately collinear; and the distance between the latter two is equal to $10^{0{\cdot}82915} = 6{\cdot}748$ times the distance between the former two. This enables us to carry out the integrations.

The profile shape and velocity distribution are given in Fig. 2.

TABLE 4

$\cos\theta$	1 $\log_{10}(\frac{1}{2}q_{Ja})$	2 χ (deg.)	3 $\log_{10}\left(\frac{1}{q_0}\right)$	4 $\frac{1}{q_0}\cos\chi$	5 $\frac{1}{q_0}\sin\chi$	6 $\frac{x}{2}$	7 $\frac{y}{2}$	8 X	9 Y	10 q_a
−1	0·25978	90	∞	1·0466	∞	0	0	0	0	1·8561
−0·975	0·23665	58·81	0·27165	0·9680	1·5973	0·02518	0·07031	0·0200	0·0560	1·9368
−0·95	0·18994	56·44	0·15000	0·7808	1·1771	0·04749	0·10030	0·0378	0·0799	2·0017
−0·9	0·12894	49·81	0·04083	0·7090	0·8392	0·08473	0·15015	0·0675	0·1196	2·0588
−0·8	0·05815	39·91	$\bar{1}$·14403	0·6681	0·5588	0·15358	0·21715	0·1223	0·1729	2·1090
−0·7	0·01297	34·00	$\bar{1}$·89688	0·6538	0·4410	0·21968	0·26705	0·1749	0·2126	2·1151
−0·6	$\bar{1}$·97877	29·18	$\bar{1}$·86344	0·6375	0·3560	0·28425	0·30690	0·2263	0·2444	2·1281
−0·5	$\bar{1}$·95054	24·99	$\bar{1}$·83998	0·6269	0·2922	0·34747	0·33931	0·276	0·2702	2·1301
−0·4	$\bar{1}$·92589	21·57	$\bar{1}$·82114	0·6160	0·2435	0·40961	0·36609	0·3262	0·2915	2·1319
−0·3	$\bar{1}$·90361	18·41	$\bar{1}$·80294	0·6027	0·2006	0·47055	0·38829	0·3747	0·3092	2·1453
−0·2	$\bar{1}$·88296	15·25	$\bar{1}$·78519	0·5883	0·1604	0·53010	0·40634	0·4221	0·3235	2·1668
−0·1	$\bar{1}$·86342	11·89	$\bar{1}$·76781	0·5733	0·1207	0·58818	0·42039	0·4683	0·3347	2·1943
0	$\bar{1}$·84467	8·25	$\bar{1}$·75074	0·5575	0·0808	0·64472	0·43046	0·5134	0·3428	2·2260
+0·1	$\bar{1}$·82644	+ 4·17	$\bar{1}$·73394	0·5405	+0·0394	0·69962	0·43647	0·5571	0·3475	2·2610
0·2	$\bar{1}$·80852	− 0·49	$\bar{1}$·71741	0·5217	−0·0045	0·75273	0·43822	0·5994	0·3489	2·2982
0·3	$\bar{1}$·79070	− 6·01	$\bar{1}$·70112	0·4997	−0·0526	0·80380	0·43577	0·6400	0·3470	2·3365
0·4	$\bar{1}$·77288	−12·75	$\bar{1}$·68506	0·4723	−0·1069	0·85240	0·42780	0·6787	0·3406	2·3755
0·5	$\bar{1}$·75486	−21·51	$\bar{1}$·66925	0·4344	−0·1712	0·89774	0·41390	0·7148	0·3296	2·4139
0·6	$\bar{1}$·73640	−34·12	$\bar{1}$·65368	0·3729	−0·2526	0·93810	0·39270	0·7470	0·3127	2·4506
0·7	$\bar{1}$·71720	−56·05	$\bar{1}$·63835	0·2429	−0·3607	0·96889	0·36203	0·7715	0·2883	2·4835
0·75	$\bar{1}$·70716	−78·48	1·63258	0·0857	−0·4201	0·98532	0·32297	0·7846	0·2572	2·4976
0·8	$\bar{1}$·69667	−∞	$\bar{1}$·62328 0·45243	—	—	0·98222	0·31346	0·7821	0·2496	2·5092 0·37188
0·85	$\bar{1}$·68557	−74·72	0·44499	0·7342	−2·6875	0·96078	0·24695	0·7650	0·1966	0·37307
0·9	$\bar{1}$·67345	−47·46	0·43761	1·8520	−2·0183	1·02391	0·11904	0·8153	0·0948	0·37340
0·95	$\bar{1}$·65931	−28·40	0·43031	2·3692	−1·2810	1·13446	0·04625	0·9033	0·0368	0·37200
1	$\bar{1}$·63274	0	0·42306	2·6489	0	1·25587	0	1	0	0·36013

APPENDIX III

Calculations for "Direct Design at Incidence"

The conjugate of $\log \dfrac{\cos \frac{1}{2}\theta}{\cos(\frac{1}{2}\theta - \alpha)}$ is

$$-\frac{\sin\theta}{\pi}\int_0^{\pi} \frac{\log[\cos\frac{1}{2}\phi/\cos(\frac{1}{2}\phi-\alpha)]}{\cos\theta - \cos\phi}\,d\phi \quad \ldots \quad \text{(III.1)}$$

$$= \frac{2t}{\pi(1+t^2)}\int_0^{\infty} \frac{\log(a+p)}{\dfrac{1-t^2}{1+t^2} - \dfrac{1-p^2}{1+p^2}}\cdot\frac{2dp}{1+p^2}, \quad \ldots \quad \text{(III.2)}$$

$\left[\text{where } a = \cot\alpha, p = \tan\dfrac{\phi}{2}, \text{t} = \tan\dfrac{\theta}{2}\right]$,

$$= \frac{2t}{\pi}\int_0^{\infty}\frac{\log(a+p)}{p^2-t^2}\,dp = \frac{2T}{\pi}\int_0^{\infty}\frac{\log(1+P)}{P^2-T^2}\,dP, \quad \ldots \quad \text{(III.3)}$$

where $\dfrac{p}{a} = P, \dfrac{t}{a} = T$. Call this

$$f(T) = \frac{1}{\pi}\int_0^{\infty}\left(\frac{1}{P-T} - \frac{1}{P+T}\right)\log(1+P)\,dP.$$

Then

$$f'(T) = -\frac{1}{\pi}\int_0^{\infty}\log(1+P)\ .\ d\left(\frac{1}{P-T}+\frac{1}{P+T}\right)$$

$$= \frac{1}{\pi}\int_0^{\infty}\frac{1}{1+P}\left(\frac{1}{P-T}+\frac{1}{P+T}\right)dP$$

$$= \frac{1}{\pi}\int_0^{\infty}\left[\left(\frac{1}{P-T}-\frac{1}{1+P}\right)\frac{1}{1+T} + \left(\frac{1}{1+P}-\frac{1}{P+T}\right)\frac{1}{T-1}\right]dP$$

$$= \frac{2}{\pi}\frac{\log T}{T^2-1}. \quad \ldots \quad \text{(III.4)}$$

But $f(0) = 0$, hence $f(T) = \dfrac{2}{\pi}\displaystyle\int_0^{T}\frac{\log X}{x^2-1}\,dx. \quad \ldots \quad \text{(III.5)}$

The Fourier constants are determined as follows.

$$K(\alpha) = -\int_0^{\infty}\log(a+t)\,d\left(\frac{2t}{1+t^2}\right) = \int_0^{\infty}\frac{1}{a+t}\cdot\frac{2t}{1+t^2}\,dt$$

$$= \int_0^{\infty}\left(-\frac{a}{a+t}+\frac{1+at}{1+t^2}\right)\frac{2dt}{1+a^2}$$

$$= \frac{2}{1+a^2}\left[a\log\frac{\sqrt{(1+t^2)}}{a+t} + \tan^{-1}t\right]_0^{\infty} = \frac{2}{1+a^2}\left(\frac{\pi}{2}+a\log a\right)$$

$$= \pi\sin^2\alpha + \sin 2\alpha\log\cot\alpha. \quad \ldots \quad \text{(III.6)}$$

$$-L(\alpha) = \int_0^{\pi} \log \frac{\cos \frac{1}{2}\theta}{\cos(\frac{1}{2}\theta - d)}\, d\theta = 2\int_0^{\pi/2} \log \cos\theta\, d\theta - 2\int_{-a}^{\frac{\pi}{2}-a} \log\cos\theta\, d\theta$$

$$= 2\int_0^{a} \log \tan\theta\, d\theta$$

$$= 2\int_0^{\tan a} \frac{\log x}{1+x^2}\, dx. \qquad \ldots \qquad \text{(III.7)}$$

$$F(T) = \frac{360}{\pi^2}\int_0^{T} \frac{\log x}{x^2-1}\, dx$$ is tabulated in Table 5, for $T = 0$ to 1.

For $T > 1$, the formula $F(T) = 90 - F\left(\frac{1}{T}\right)$ should be used. For very small T, interpolation became inaccurate owing to the logarithmic term and it is advisable to use the expression

$$F(x) = 83{\cdot}98823\left\{\left(\log_{10}\frac{1}{x}\right)\left(x + \frac{x^3}{3} + \frac{x^5}{5} + \ldots\right)\right.$$

$$\left. + 0{\cdot}4342945\left(x + \frac{x^3}{9} + \frac{x^5}{25} + \ldots\right)\right\}. \qquad \ldots \qquad \text{(III.8)}$$

TABLE 5

T	$F(T)$		
1	45·000	368	
0·98	44·632	376	8
0·96	44·256	384	8
0·94	43·872	392	8
0·92	43·480	401	9
0·90	43·079	408	7
0·88	42·671	418	10
0·86	42·253	427	9
0·84	41·826	437	10
0·82	41·389	447	10
0·80	40·942	458	11
0·78	40·484	468	10
0·76	40·016	480	12
0·74	39·536	491	11
0·72	39·045	504	13
0·70	38·541	517	13
0·68	38·024	530	13
0·66	37·494	544	14
0·64	36·950	559	15
0·62	36·391	575	16
0·60	35·816	590	15
0·58	35·226	608	18
0·56	34·618	625	17
0·54	33·993	644	19
0·52	33·349	664	20
0·50	32·685	340	
0·49	32·345	345	5
0·48	32·000	350	5
0·47	31·650	357	7
0·46	31·293	362	5
0·45	30·931	368	6
0·44	30·563	375	7
0·43	30·188	381	6
0·42	29·807	387	6
0·41	29·420	395	8
0·40	29·025	401	6
0·39	28·624	409	8
0·38	28·215	416	7
0·37	27·799	424	8
0·36	27·375	433	9
0·35	26·942	440	7
0·34	26·502	450	10
0·33	26·052	458	8
0·32	25·594	468	10
0·31	25·126	477	9
0·30	24·649	488	11
0·29	24·161	499	11
0·28	23·662	509	10
0·27	23·153		

T	$F(T)$		
0·27	23·153	521	
0·26	22·632	533	12
0·25	22·099	546	13
0·24	21·553	559	13
0·23	20·994	573	14
0·22	20·421	588	15
0·21	19·833	603	15
0·20	19·230	308	
0·195	18·922	312	4
0·19	18·610	317	5
0·185	18·293	321	4
0·18	17·972	325	4
0·175	17·647	331	6
0·17	17·316	335	4
0·165	16·981	340	5
0·16	16·641	346	6
0·155	16·295	351	5
0·15	15·944	357	6
0·145	15·587	363	6
0·14	15·224	369	6
0·135	14·855	375	6
0·13	14·480	382	7
0·125	14·098	388	6
0·12	13·710	396	8
0·115	13·314	404	8
0·11	12·910	412	8
0·105	12·498	419	7
0·10	12·079	429	10
0·095	11·650	438	9
0·09	11·212	448	10
0·085	10·764	458	10
0·08	10·306	469	11
0·075	9·837	481	12
0·07	9·356	494	13
0·065	8·862	508	14
0·06	8·354	523	15
0·055	7·831	539	16
0·05	7·292	557	18
0·045	6·735	577	20
0·04	6·158	600	23
0·035	5·558	625	25
0·03	4·933	656	31
0·025	4·277	693	37
0·02	3·584	739	46
0·015	2·845	800	61
0·01	2·045	896	96
0·005	1·149	1149	253
0	0		

APPENDIX IV

"Direct Design at Incidence" used to produce Fairly Thick Suction Aerofoil. Accurate Numerical Methods

In (16) and (17) we take $\alpha = \tan^{-1} \frac{1}{8}$, $\beta = 36$ deg. Then $K(\alpha) = \dfrac{\pi}{65} + \dfrac{16}{65} \log 8 = 0 \cdot 5601947$, hence $k = 0 \cdot 9530602$, and $e^k = 2 \cdot 593635$. Now χ in degrees is

$$F(T) + k \cdot \frac{180}{\pi^2} \log_e 10 \cdot [\log_{10} \sin \tfrac{1}{2} (\theta + 36 \text{ deg.}) - \log_{10} \sin \tfrac{1}{2} (\theta - 36 \text{ deg.})]. \quad .. \quad \text{(IV.1)}$$

The expression in square brackets is tabulated in Table 6, column 1. Its coefficient is evaluated as $40 \cdot 02292$. $F(T)$ was obtained as indicated in Appendix III and the resulting value of χ shown in column 2, reduced to degrees and minutes. Now

$$\frac{2}{q_0} = \frac{2 \cos (\frac{1}{2}\theta - \alpha)}{\cos \frac{1}{2}\theta} \cdot \frac{1}{S} = (\cot \alpha + \tan \tfrac{1}{2}\theta) \cdot \frac{2 \sin \alpha}{S}. \quad .. \quad .. \quad \text{(IV.2)}$$

Sin θ (cot α + tan $\frac{1}{2}\theta$) has been tabulated in column 3, and multiplied by cos χ and sin χ respectively in columns 4 and 5, to

$$\left(\frac{2 \sin \alpha}{S}\right)^{-1} \frac{dx}{d\theta} \text{ and } \left(\frac{2 \sin \alpha}{S}\right)^{-1} \frac{dy}{d\theta}. \quad .. \quad .. \quad .. \quad .. \quad \text{(IV.3)}$$

In columns 6 and 7 these two expressions are integrated up from the two ends (taking 2 deg. as the unit, instead of $180/\pi$). The method of integration was that of Whittaker and Robinson, "Calculus of Observations," page 147, except at the leading edge for x where the logarithmic singularity makes it inaccurate. Here the following easily verifiable formulae was used :—

$$\int_0^x (ay \log y + \ldots)dy = 1 \text{ Simpson} - 0 \cdot 01895\, ax^2 = 2 \text{ Simpson} - 0 \cdot 00479 ax^2$$
$$= 3 \text{ Simpson} - 0 \cdot 00214 ax^2 ;$$
$$\int_x^{3x} (ay \log y + \ldots)dy = 1 \text{ Simpson} - 0 \cdot 00326 ax^2,$$
$$\int_{3x}^{5x} = 1 \text{ Simpson} - 0 \cdot 000355 ax^2, \quad .. \quad .. \quad .. \quad .. \quad .. \quad \text{(IV.4)}$$

where "n Simpson" means the formula of Simpson's rule used with $2n + 1$ separate values of the integrand. Simpson's rule was also used near the suction slot.

At the slot itself we again employ the theory of the logarithmic spiral. We have $\phi = \tan^{-1} \dfrac{k}{\pi} + 16$ deg. 52 min. The mean value of χ at $\theta = 35$ deg. and 37 deg. is $-$ 67 deg. 21 min. The ϑ of Appendix II is then 84 deg. 13 min., and the following equation must hold :—

$$\frac{(c - 36 \cdot 501295 \,.\, 2 \cdot 593635) - 466 \cdot 54745}{54 \cdot 58371 - 18 \cdot 06961 \,.\, 2 \cdot 593635} = \cot 84 \text{ deg. } 13 \text{ min.} \quad \text{(IV.5)}$$

(remembering that the two parts of S in (IV.3) differ by a factor e^k). This gives $c = 562 \cdot 000161$, c being the chord on which the values forward of the slot in column 6 are based. The true chord is seen from (IV.3) to be

$$\frac{2 \sin \alpha}{e^l} \cdot \frac{\pi}{90} \cdot c. \quad .. \quad .. \quad .. \quad .. \quad .. \quad .. \quad .. \quad \text{(IV.6)}$$

But $\quad L(\alpha) = 2 \displaystyle\int_0^{1/8} \frac{\log (1/x)}{1 + x^2}\, dx$ is found to be $0 \cdot 766715$, so $l = \dfrac{k}{5} + \dfrac{L(\alpha)}{\pi} = 0 \cdot 434665$.

Hence $\quad e^l = 1 \cdot 5445$. But $C_L = 8\pi \sin \alpha/\text{chord} = \dfrac{4 \,.\, e^l \,.\, 90}{c} = 0 \cdot 98936$. .. (IV.7)

The final values of X and Y, reduced with respect to the chord, are given in Table 6, columns 8 and 9. It is seen that the aerofoil is $34 \cdot 0$ per cent. thick and has the suction slot at 83 per cent. chord. Its shape is shown in Fig. 3.

TABLE 6

θ (deg.)	1 $\log_{10}\sin\frac{1}{2}(\theta+36 \text{ deg.}) - \log_{10}\sin\frac{1}{2}(\theta-36 \text{ deg.})$	2 χ	3 $(8+\tan\frac{1}{2}\theta)\times\sin\theta$	4 $\therefore\cos\chi$	5 $\therefore\sin\chi$	6 x	7 y	8 X	9 Y
180	0	90°	2	0	2	0	0	0	0
179	0·0024629	80° 33·82′	2·1394662	0·3507687	2·1105158	—	—	—	—
178	0·0049262	74° 36·29′	2·2785870	0·6049074	2·1968263	0·331294	2·10648	0·000589	0·003748
177	0·0073904	69° 54·11′	2·4173192	0·8307282	2·2701173	—	—	—	—
176	0·0098558	65° 58·49′	2·5556168	1·0404885	2·3342153	1·159309	4·37507	0·002063	0·007785
172	0·0197382	54° 36·58′	3·1036528	1·7974607	2·5301456	3·919042	9·22845	0·006973	0·016421
168	0·0296742	46° 58·13′	3·6414413	2·4849053	2·6618302	8·300481	14·42954	0·014770	0·025675
164	0·0396913	41° 16·54′	4·1663612	3·1312054	2·7484760	13·667136	19·84659	0·024319	0·035314
160	0·0498179	36° 46·36′	4·6758532	3·7454379	2·7991598	20·803673	25·39979	0·037017	0·045195
156	0·0600837	33° 3·70′	5·1674380	4·3307466	2·8190514	28·884614	31·02285	0·051396	0·055201
152	0·0705203	29° 54·48′	5·6387205	4·8877957	2·8115157	38·107911	36·65779	0·067808	0·065227
148	0·0811612	27° 9·75′	6·0874026	5·4160558	2·7789949	48·416654	42·25230	0·086151	0·075182
144	0·0920424	24° 43·48′	6·5112995	5·9143970	2·7234044	59·752213	47·75842	0·106321	0·084979
140	0·1032033	22° 31·41′	6·9083452	6·3813939	2·6463273	72·053358	53·13161	0·128209	0·094540
136	0·1146868	20° 30·43′	7·2766071	6·8154769	2·5491737	85·255848	58·33036	0·151701	0·103791
132	0·1265408	18° 38·16′	7·6142890	7·2150551	2·4331818	99·292263	63·31575	0·176677	0·112661
128	0·1388187	16° 52·78′	7·9197479	7·5785390	2·2996152	114·091997	68·05119	0·203011	0·121087
124	0·1515802	15° 12·82′	8·1914938	7·9044139	2·1519062	129·581337	72·50554	0·230572	0·129013
120	0·1648935	13° 37·06′	8·4282032	8·1912738	1·9843513	145·683636	76·64444	0·259223	0·136370
116	0·1788366	12° 4·47′	8·6287230	8·4378246	1·8049856	162·319237	80·43584	0·288824	0·143124
112	0·1934996	10° 34·15′	8·7920779	8·6466429	1·6126640	179·409007	83·85556	0·319233	0·149209
108	0·2089876	9° 5·21′	8·9174690	8·8055557	1·4083457	196·868671	86·87842	0·350300	0·154588
104	0·2254241	7° 37·15′	9·0042874	8·9247903	1·1938596	214·605987	89·48231	0·381861	0·159221
100	0·2429562	6° 8·82′	9·0521106	9·0000646	0·9692973	232·538223	91·64700	0·413769	0·163073
96	0·2617602	4° 39·71′	9·0607037	9·0307282	0·7364051	250·576510	93·35356	0·445866	0·166109
92	0·2820509	3° 11·08′	9·0300259	9·0160808	0·5016568	268·631596	94·59302	0·477992	0·168315
88	0·3040929	+ 1° 35·68′	8·9602269	8·9477964	+0·2519553	286·602279	95·34803	0·509968	0·169658
84	0·3366216	− 0° 21·34′	8·8516467	8·8514759	−0·0549466	304·408562	95·54595	0·541652	0·170011
80	0·3639552	− 2° 4·64′	8·7048143	8·6990935	−0·3155347	321·967641	95·17195	0·572896	0·169345
76	0·3943688	− 3° 54·27′	8·5204437	8·5006678	−0·5801885	339·175099	94·27688	0·603514	0·167752
72	0·4285918	− 5° 52·15′	8·2994350	8·2559294	−0·8486770	355·939460	92·84867	0·633344	0·165211
68	0·4676195	− 8° 0·81′	8·0428646	7·9643276	−1·1212276	372·166646	90·87408	0·662218	0·161698
64	0·5005788	− 9° 54·28′	7·7519809	7·6364400	−1·3334128	387·775315	88·42037	0·689991	0·157332
60	0·5531946	−12° 34·47′	7·4282032	7·2500281	−1·6171852	402·671152	85·47680	0·716497	0·152094
56	0·6172639	−15° 41·86′	7·0731079	6·8093001	−1·9137086	416·740293	81·94876	0·741531	0·145816
52	0·6982160	−10° 29·48′	6·6884250	6·3051247	−2·2316586	429·867011	77·80847	0·764888	0·138449
48	0·8062763	−24° 22·13′	6·2760278	5·7168852	−2·5895456	441·907522	72·99735	0·786312	0·129888
44	0·9644830	−31° 15·24′	5·8379274	4·9907023	−3·0289094	452·645840	67·40278	0·805419	0·119934
40	1·2465228	−43° 5·87′	5·3762563	3·9256784	−3·6733067	461·838844	60·67947	0·821777	0·107971
39	1·3665281	−48° 2·44′	5·1822302	3·4648541	−3·8536085	—	—	—	—
38	1·5376077	−55° 1·67′	5·1372812	2·9445786	−4·2096454	465·293769	56·79657	0·829189	0·101061
37	1·8335457	−67° 0·76′	5·0158845	1·9588413	−4·6476744	466·547446	54·58371	0·830155	0·097124
36	+∞	−∞	4·8932654	—	—	466·764958	52·43610	0·830542	0·093303
35	1·8436052	−67° 41·85′	4·7694592	1·8099936	−4·4126707	36·501295	18·06961	0·831546	0·083391
34	1·5167360	−54° 45·43′	4·6445056	2·7130796	−3·7696995	35·339370	15·93446	0·836909	0·073538
33	1·3352090	−47° 38·07′	4·5184414	3·0602911	−3·3242942	—	—	—	—
32	1·2047425	−42° 33·44′	4·3913063	3·2353696	−2·9699617	32·307768	12·69499	0·850899	0·058587
28	0·8806252	−30° 9·84′	3·8728252	3·3484087	−1·9460048	25·971342	7·83036	0·880142	0·036137
24	0·6797354	−22° 43·13′	3·3403473	3·0812713	−1·2900732	19·516850	4·84126	0·909930	0·021419
20	0·5280540	−17° 15·77′	2·7964682	2·6704968	−0·8298673	13·747111	2·54839	0·936557	0·011761
16	0·4021718	−12° 50·53′	2·2438375	2·1877093	−0·4987290	8·879485	1·23885	0·959021	0·005717
12	0·2914344	− 9° 6·52′	1·6851460	1·6638961	−0·2672551	5·022575	0·48760	0·976821	0·002250
8	0·1899002	− 5° 46·22′	1·1231167	1·1174258	−0·1129195	2·238438	0·11953	0·989670	0·000552
4	0·0937136	− 2° 43·58′	0·5604880	0·5598536	−0·0266599	0·560044	0·00533	0·997415	0·000025
0	0	0	0	0	0	0	0	1	0

APPENDIX V

Thicker Suction Aerofoil Computed (to Less Numerical Accuracy) by Direct Design at Incidence

As a second example from our doubly infinite series of suction aerofoils with step function velocity distribution on the upper surface at incidence α, we take $\alpha = \tan^{-1}\frac{1}{5}$, $\beta = \cos^{-1} 0\cdot9$.

TABLE 7

$\cos\theta$	χ (deg.)	$(\cot\alpha+\tan\frac{1}{2}\theta)\left\{\begin{matrix}e^k\\1\end{matrix}\right\}$	$\ldots\cos\chi$	$\ldots\sin\chi$	$\dfrac{xe^l}{2\sin\alpha}$	$\dfrac{ye^l}{2\sin\alpha}$	X	Y
$-0\cdot1$	90	∞	$\log\infty$	∞	0	0	0	0
$-0\cdot975$	$55\cdot29$	$13\cdot8882$	$7\cdot9082$	$11\cdot4167$	—	—	—	—
$-0\cdot95$	$46\cdot75$	$11\cdot2450$	$7\cdot7048$	$8\cdot1905$	$0\cdot4$	$0\cdot6$	$0\cdot032$	$0\cdot043$
$-0\cdot9$	$39\cdot14$	$9\cdot3589$	$7\cdot2589$	$5\cdot9075$	$0\cdot774$	$0\cdot945$	$0\cdot062$	$0\cdot076$
$-0\cdot85$	$34\cdot57$	$8\cdot5119$	$7\cdot0089$	$4\cdot8297$	$1\cdot131$	$1\cdot211$	$0\cdot091$	$0\cdot098$
$-0\cdot8$	$31\cdot09$	8	$6\cdot8509$	$4\cdot1310$	$1\cdot477$	$1\cdot435$	$0\cdot119$	$0\cdot116$
$-0\cdot7$	$25\cdot89$	$7\cdot3805$	$6\cdot6398$	$3\cdot2226$	$2\cdot152$	$1\cdot802$	$0\cdot174$	$0\cdot145$
$-0\cdot6$	$21\cdot90$	7	$6\cdot4949$	$2\cdot6109$	$2\cdot808$	$2\cdot094$	$0\cdot226$	$0\cdot169$
$-0\cdot5$	$18\cdot53$	$6\cdot7320$	$6\cdot3830$	$2\cdot1394$	$3\cdot452$	$2\cdot332$	$0\cdot278$	$0\cdot188$
$-0\cdot4$	$15\cdot52$	$6\cdot5275$	$6\cdot2895$	$1\cdot7466$	$4\cdot086$	$2\cdot526$	$0\cdot330$	$0\cdot204$
$-0\cdot3$	$12\cdot75$	$6\cdot3628$	$6\cdot2059$	$1\cdot4043$	$4\cdot171$	$2\cdot683$	$0\cdot380$	$0\cdot216$
$-0\cdot2$	$10\cdot06$	$6\cdot2247$	$6\cdot1290$	$1\cdot0885$	$5\cdot327$	$2\cdot808$	$0\cdot430$	$0\cdot226$
$-0\cdot1$	$7\cdot44$	$6\cdot1055$	$6\cdot0541$	$0\cdot7906$	$5\cdot937$	$2\cdot902$	$0\cdot471$	$0\cdot234$
0	$4\cdot76$	6	$5\cdot9793$	$0\cdot4979$	$6\cdot538$	$2\cdot966$	$0\cdot527$	$0\cdot239$
$+0\cdot1$	$+\ 1\cdot97$	$5\cdot9045$	$5\cdot9010$	$+\ 0\cdot2030$	$7\cdot132$	$3\cdot001$	$0\cdot575$	$0\cdot242$
$0\cdot2$	$-\ 1\cdot03$	$5\cdot8165$	$5\cdot8156$	$-\ 0\cdot1045$	$7\cdot718$	$3\cdot006$	$0\cdot622$	$0\cdot242$
$0\cdot3$	$-\ 4\cdot22$	$5\cdot7338$	$5\cdot7183$	$-\ 0\cdot4219$	$8\cdot295$	$2\cdot980$	$0\cdot669$	$0\cdot240$
$0\cdot4$	$-\ 8\cdot09$	$5\cdot6547$	$5\cdot5984$	$-\ 0\cdot7958$	$8\cdot861$	$2\cdot919$	$0\cdot715$	$0\cdot235$
$0\cdot5$	$-12\cdot68$	$5\cdot5773$	$5\cdot4413$	$-\ 1\cdot2243$	$9\cdot413$	$2\cdot818$	$0\cdot759$	$0\cdot227$
$0\cdot6$	$-18\cdot62$	$5\cdot5$	$5\cdot2121$	$-\ 1\cdot7561$	$9\cdot945$	$2\cdot669$	$0\cdot802$	$0\cdot215$
$0\cdot7$	$-27\cdot28$	$5\cdot4201$	$4\cdot8173$	$-\ 2\cdot4842$	$10\cdot446$	$2\cdot457$	$0\cdot842$	$0\cdot198$
$0\cdot8$	$-43\cdot28$	$5\cdot3333$	$3\cdot8827$	$-\ 3\cdot6563$	$10\cdot891$	$2\cdot150$	$0\cdot878$	$0\cdot173$
$0\cdot85$	$-61\cdot03$	$5\cdot2847$	$2\cdot5596$	$-\ 4\cdot6234$	$11\cdot052$	$1\cdot943$	$0\cdot891$	$0\cdot157$
$0\cdot9$	$-\ \infty$	$28\cdot55, 5\cdot2294$	—	—	—	—	$0\cdot893$	$0\cdot141$
$0\cdot95$	$-48\cdot27$	$28\cdot11$	$18\cdot71$	$-20\cdot98$	$c-1\cdot193$	$0\cdot629$	$0\cdot904$	$0\cdot051$
$0\cdot975$	$-29\cdot28$	$27\cdot85$	$24\cdot29$	$-13\cdot62$	$c-0\cdot620$	$0\cdot256$	$0\cdot950$	$0\cdot021$
1	0	$27\cdot24$	$27\cdot24$	0	0	0	1	0

Everything is carried through (with the smaller range of points, and taking $\cos\theta$ instead of θ as independent variable) as in Appendix IV. The greatest inaccuracy occurs in the estimation of the values of $xe^l/2\sin\alpha$ and $ye^l/2\sin\alpha$ at $\cos\theta = -0\cdot95$. Near the slot, too, the paucity of points leads to inaccuracy. By logarithmic spiral theory we obtain $c = 12\cdot4$, and hence the figures in the last two columns of Table 7. The true chord is $2c\sin\alpha/e^l$, and hence

$$C_L = 4\pi e^l/c = 1\cdot88\ .$$

The profile shape and velocity distribution are given in Fig. 4.

APPENDIX VI

Low-drag Wing with Upper Surface Velocity (at Incidence) Quite Flat up to Half Chord

We take the conditions of (19), with $\alpha = \tan^{-1} 0\cdot04$ and $\beta = \cos^{-1} 0\cdot1$. The former is chosen to give C_L approximately $0\cdot26$, the latter is chosen because it is found that for fairly thin aerofoils this point generally corresponds to half chord. (20) then gives $k = 0\cdot38234$, $e^k = 1\cdot4657$, $l = 0\cdot2106$, $e^l = 1\cdot2345$ and (22) becomes (in degrees)

$$\chi = F\left(\tfrac{1}{25}\tan\tfrac{1}{2}\theta\right) - 10\cdot255\sin\theta + 21\cdot906(\cos\theta - \cos\beta)\frac{1}{\pi}\log\frac{\sin\frac{1}{2}(\theta-\beta)}{\sin\frac{1}{2}(\theta+\beta)}\ . \quad .. \quad \text{(VI.1)}$$

This is tabulated in Table 8, column 1. In column 2 we have

$$\frac{e^l}{q_0} \sec \alpha = (1 + \tan \alpha \tan \tfrac{1}{2}\theta) \begin{Bmatrix} 1 \\ e^{k(\cos\theta - \cos\beta)} \end{Bmatrix} , \quad \ldots \quad \ldots \quad \ldots \quad \ldots \quad \text{(VI.2)}$$

so that columns 3 and 4 (obtained by multiplying this by cos χ and sin χ) give

$$\tfrac{1}{2}e^l \sec \alpha \frac{dx}{d(\cos\theta)} \text{ and } \tfrac{1}{2}e^l \sec \alpha \frac{dy}{d(\cos\theta)} .$$

Columns 5 and 6 give the integrated values of $10e^l \sec \alpha . x$ and $15e^l \sec \alpha . y$. The chord is found to be

$$\frac{45\cdot5}{10e^l \sec \alpha} \text{ so that } C_L = \frac{8\pi \,.\, 10e^l \tan \alpha}{45\cdot5} = \frac{80\pi \,.\, 1\cdot2345}{25 \,.\, 45\cdot5} = 0\cdot273 .$$

Columns 7, 8 and 9 give the final figures of shape and velocity distribution which are plotted in Fig. 5. The thickness 13 per cent. for such a C_L range is exceptionally low. But the maximum lift of the wing is unlikely to be high.

TABLE 8

cos θ	1 χ (deg.)	2 $\frac{e^l}{q_0}$ sec α	3 . . . cos χ	4 . . . sin χ	5 $10e^lx$ sec α	6 $15e^ly$ sec α	7 X	8 Y	9 q_a
−1	90	∞	∞	∞	45·5	0	0	0	1·2034
−0·9	16·05	1·17436	1·1286	0·3247	43·0607	1·716	0·054	0·0251	1·2034
−0·8	11·46	1·12000	1·0977	0·2225	40·8344	2·523	0·103	0·0370	1·2034
−0·7	8·81	1·09522	1·0823	0·1677	38·6544	3·098	0·150	0·0454	1·2034
−0·6	6·86	1·08000	1·0723	0·1290	36·4998	3·545	0·198	0·0519	1·2034
−0·5	5·25	1·06928	1·0648	0·0978	34·3627	3·880	0·245	0·0568	1·2034
−0·4	3·82	1·06110	1·0587	0·0707	32·2392	4·136	0·291	0·0606	1·2034
−0·3	2·46	1·05451	1·0535	0·0453	30·1270	4·306	0·338	0·0631	1·2034
−0·2	+1·10	1·04899	1·0488	+0·0201	28·0247	4·408	0·384	0·0646	1·2034
−0·1	−0·35	1·04422	1·0442	−0·0064	25·9317	4·425	0·430	0·0648	1·2034
0	−2·01	1·04000	1·0394	−0·0365	23·8481	4·366	0·476	0·0640	1·2034
+0·1	−4·50	1·03618	1·0330	−0·0813	21·7757	4·192	0·521	0·0614	1·2034
0·2	−6·85	1·07283	1·0652	−0·1280	19·6775	3·876	0·568	0·0568	1·1582
0·3	−8·09	1·11108	1·1000	−0·1564	17·5123	3·442	0·615	0·0504	1·1148
0·4	−8·85	1·15077	1·1371	−0·1770	15·2752	2·946	0·664	0·0432	1·0745
0·5	−9·08	1·19221	1·1772	−0·1882	12·9609	2·389	0·715	0·0350	1·0327
0·6	−8·96	1·23491	1·2198	−0·1923	10·5639	1·823	0·768	0·0267	0·9940
0·7	−8·41	1·27893	1·2652	−0·1870	8·0307	1·245	0·824	0·0182	0·9567
0·8	−7·34	1·32432	1·3134	−0·1692	5·4521	0·714	0·880	0·0105	0·9208
0·9	−5·46	1·37026	1·3640	−0·1304	2·7747	0·267	0·939	0·0039	0·8863
1	0	1·41070	1·4107	0	0	0	1	0	0·8530

APPENDIX VII

Thicker Version of the Aerofoil of Appendix VI

Taking everything as in Appendix VI except that cot $\alpha = 14$ instead of 25, we obtained the following values of X, Y, q_a :—

They are plotted in Fig. 6. The aerofoil is found to be 19·2 per cent. thick and has a C_L range of 0·508.

TABLE 9

$\cos\theta$	X	Y	q_a
-1	0	0	1·376
$-0·9$	0·051	0·0368	1·376
$-0·8$	0·100	0·0543	1·376
$-0·7$	0·147	0·0666	1·376
$-0·6$	0·194	0·0763	1·376
$-0·5$	0·240	0·0836	1·376
$-0·4$	0·285	0·0893	1·376
$-0·3$	0·331	0·0930	1·376
$-0·2$	0·375	0·0954	1·376
$-0·1$	0·420	0·0960	1·376
0	0·464	0·0950	1·376
$+0·1$	0·508	0·0915	1·376
0·2	0·552	0·0852	1·300
0·3	0·599	0·0761	1·228
0·4	0·648	0·0656	1·160
0·5	0·699	0·0536	1·095
0·6	0·753	0·0411	1·035
0·7	0·809	0·0281	0·977
0·8	0·869	0·0160	0·923
0·9	0·933	0·0053	0·872
1	1	0	0·823

APPENDIX VIII

Thin Aerofoil with High Maximum Lift, obtained by Forward Suction

Dr. Goldstein's idea was that an ordinary thin aerofoil at a high C_L (above the stall) has a (theoretical) velocity distribution with a very high peak near the leading edge, followed by a more gradual decline over the main part of the chord. The rear side of this peak possesses a very steep adverse velocity gradient, which is the cause of the breakaway associated with stalling. But if the drop from the summit to the foothills is replaced by a sheer precipice, by a discontinuity in fact where the boundary layer is sucked away, and the remainder of the velocity curve given an even declivity down to the trailing edge, it is to be hoped (i) that breakaway will be avoided (ii) that the thickness will not be too much increased.

We may approximate to this new velocity distribution with the formula (23) of the main paper, if β is taken near to π.

At first $\alpha = \tan^{-1}\frac{1}{3}$ was taken (corresponding to $C_L \simeq 2·3$). With $\beta = 160$ deg. equations (24) give

$$\left.\begin{aligned} b &= 0·60609 - 0·16448a, \\ c &= 0·95553 - 0·32235a. \end{aligned}\right\} \quad \ldots \quad \text{(VIII.1)}$$

Now $q_0 = S\dfrac{\cos\frac{1}{2}\theta}{\cos(\frac{1}{2}\theta - \alpha)}$, and this is zero at $\theta = \pi$, rises up to a sharp peak at $\theta = \beta$, drops suddenly and begins to rise again, attaining a maximum around $\theta = 120$ deg. or so, and then falling off down to the trailing edge. The value of the peak at β is

$$e^a = \frac{\cos\frac{1}{2}\beta}{\cos(\frac{1}{2}\beta - \alpha)} = 0·3647e^a \quad \ldots \quad \text{(VIII.2)}$$

in our case. It is soon seen on inspection that the absolute maximum of q_0 will be least when a is so chosen that the two local maxima are equal. By trial and error it is found that this least maximum of q_0 occurs when $a = 1·271$ and its value is $1·3$. But of course an aerofoil whose maximum velocity at zero C_L at $1 \cdot 3$ times the velocity at infinity cannot be called a thin aerofoil, and nothing can be gained by drawing it out.

To reduce this the slot was moved forward to $\beta = 170$ deg. This altered (VIII.1) and (VIII.2) to

$$\left.\begin{aligned} b &= 0 \cdot 50470 - 0 \cdot 06658a, \\ c &= 0 \cdot 75891 - 0 \cdot 13248a. \end{aligned}\right\} \quad \text{Peak of } q_0 = 0 \cdot 21917 e^a \; . \qquad \ldots \qquad \ldots \text{(VIII.3)}$$

Under these conditions the least maximum is found to be $1 \cdot 27$, only a slight reduction.

It is therefore necessary to aim for a lower C_L, and our final aerofoil was designed with $\alpha = \tan^{-1} \frac{1}{8}$ and $\beta = 170$ deg. We have then

$$\left.\begin{aligned} b &= 0 \cdot 28392 - 0 \cdot 06658a, \\ c &= 0 \cdot 43597 - 0 \cdot 13248a. \end{aligned}\right\} \quad \text{Peak of } q_0 = 0 \cdot 41497 e^a \; . \qquad \ldots \qquad \ldots \text{(VIII.4)}$$

The least maximum of q_0 is $1 \cdot 19$, which gives $a = 1 \cdot 05352$, $b = 0 \cdot 21378$, $c = 0 \cdot 29640$. We have by (25)

$$\chi = (0 \cdot 83974 + 0 \cdot 29640 \cos \theta) \frac{1}{\pi} \log \frac{\sin \frac{1}{2} (\theta - 170 \text{ deg.})}{\sin \frac{1}{2} (\theta + 170 \text{ deg.})}$$

$$- 0 \cdot 27993 \sin \theta + F (\tfrac{1}{8} \tan \tfrac{1}{2} \theta) \ldots \qquad \ldots \qquad \ldots \qquad \ldots \qquad \ldots \text{(VIII.5)}$$

In degrees it can be written

$$\chi = (35 \cdot 264 + 12 \cdot 447 \cos \theta) (\log_{10} \sin \tfrac{1}{2} (\theta - 170 \text{ deg.})$$

$$- \log_{10} \sin \tfrac{1}{2} (\theta + 170 \text{ deg.})) - 16 \cdot 039 \sin \theta + F (\tfrac{1}{8} \tan \tfrac{1}{2} \theta) \; . \quad \text{(VIII.6)}$$

Table 10, columns 1–4 give auxiliary functions for the tabulation of χ which is carried out in column 5. Column 6 gives

$$\frac{e^a \sec \alpha}{q_0} \sin \theta = (1 + \tfrac{1}{8} \tan \tfrac{1}{2} \theta) \sin \theta \left\{ \frac{1}{e^{(a - b)} + \cos \theta} \right\} , \qquad \ldots \qquad \ldots \qquad \ldots \qquad \ldots \text{(VIII.7)}$$

the exponential being calculated as antilog ($0 \cdot 010432$ col. 4). In columns 7 and 8 this is multiplied by cos χ and sin χ respectively and in columns 9 and 10 integrated by Simpson's rule to give

$$\frac{27}{\pi} e^a \sec \alpha \left\{ \frac{x}{c - x} \right\} \text{ and } \frac{27}{\pi} e^a \sec \alpha \, . \, y \quad \ldots \quad \ldots \qquad \ldots \qquad \ldots \qquad \ldots \text{(VIII.8)}$$

respectively. Logarithmic spiral theory $\left(\text{with } \phi = \tan^{-1} \dfrac{a - (b - c \cos \beta)}{\pi} = 9 \cdot 89 \text{ deg.}\right)$ now gives $c = 92 \cdot 584$, yielding the reduced values of X and Y in columns 11 and 12. The true chord is

$$92 \cdot 584 \, . \frac{\pi}{27} \, . \, e^{-a} \cos \alpha \qquad \ldots \qquad \ldots \qquad \ldots \qquad \ldots \qquad \ldots \qquad \ldots \text{(VIII.9)}$$

and we deduce

$$C_L = \frac{8\pi \sin \alpha}{\text{chord}} = \frac{27 e^a}{92 \cdot 584} = 0 \cdot 836 \; . \qquad \ldots \qquad \ldots \qquad \ldots \qquad \ldots \qquad \ldots \text{(VIII.10)}$$

Finally q_a is tabulated in column 13, and the shape and velocity distribution at incidence plotted in Fig 7.

TABLE 10

	1	2	3	4	5	6	7	8	9	10	11	12	13
θ (deg.)	log sin $\frac{1}{2}$ (θ+170 deg.) —log sin $\frac{1}{2}$ (θ—170 deg.)	$\frac{1}{8}\tan\frac{1}{2}\theta$	F	$35{\cdot}264 + 12{\cdot}447 \cos\theta$	χ (deg.)	$\dfrac{e^{a}\sec\alpha}{q_0}\sin\theta$	$\ldots\cos\chi$	$\ldots\sin\chi$	$\dfrac{27}{\pi}e^{a}\sec\alpha\begin{Bmatrix}x\\ c-x\end{Bmatrix}$	$\dfrac{27}{\pi}e^{a}\sec\alpha\cdot y$	X	Y	q_a
180	0	∞	90	22·817	90·00	0·2500	0	0·2500	0	0	0	0	2·8677
177·5	0·22130	5·729	72·383	22·824	66·63	0·2935	0·1164	0·2694	0·045	0·196	0·0005	0·0021	2·8677
175	0·47602	2·863	63·090	22·864	50·81	0·3367	0·2128	0·2610	0·170	0·397	0·0018	0·0043	2·8677
172·5	0·84345	1·9071	56·509	22·923	35·08	0·3795	0·3106	0·2181	0·365	0·579	0·0039	0·0063	2·8677
170		1·4287	51·461	23·006	—	—	—	—	—	—	0·0075	0·0073	1·6581
167·5	0·95149	1·14137	47·410	23·112	21·95	0·8036	0·7453	0·3004	91·307	0·849	0·0138	0·0092	1·6539
165	0·69566	0·94944	44·053	23·241	23·73	0·8775	0·8033	0·3531	90·727	1·097	0·0201	0·0118	1·6489
162·5	0·56040	0·81214	41·214	23·393	23·28	0·9512	0·8738	0·3759	—	—	—	—	—
160	0·47270	0·70891	38·765	23·568	22·14	1·0245	0·9490	0·3769	89·415	1·655	0·0342	0·0179	1·6361
150	0·29438	0·46651	31·525	24·485	16·30	1·3136	1·2608	0·3687	86·103	2·794	0·0700	0·0302	1·6007
140	0·21295	0·34343	26·653	25·729	10·80	1·5936	1·5651	0·3003	81·858	3·807	0·1159	0·0411	1·5540
130	0·16492	0·26806	23·052	27·263	6·27	1·8593	1·8482	0·2031	76·733	4·567	0·1712	0·0493	1·4982
120	0·13264	0·21663	20·223	29·040	+ 2·48	2·1040	2·1020	+0·0910	70·798	5·011	0·2353	0·0541	1·4362
110	0·10910	0·17852	17·876	31·007	— 0·58	2·3174	2·3173	—0·0235	64·160	5·110	0·3070	0·0552	1·3704
100	0·09090	0·14897	15·870	33·102	— 2·93	2·4889	2·4085	—0·1272	56·941	4·880	0·3850	0·0527	1·3038
90	0·07618	0·12500	14·098	35·264	— 4·63	2·6053	2·5968	—0·2103	49·303	4·368	0·4675	0·0472	1·2383
80	0·06387	0·10489	12·489	37·425	— 5·70	2·6529	2·6398	—0·2635	41·429	3·648	0·5525	0·0394	1·1763
70	0·05328	0·08753	10·992	39·521	— 6·19	2·6191	2·6038	—0·2824	33·544	2·821	0·6377	0·0305	1·1189
60	0·04392	0·07217	9·566	41·487	— 6·15	2·4938	2·4794	—0·2672	25·894	1·988	0·7203	0·0215	1·0658
50	0·03546	0·05829	8·177	43·265	— 5·64	2·2715	2·2605	—0·2232	18·762	1·247	0·7974	0·0135	1·0235
40	0·02766	0·04550	6·791	44·799	— 4·76	1·9530	1·9461	—0·1621	12·427	0·666	0·8658	0·0072	0·9868
30	0·02036	0·03349	5·372	46·043	— 3·58	1·5469	1·5439	—0·0966	7·173	0·278	0·9225	0·0030	0·9580
20	0·01340	0·02204	3·871	46·960	— 2·24	1·0695	1·0687	—0·0418	3·236	0·076	0·9650	0·0008	0·9373
10	0·00665	0·01094	2·201	47·522	— 0·90	0·5420	0·5419	—0·0085	—	—	—	—	—
0	0	0	0	47·711	0	0	0	0	0	0	1	0	0·9207

The thickness is found to be 11 per cent. The minimum of dq_a/dx is just over -1. It is generally found that an adverse velocity gradient of this magnitude does not produce separation.

This aerofoil was the prototype of a large series of aerofoils (mostly cambered) with leading-edge suction. These are discussed in a forthcoming report. The latest ones have (according to theory) most excellent characteristics for high-speed flight.

APPENDIX IX

The Obtaining of a Leading-edge Radius of Curvature in the Method of Direct Design at Incidence

(29) is equivalent to the choice of $\log q_0$ as

$$\log \frac{\cos \frac{1}{2}\theta}{\cos (\frac{1}{2}\theta - \alpha)} + \log S + \left\{ \begin{array}{ll} \dfrac{\sin n(\pi - \theta) - 1}{2n \tan \alpha} & \left(\theta = \pi - \dfrac{\pi}{2n} \text{ to } \pi\right) \\ 0 & \left(\theta = 0 \text{ to } \pi - \dfrac{\pi}{2n}\right) \end{array} \right\} . \qquad \text{(IX.1)}$$

χ is the conjugate of this. Now the conjugate of the last term is

$$-\frac{\sin \theta}{\pi} \int_{\pi - \pi/2n}^{\pi} \frac{\sin n(\pi - t) - 1}{2n \tan \alpha} \frac{dt}{\cos \theta - \cos t} . \qquad \text{(IX.2)}$$

Writing $\pi - \theta$ for θ, we find that the conjugate is proportional to

$$I = \sin \theta \int_0^{\pi/2n} \frac{1 - \sin nt}{\cos \theta - \cos t} dt . \qquad \text{(IX.3)}$$

We use two asymptotic formulae for this expression, when n is fairly large: Firstly, when θ is large compared with $\pi/2n$ it approximates to

$$\frac{\sin \theta}{\cos \theta - 1} \int_0^{\pi/2n} (1 - \sin nt)\, dt = -\frac{\pi - 2}{2n} \cot \frac{\theta}{2} \qquad \text{(IX.4)}$$

and when θ is small compared with $\pi/2n$ we proceed as follows:—

If $I^* = \displaystyle\int_0^{\pi/2n} \frac{\sin n\theta \sin t - \sin \theta \sin nt}{\cos \theta - \cos t} dt$, then the derivative of the integrand with respect to θ is

$$\frac{(\cos \theta - \cos t)(n \cos n\theta \sin t - \cos \theta \sin nt) + \sin \theta (\sin n\theta \sin t - \sin \theta \sin nt)}{(\cos \theta - \cos t)^2} \qquad \text{(IX.5)}$$

and so

$$\left[\frac{dI^*}{d\theta}\right]_{\theta = 0} = \int_0^{\pi/2n} \frac{n \sin t - \sin nt}{1 - \cos t} dt \simeq \int_0^{\pi/2n} \frac{nt - \sin nt}{\frac{1}{2}t^2} dt$$

$$= 2n \int_0^{\pi/2} \frac{u - \sin u}{u^2} du = 0 \cdot 38718n . \qquad \text{(IX.6)}$$

But

$$I = I^* + \int_0^{\pi/2n} \frac{\sin\theta - \sin n\theta \sin t}{\cos\theta - \cos t}\,dt$$

$$= I^* + \log \frac{\sin \frac{1}{2}\left(\dfrac{\pi}{2n} - \theta\right)}{\sin\frac{1}{2}\left(\theta + \dfrac{\pi}{2n}\right)} - \sin n\theta \log \frac{\cos\theta - \cos\dfrac{\pi}{2n}}{1 - \cos\theta}$$

$$\simeq 0\cdot38718 n\theta - \cot\frac{\pi}{4n} - n\theta \log \frac{1 - \cos\dfrac{\pi}{2n}}{\frac{1}{2}\theta^2} \text{ as } \theta \to 0,$$

$$\simeq \left(0\cdot38718 - \frac{4}{\pi}\right) n\theta - 2n\theta \log \frac{\pi}{2n\theta}\,. \qquad \text{(IX.7)}$$

Now the conjugate of the first term of (IX.1) is

$$\frac{2}{\pi}\int_0^{\tan\alpha\tan\frac{1}{2}\theta} \frac{\log x}{x^2 - 1}\,dx = \frac{\pi}{2} - \frac{2}{\pi}\int_0^{\cot\alpha\cot\frac{1}{2}\theta} \frac{\log x}{x^2 - 1}\,dx, \qquad \text{(IX.8)}$$

and for $\theta = \pi - \delta$, δ small, this approximates to

$$\frac{\pi}{2} - \frac{2}{\pi}\left(\frac{\delta}{2}\cot\alpha\right)\left(\log\frac{2}{\delta\cot\alpha} + 1\right)\,. \qquad \text{(IX.9)}$$

Hence this, added to (IX.2), gives

$$\frac{\pi}{2} - \frac{\delta\cot\alpha}{\pi}\log\frac{2e}{\delta\cot\alpha} - \frac{1}{2\pi n\tan\alpha}\left[\left(0\cdot38718 - \frac{4}{\pi}\right)n\delta - 2n\delta\log\frac{\pi}{2n\delta}\right] \qquad \text{(IX.10)}$$

$$= \frac{\pi}{2} - \delta\cot\alpha\left[\frac{1}{\pi}\log\frac{2e}{\delta\cot\alpha} + \frac{0\cdot38718 - 4\pi^{-1}}{2\pi} - \frac{1}{\pi}\log\frac{\pi}{2n\delta}\right]$$

$$= \frac{\pi}{2} - \delta\cot\alpha\left[\frac{1}{\pi}\log\frac{4ne}{\pi\cot\alpha} - 0\cdot14102\right]$$

$$= \frac{\pi}{2} - \delta\cot\alpha\left[0\cdot25418 + \log(n\tan\alpha)\right]\,. \qquad \text{(IX.11)}$$

It is observed that the $\delta \log \frac{1}{\delta}$ term, which was producing the zero radius of curvature, has gone out owing to our new measures.

The actual value of χ near the leading edge has an extra term due to the conjugate of log S (*see* (IX.1)), which will vary according to the type of aerofoil chosen. This will *increase* the quantity in square brackets, but it is found that it does so by only a small amount, which we will here write A. Then

$$\left[\frac{d\chi}{d\theta}\right]_{\theta=\pi} = \cot\alpha\,(0\cdot25418 + \log(n\tan\alpha)) + A\,. \qquad \text{(IX.12)}$$

On the other hand

$$\frac{ds}{d\theta} = \frac{2}{q_0}\sin\theta = 4\sin\tfrac{1}{2}\theta\cos(\tfrac{1}{2}\theta - \alpha)\frac{1}{S}e^{\frac{1 - \sin n(\pi - \theta)}{2n\tan\alpha}}$$

$$= \frac{4\sin\alpha}{Q}e^{\frac{\cot\alpha}{2n}} \text{ at } \theta = \pi, \qquad \text{(IX.13)}$$

where Q is the maximum velocity at incidence α. Hence ϱ_L, the radius of curvature at the leading edge, is given by

$$\varrho_L = \left[\frac{ds}{d\chi}\right]_{\theta=\pi} = \frac{4\sin^2\alpha\, e^{\frac{\cot\alpha}{2n}}}{Q\cos\alpha\,(0\cdot25418 + \log(n\tan\alpha) + A)}\,. \qquad \text{(IX.14)}$$

It is customary to refer ϱ_L to the chord of the aerofoil, which is rather under 4. Clearly a rough approximation to ϱ_L/c is $\dfrac{\alpha^2}{\log(1{\cdot}2906\, n \tan\alpha)}$, $1{\cdot}2906$ being $e^{0{\cdot}25418}$.

For $n < \dfrac{\cot\alpha}{1{\cdot}2906} = 0{\cdot}7748 \cot\alpha$, ϱ_L is negative and the leading edge is concave, giving an unevenness of surface which is very likely to produce turbulence in the boundary layer and is quite inacceptable. To obtain a large positive ϱ_L, it is necessary to take n just greater than $0{\cdot}7748 \cot\alpha$, say the next or next but one integer.

APPENDIX X

Low-drag Wing as in Appendix VI, but with Leading-edge Radius of Curvature

We take $\alpha = \tan^{-1} 0{\cdot}04$ and $\beta = \cos^{-1} 0{\cdot}1$ as in Appendix VI, but now we have (IX.1) holding, which becomes

$$\log q_0 = \log \frac{\cos \frac{1}{2}\theta}{\cos(\frac{1}{2}\theta - \alpha)} + \left\{ \begin{array}{ll} l & (\beta < \theta < \pi) \\ l - k(\cos\theta - \cos\beta) & (0 < \theta < \beta) \end{array} \right\}$$
$$+ \left\{ \begin{array}{ll} \dfrac{\sin n(\pi - \theta) - 1}{2n \tan\alpha} & \left(\pi - \dfrac{\pi}{2n} < \theta < \pi\right) \\ 0 & \left(0 < \theta < \pi - \dfrac{\pi}{2n}\right) \end{array} \right\} \quad \ldots \quad \ldots \quad \ldots \quad (X.1)$$

The conditions (7) become

$$\left. \begin{array}{r} l\pi - k(\sin\beta - \beta\cos\beta) - L(\alpha) - \dfrac{\pi - 2}{4n^2 \tan\alpha} = 0, \\ -k(\frac{1}{2}\beta - \frac{1}{4}\sin 2\beta) - K(\alpha) + \dfrac{1}{2n\tan\alpha}\left(\dfrac{n^2}{n^2 - 1}\sin\dfrac{\pi}{2n} - \dfrac{n}{n^2 - 1}\right) = 0. \end{array} \right\} \quad \ldots \quad \ldots \quad (X.2)$$

n must be taken just greater than $0{\cdot}7748 \,.\, 25 = 19{\cdot}37$. We choose $n = 20$. Then (X.2) gives $k = 0{\cdot}40835$, $l = 0{\cdot}22328$, $e^l = 1{\cdot}2502$.

We take for our points those defined by $\cos\theta = 1, 0{\cdot}9, 0{\cdot}8, \ldots, -0{\cdot}8, -0{\cdot}9, -0{\cdot}925, -0{\cdot}95, -0{\cdot}975, -1$. For all these except the last we use the approximation (IX.4) for the conjugate of $1 - \sin nt$. This leads to the expression

$$\chi = F(0{\cdot}04 \tan \tfrac{1}{2}\theta) + 23{\cdot}397 (\cos\theta - \cos\beta) \frac{1}{\pi} \log_e \frac{\sin \frac{1}{2}(\theta - \beta)}{\sin \frac{1}{2}(\theta + \beta)}$$
$$- 10{\cdot}952 \sin\theta + 0{\cdot}32531 \tan \tfrac{1}{2}\theta \,, \quad \ldots \quad \ldots \quad \ldots \quad \ldots \quad (X.3)$$

which is tabulated in Table 11, column 3. The expression

$$\frac{e^l \sec\alpha}{q_0} = (1 + 0{\cdot}04 \tan \tfrac{1}{2}\theta) \left\{ \begin{array}{ll} 1 & \left(\dfrac{39\pi}{40} > \theta > \beta\right) \\ \text{antilog}\,(0{\cdot}17734 (\cos\theta - \cos\beta)) & (\beta > \theta > 0) \end{array} \right\}$$

is given in column 4, and multiplied by $\cos\chi$ and $\sin\chi$ in columns 5 and 6. By the formulae of Appendix IX we have

$$\left[\frac{d\chi}{d\theta}\right]_{\theta = \pi} = 25\,(0{\cdot}03104) + 0{\cdot}40835 - 0{\cdot}40835 \,.\, 1{\cdot}1 \frac{\beta}{\pi} \frac{1}{\pi} \,.\, \tan \tfrac{1}{2}\beta$$
$$= 0{\cdot}99415 \,. \quad \ldots \quad \ldots \quad \ldots \quad \ldots \quad \ldots \quad \ldots \quad \ldots \quad (X.4)$$

But $$\left[\frac{ds}{d\theta}\right]_{\theta=\pi} = 4 \sin \alpha \, e^{\frac{1}{2n \tan \alpha} - l} - 0\cdot 23888, \text{ giving}$$

$$\varrho_L = \left[\frac{ds}{d\chi}\right]_{\theta=\pi} = 0\cdot 24029. \text{ Also the value of } \frac{e^l \sec \alpha}{q_0} \cos \chi \text{ at}$$

$$\theta = \pi \text{ is } \lim_{\delta \to 0} \frac{0\cdot 08}{\delta} e^{\frac{1}{2n \tan \alpha}} \left[\frac{d\chi}{d\theta}\right]_{\theta=\pi} \delta = e^{0\cdot 625}\, 0\cdot 08 \,.\, 0\cdot 99415 = 0\cdot 1486.$$

This value is very small compared with the other terms in column 5, and leads to a difficulty in the estimation of the first term of column 7 (columns 7 and 8 are obtained by integrating columns 5 and 6 from $\theta = \delta$ upwards by Simpson's rule, assisted at certain points by the cubic 1 : 3 : 3 : 1 rule). The value 68·1 is probably correct to 3 figures but it is difficult to see how more accuracy could be obtained, short of taking many more points and using a better formula than (IX.4) at some of them. By taking n greater, say 28, the value at $\theta = \pi$ could be made nearer the others, but the uncertainty would remain and ϱ_L be far smaller.

The final aerofoil is seen to be 14·1 per cent. thick. The true chord is $\dfrac{68\cdot 1 \cos \alpha}{15 e^l} = 3\cdot 63$, $\dfrac{\varrho_L}{\text{chord}} = 0\cdot 0662$, and the C_L range is $\dfrac{8\pi \sin \alpha}{3\cdot 63} = 0\cdot 277$. The shape and velocity distribution are plotted in Fig. 8.

TABLE 11

	1	2	3	4	5	6	7	8	9	10	11
$\cos\theta$	$0\cdot 04 \tan \frac{1}{2}\theta$	F	χ (deg.)	$\dfrac{e^l \sec \alpha}{q_0}$	$\ldots \cos\chi$	$\ldots \sin\chi$	$\dfrac{15e^l}{\cos\alpha}(c-x)$	$\dfrac{15e^l}{\cos\alpha} y$	X	Y	q_α
−1	∞	90·000	90·00	∞	0·1486	∞	68·1	0	0	0	0·6692
−0·975	0·35553	27·183	29·28	1·35553	1·1823	0·6630	67·407	0·887	0·0102	0·0130	1·2502
−0·95	0·24980	22·088	22·98	1·24980	1·1506	0·4879	66·534	1·312	0·0230	0·0193	1·2502
−0·925	0·20265	19·391	19·63	1·20265	1·1328	0·4040	65·678	1·642	0·0356	0·0241	1·2502
−0·9	0·17436	17·605	17·38	1·17436	1·1207	0·3508	64·833	1·925	0·0480	0·0283	1·2502
−0·8	0·12000	13·710	12·28	1·12000	1·0944	0·2382	61·515	2·788	0·0967	0·0409	1·2502
−0·7	0·09522	11·669	9·39	1·09522	1·0805	0·1787	58·255	3·407	0·1446	0·0500	1·2502
−0·6	0·08000	10·306	7·28	1·08000	1·0713	0·1369	55·027	3·878	0·1920	0·0569	1·2502
−0·5	0·06928	9·286	5·55	1·06928	1·0643	0·1034	51·825	4·237	0·2390	0·0622	1·2502
−0·4	0·06110	8·467	3·99	1·06110	1·0585	0·0738	48·640	4·503	0·2858	0·0661	1·2502
−0·3	0·05451	7·779	2·54	1·05451	1·0535	0·0467	45·473	4·682	0·0323	0·0688	1·2502
−0·2	0·04899	7·181	+ 1·08	1·04899	1·0488	+0·0198	42·319	4·783	0·3786	0·0702	1·2502
−0·1	0·04422	6·646	− 0·46	1·04422	1·0442	−0·0084	39·180	4·800	0·4247	0·0705	1·2502
0	0·04000	6·158	− 2·24	1·04000	1·0392	−0·0407	36·054	4·728	0·4706	0·0694	1·2502
+0·1	0·03618	5·702	− 4·90	1·03618	1·0324	−0·0885	32·946	4·540	0·5162	0·0667	1·2502
0·2	0·03266	5·269	− 7·42	1·0757	1·0667	−0·1389	29·799	4·200	0·5624	0·0617	1·2002
0·3	0·02935	4·849	− 8·73	1·1169	1·1040	−0·1695	26·543	3·727	0·6102	0·0547	1·1522
0·4	0·02619	4·436	− 9·48	1·1599	1·1441	−0·1910	23·173	3·192	0·6597	0·0469	1·1061
0·5	0·02309	4·017	− 9·78	1·2046	1·1871	−0·2046	19·676	2·589	0·7111	0·0380	1·0619
0·6	0·02000	3·584	− 9·65	1·2510	1·2333	−0·2097	16·047	1·973	0·7644	0·0290	1·0193
0·7	0·01680	3·116	− 9·07	1·2991	1·2828	−0·2048	12·273	1·340	0·8198	0·0197	0·9785
0·8	0·01333	2·587	− 7·91	1·3486	1·3357	−0·1856	8·347	0·759	0·8774	0·0111	0·9394
0·9	0·00918	1·906	− 5·88	1·3991	1·3917	−0·1433	4·255	0·250	0·9375	0·0037	0·9018
1	0	0	0	1·4441	1·4441	0	0	0	1	0	0·8658

APPENDIX XI

Cambered Suction Aerofoil with Incidence Range 0 to 20 deg.

We take $\log q_0$ as in (30), with $\alpha = 20$ deg., $\beta_1 = \alpha = 20$ deg., and β_2 (in virtue of (34)) $= 64 \cdot 30$ deg. Then

$$\left.\begin{aligned} k = \frac{\pi \sin 20 \text{ deg.}}{1 - \cos 84 \cdot 30 \text{ deg.}} = 1 \cdot 19298,\ e^k = 3 \cdot 2969\ , \\ k \cdot \frac{180}{\pi^2} \log_e 10 = 50 \cdot 098,\ \tan \tfrac{1}{2}\alpha = 0 \cdot 17633\ . \end{aligned}\right\} \quad \ldots \quad \ldots \quad \text{(XI.1)}$$

Hence χ, in degrees, has the form

$$F\,(0 \cdot 17633 \tan \tfrac{1}{2}|\vartheta|) + 50 \cdot 098 \log_{10} \frac{\sin \frac{1}{2}\theta}{\sin \frac{1}{2}(\vartheta + 84 \cdot 30 \text{ deg.})} + \text{const.}$$

$$= \text{F}\,(0 \cdot 17633 \tan \tfrac{1}{2}|\vartheta|) - 50 \cdot 098 \log_{10}|0 \cdot 74139 + 0 \cdot 67107 \cot \tfrac{1}{2}\vartheta| \quad \text{(XI.2)}$$

plus a different constant, which we ignore. χ is tabulated in Table 12, column 4, after certain auxiliary quantities have been found.

Now

$$\frac{ds}{d\theta} = \frac{2}{q_0} \sin \theta = \left\{\begin{array}{l} 4 \sin \frac{\theta}{2} \cos\left(\frac{\theta}{2} - \alpha\right) \\ 2 \sin \theta \end{array}\right. \times \left\{\begin{array}{l} e^{-l} \\ e^{-l+k} \end{array}\right\}$$

$$= \left\{\begin{array}{l} \sin \vartheta + \sin 20 \text{ deg. } (0 \text{ deg.} < \vartheta < 180 \text{ deg.}) \\ |\sin (340 \text{ deg.} - \vartheta)|\,(180 \text{ deg.} < \vartheta < 360 \text{ deg.}) \end{array}\right\}$$

$$\times \left\{\begin{array}{l} 2e^{-l}\ (0 \text{ deg.} < \vartheta < 275 \cdot 70 \text{ deg.}) \\ 2e^{-l+k}\ (275 \cdot 70 \text{ deg.} < \vartheta < 360 \text{ deg.}) \end{array}\right\} \quad \ldots \quad \text{(XI.3)}$$

$\frac{1}{2}e^l \dfrac{ds}{d\theta}$ is tabulated in column 5 and multiplied by $\cos \chi$ and $\sin \chi$ in columns 6 and 7. These are integrated up from the trailing edge (which is $\vartheta = 340$ deg.) in columns 8 and 9 to give $\frac{1}{2}e^l \dfrac{180}{\pi} x$ and $\frac{1}{2}e^l \dfrac{180}{\pi} y$, in *some* co-ordinate system with the trailing edge at the origin. The aerofoil is drawn on the right of Fig. 9. On the left are shown the fairing, centre-line, and velocity distributions at incidences 0 deg. and 20 deg. The chord is measured to be 164, so

$$\text{True chord} = \frac{164}{57 \cdot 296} \cdot \frac{2}{1 \cdot 7931} = 3 \cdot 1926\ , \quad \ldots \quad \ldots \quad \ldots \quad \ldots \quad \ldots \quad \text{(XI.4)}$$

since $l = k \dfrac{\beta_1 + \beta_2}{2\pi} + \dfrac{1}{\pi} L(10 \text{ deg.}) = 0 \cdot 27936 + 0 \cdot 30465 = 0 \cdot 58401$ and $e^l = 1 \cdot 7931$. Hence the C_L at incidence 20 deg. is

$$\frac{8\pi}{3 \cdot 1926} \sin 20 \text{ deg.} = 2 \cdot 69\ . \quad \ldots \quad \ldots \quad \ldots \quad \ldots \quad \ldots \quad \ldots \quad \ldots \quad \ldots \quad \text{(XI.5)}$$

TABLE 12

	1	2	3	4	5	6	7	8	9	10	11
ϑ (deg.)	$0{\cdot}17633 \tan \frac{1}{2}\vartheta$	F	$0{\cdot}74139$ $+0{\cdot}67107$ $\cot \vartheta/2$	χ	$\frac{e^t}{q_0}$	$\ldots \sin\chi$	$\ldots \cos\chi$	x	y	q_0	q_a
0	0	0	∞	−∞	0·34202	—	—	5·443	− 9·756	1·7931	1·7931
5	0·00770	1·648	16·1116	−58·83	0·42918	−0·3672	0·2221	5·714	−11·332	1·7657	1·7931
10	0·01543	2·910	8·4117	−43·43	0·51567	−0·3545	0·3745	7·216	−14·944	1·7386	1·7931
20	0·03109	5·071	4·5472	−27·88	0·68404	−0·3199	0·6046	12·194	−18·349	1·6848	1·7931
30	0·04725	6·988	3·2459	−18·63	0·84202	−0·2690	0·7979	19·185	−21·288	1·6313	1·7931
40	0·06418	8·779	2·5851	−11·89	0·98481	−0·2029	0·9637	28·060	−23·678	1·5767	1·7931
50	0·08222	10·510	2·1805	− 6·45	1·10806	−0·1245	0·1010	38·364	−25·305	1·5206	1·7931
60	0·10180	12·228	1·9037	− 1·78	1·20805	−0·0375	1·2075	49·978	−26·140	1·4616	1·7931
70	0·12347	13·980	1·6998	+ 2·44	1·28171	+0·0546	1·2805	62·403	−26·038	1·3990	1·7931
80	0·14796	15·799	1·5411	6·39	1·32683	0·1477	1·3186	75·471	−25·044	1·3308	1·7931
90	0·17633	17·734	1·4125	10·22	1·34202	0·2381	1·3207	88·655	−23·093	1·2555	1·7931
100	0·21014	19·841	1·3045	14·06	1·32683	0·3223	1·2871	101·766	−20·303	1·1703	1·7931
110	0·25183	22·197	1·2113	18·03	1·28171	0·3967	1·2187	114·281	−16·679	1·0717	1·7931
120	0·30541	24·908	1·1288	22·27	1·20805	0·4578	1·1179	126·032	−12·413	0·9541	1·7931
130	0·37814	28·138	1·0543	26·99	1·10806	0·5029	0·9874	136·540	− 7·577	0·8091	1·7931
140	0·48446	32·155	0·98564	32·47	0·98481	0·5287	0·8308	145·693	− 2·420	0·6227	1·7931
150	0·65807	37·442	0·92120	39·23	0·84202	0·5325	0·6522	153·083	+ 2·924	0·3698	1·7931
160	1	45·000	0·85972	48·29	0·68404	0·5106	0·4551	158·676	8·145	0	1·7931
170	2·01543	57·444	0·80010	62·30	0·51567	0·4566	+0·2397	162·124	13·029	0·6038	1·7931
180	∞	90·000	0·74139	96·51	0·34202	0·3398	−0·0388	163·259	17·064	1·7931	1·7931
190		122·556	0·68268	130·86	0·5	0·3782	−0·3271	161·315	20·696	1·7931	0·6038
200		135·000	0·62306	145·29	0·64279	0·3660	−0·5284	157·007	24·463	1·7931	0
210		142·558	0·56158	155·11	0·76604	0·3224	−0·6949	150·863	27·911	1·7931	0·3698
220		147·845	0·49714	163·05	0·86603	0·2525	−0·8284	143·219	30·823	1·7931	0·6227
230		151·862	0·42846	170·30	0·93969	0·1583	−0·9263	134·414	32·880	1·7931	0·8091
240		155·092	0·35395	177·69	0·98481	0·0397	−0·9840	124·827	33·908	1·7931	0·9541
250		157·803	0·27150	186·17	1	−0·1076	−0·9942	114·892	33·579	1·7931	1·0717
260		160·159	0·17829	197·68	0·98481	−0·2991	−0·9383	105·164	31·608	1·7931	1·1703
270		162·266	0·07032	220·02	0·93969	−0·6043	−0·7197	94·176	23·659	1·7931	1·2555
280		164·201	0·05836	226·02	2·85521	−2·0546	−1·9828	88·977	14·602	0·5439	0·4037
290		166·020	0·21700	199·26	2·52556	−0·8331	−2·3843	66·146	+ 0·907	0·5439	0·4243
300		167·772	0·42094	186·60	2·11921	−0·2436	−2·1051	43·559	− 4·167	0·5439	0·4433
310		169·490	0·69773	177·32	1·64845	+0·0771	−1·6468	24·641	− 4·860	0·5439	0·4612
320		171·221	1·1024	169·10	1·12761	0·2133	−1·1071	10·896	− 3·238	0·5439	0·4782
330		173·012	1·7631	160·67	0·57251	+0·1896	−0·5404	2·588	− 1·128	0·5439	0·4948
340		174·929	3·0644	150·56	0	0	0	0	0	0·5439	0·5110
350		177·090	6·9289	134·97	0·57251	−0·4052	+0·4045	2·136	− 2·215	0·5439	0·5273
355		178·352	14·629	119·98	0·85330	−0·7392	0·4263	4·550	− 4·560	0·5439	0·5356
360		180·000	∞	−∞	1·12761	—	—	5·443	− 9·756	0·5439	0·5439

APPENDIX XII

Calculations for Cambered Aerofoils

By (10), the χ corresponding to (30) is

$$\frac{1}{2\pi}\int_0^\pi \log\left|\frac{\cos\frac{1}{2}(\phi+\alpha)}{\cos\frac{1}{2}(\phi-\alpha)}\right| \cot\tfrac{1}{2}(\theta-\phi)\,d\phi - \frac{1}{2\pi}\int_{\beta_2}^{\beta_1} k\cot\tfrac{1}{2}(\theta-\phi)\,d\phi. \quad \ldots \quad \text{(XII.1)}$$

The first term can be written (with $a = \cot\frac{1}{2}\alpha$, $t = \tan\frac{1}{2}\theta$, $p = \tan\frac{1}{2}\phi$)

$$\frac{1}{\pi}\int_0^\infty \log\frac{|a-p|}{a+p}\cdot\frac{1+tp}{t-p}\cdot\frac{dp}{1+p^2} = g(a, t)\,. \quad \ldots \quad \text{(XII.2)}$$

Now

$$\frac{\partial}{\partial a} g(a,t) = \frac{1}{\pi}\int_0^\infty \left(\frac{1}{a-p} - \frac{1}{a+p}\right)\frac{1+tp}{t-p}\cdot\frac{dp}{1+p^2}$$

$$= \frac{1}{\pi}\int_0^\infty \left[\frac{\frac{1+at}{t-a}\,\frac{1}{1+a^2}}{a-p} + \frac{\frac{1}{a-t}}{t-p} + \frac{\frac{-1+ap}{1+a^2}}{1+p^2} - \frac{\frac{1-at}{t+a}\,\frac{1}{1+a^2}}{a+p} - \frac{\frac{1}{a+t}}{t-p} - \frac{\frac{1+ap}{1+a^2}}{1+p^2}\right] dp$$

$$= \frac{1}{\pi}\Big[-\frac{1+at}{t-a}\,\frac{1}{1+a^2}\log|a-p| - \frac{1}{a-t}\log|t-p| - \frac{1}{1+a^2}\tan^{-1}p$$

$$+ \frac{a}{1+a^2}\log\sqrt{(1+p^2)} - \frac{1-at}{t+a}\,\frac{1}{1+a^2}\log(a+p) + \frac{1}{a+t}\log|t-p|$$

$$- \frac{1}{1+a^2}\tan^{-1}p - \frac{a}{1+a^2}\log\sqrt{(1+p^2)}\Big]_0^\infty$$

$$= \frac{1}{\pi}\left[\frac{2t}{t^2-a^2}\log\frac{a}{|t|} - \frac{\pi}{1+a^2}\right]. \quad \ldots \quad \text{(XII.3)}$$

But $g(0, t) = 0$. Hence

$$g(a, t) = \frac{2}{\pi}\int_0^a \frac{t}{t^2-x^2}\log\frac{x}{t}\,dx - \tan^{-1}a$$

$$= \frac{2}{\pi}\int_0^{a/t} \frac{\log y}{1-y^2}\,dy - \tan^{-1}a$$

$$= -\frac{\pi}{2} + F\left(\frac{t}{a}\right) - \left(\frac{\pi}{2} - \frac{\alpha}{2}\right). \quad \ldots \quad \text{(XII.4)}$$

Hence (36) holds.

To get the Fourier constants of (37) we want

$$\int_0^{\pi-\delta\alpha} \log\left|\frac{\cos\frac{1}{2}(\vartheta+\alpha)}{\cos\frac{1}{2}(\vartheta-\alpha)}\right| \cos\vartheta\, d\vartheta = \sin\delta\alpha \log\frac{\sin\frac{1}{2}(\alpha-\delta\alpha)}{\sin\frac{1}{2}(\alpha+\delta\alpha)} + \int_0^{\pi-\delta\alpha} \sin\vartheta \frac{\sin\alpha}{\cos\vartheta+\cos\alpha}\, d\vartheta$$

$$= \sin\delta\alpha \log\frac{\sin\frac{1}{2}(\alpha-\delta\alpha)}{\sin\frac{1}{2}(\alpha+\delta\alpha)}$$

$$+ \sin\alpha\log\frac{(\cot\frac{1}{2}(\alpha+\delta\alpha)}{(\cot\frac{1}{2}(\alpha-\delta\alpha)} = A \qquad \ldots \qquad \ldots \quad \text{(XII.5)}$$

and

$$\int_0^{\pi-\delta\alpha} \log\left|\frac{\cos\frac{1}{2}(\vartheta+\alpha)}{\cos\frac{1}{2}(\vartheta-\alpha)}\right| \sin\vartheta\, d\vartheta = -\cos\delta\alpha\log\frac{\sin\frac{1}{2}(\alpha-\delta\alpha)}{\sin\frac{1}{2}(\alpha+\delta\alpha)} - \int_0^{\pi-\delta\alpha} \cos\vartheta\frac{\sin\alpha}{\cos\vartheta+\cos\alpha}\, d\vartheta$$

$$= \cos\ \delta\alpha\ \log\frac{\sin\frac{1}{2}(\alpha-\delta\alpha)}{\sin\frac{1}{2}(\alpha+\delta\alpha)} - (\pi-\delta\alpha)\sin\alpha$$

$$-\cos\ \alpha\ \log\frac{\sin\frac{1}{2}(\alpha-\delta\alpha)}{\sin\frac{1}{2}(\alpha+\delta\alpha)} = -B, \ldots \qquad \ldots \quad \text{(XII.6)}$$

and also

$$\int_0^{\pi-\delta\alpha} \log\left|\frac{\cos\frac{1}{2}(\vartheta+\alpha)}{\cos\frac{1}{2}(\vartheta-\alpha)}\right| d\vartheta = 2\left(\int_{\alpha/2}^{\frac{\pi-\delta\alpha+\alpha}{2}} - \int_{-\alpha/2}^{\frac{\pi-\delta\alpha-\alpha}{2}}\right)\log|\cos\vartheta|\, d\vartheta$$

$$= 2\left(\int_{\frac{\alpha-\delta\alpha}{2}}^{\frac{\alpha+\delta\alpha}{2}}\log|\sin\vartheta|\, d\vartheta - 2\int_0^{\alpha/2}\log\cos\vartheta d\vartheta\right) = -C. \quad \text{(XII.7)}$$

Conditions (7) are then

$$\left.\begin{aligned} l_1(\sin(\beta-\alpha)-\sin\delta\alpha)+l_2(\sin(\beta+\alpha)+\sin\delta\alpha) &= A,\\ l_1(\cos(\beta-\alpha)+\cos\delta\alpha)-l_2(\cos(\beta+\alpha)+\cos\delta\alpha) &= B,\\ 2\pi k+l_1(\pi+\alpha-\delta\alpha-\beta)+l_2(\pi-\beta-\alpha+\delta\alpha) &= C.\end{aligned}\right\} \quad \ldots \quad \ldots \quad \ldots \quad \text{(XII.8)}$$

Finally we tabulate in Table 13 the function

$$X(\theta) = -\frac{1}{\pi}\int_0^\theta \log_e \sin\frac{\theta}{2}\, d\theta, \text{ which occurs in (41).}$$

TABLE 13

θ (deg.)	X			θ (deg.)	X			θ (deg.)	X		
0	0	3190		10	0·19107	1329	55	20	0·30526	959	28
1	0·03190	2420	770	11	0·20435	1278	50	21	0·31785	933	26
2	0·05609	2129	291	12	0·21714	1232	46	22	0·32418	908	25
3	0·07738	1940	189	13	0·22946	1190	43	23	0·33326	884	24
4	0·09678	1800	140	14	0·24136	1150	40	24	0·34210	861	23
5	0·11478	1688	112	15	0·25286	1113	37	25	0·35071	839	22
6	0·13166	1595	93	16	0·26399	1079	35	26	0·35911	818	21
7	0·14761	1516	80	17	0·27478	1046	32	27	0·36729	798	20
8	0·16276	1446	70	18	0·28524	1016	31	28	0·37528	779	19
9	0·17722	1384	62	19	0·29539	987	30	29	0·38306	760	19
			55				28	30	0·39066		18

APPENDIX XIII

Cambered Suction Aerofoil with Slots Approximately Opposite

Using the velocity distribution of (37) with $\alpha = 20$ deg., $\beta = 40$ deg., we obtain the four simultaneous equations formed by (XII.8) and $l_1 - l_2 = \log$ ($\sin \frac{1}{2} (\alpha + \delta\alpha) / \sin \frac{1}{2}(\alpha - \delta\alpha)$, from which we are to find l_1, l_2, k and δ. We solve them by finding the solution of (XII.8) for $\delta = 0$ (thus obtaining δ approximately), and then obtaining the final value of δ by trial and error. The result is :—

$$\delta = 0\cdot176,\ l_1 = 1\cdot2437,\ l_2 = 0\cdot8917,\ k = -0\cdot5448 \quad \ldots \quad \ldots \quad \text{(XIII.1)}$$

By (41) we have therefore

$$\chi = F\,(0\cdot17633 \tan \tfrac{1}{2}\vartheta) + 328\cdot28\,[\chi\,(\pi - \vartheta) - \chi\,(\pi - \vartheta - 3\cdot52 \text{ deg.})]$$
$$- 52\cdot23 \log_{10} \operatorname{cosec} \tfrac{1}{2}\,(\vartheta - 20 \text{ deg.}) + 37\cdot45 \log_{10} \operatorname{cosec} \tfrac{1}{2}\,(\vartheta + 60 \text{ deg.})\,, \quad \ldots \quad \text{(XIII.2)}$$

where for $|\pi - \vartheta| \geqslant 30$ deg. we can replace the second term by

$$14\cdot78 \log_{10} \sec \tfrac{1}{2}\,(\vartheta + 1\cdot76 \text{ deg.})\ . \quad \ldots \quad \ldots \quad \ldots \quad \ldots \quad \ldots \quad \ldots \quad \text{(XIII.3)}$$

This χ is computed in Table 14, column 1. In column 2 we have

$$\tfrac{1}{2}e^{l_2+k}\,\frac{ds}{d\theta} = \frac{e^{l_2+k}}{q_0}\sin\theta = \left\{\begin{array}{l} \sin(\theta - \alpha) + \sin\alpha \\ \\ \sin\theta \end{array}\right\} \text{ times } \left\{\begin{array}{c} e^{-(l_1-l_2)} \\ 1 \\ e^{l_2} \end{array}\right\} \quad \ldots \quad \text{(XIII.4)}$$

where $e^{-(l_1-l_2)} = 0\cdot7032$, and $e^{l_2} = 2\cdot4393$. This is multiplied by $\cos\chi$ and $\sin\chi$ in columns 3 and 4, and in columns 5 and 6 these are integrated from 0 deg. and 180 deg. in the regions behind and before the slot respectively, to give $\frac{27}{\pi}\,e^{l_2+k}\,x$ and $\frac{27}{\pi}\,e^{l_2+k}\,y$.

It is observed that two constants a and b appear. These are determined by logarithmic spiral theory. At the slot at $\vartheta = 20$ deg., $\phi = \tan^{-1} l_1/\pi = 21\cdot60$ deg., and $\frac{1}{2}$ (χ (22·5 deg.) + χ (17·5 deg.)) $- \phi = -95\cdot98$ deg.

Hence

$$[5\cdot673 - (5\cdot395 - b)] \tan 5\cdot98 \text{ deg.} = 36\cdot455 - a\ . \quad \ldots \quad \ldots \quad \ldots \quad \ldots \quad \text{(XIII.5)}$$

At the $\vartheta = -60$ deg. slot, $\phi = \tan^{-1}\dfrac{l_2}{\pi} = 15\cdot85$ deg. and $\frac{1}{2}$ (χ (− 62·5 deg.) + χ (− 57·5 deg.)) $+ \phi = 236\cdot65$ deg. Hence

$$[(-1\cdot825 - b) - (-4\cdot358)] \cot 56\cdot65 \text{ deg.} = a - 35\cdot469\ . \quad \ldots \quad \ldots \quad \ldots \quad \text{(XIII.6)}$$

These two equations give $a = 36\cdot361$, $b = 1\cdot178$. The resulting aerofoil is plotted in Fig. 10. Its thickness ratio is measured to be 41·2 per cent. Its chord is 36·7 in the scale of columns 5 and 6. Hence

$$\text{true chord} = \frac{\pi}{27}\,e^{l_2+k}\,36\cdot7 = \frac{\pi}{27}\cdot\frac{36\cdot7}{1\cdot4148} = 3\cdot02$$

and

$$C_L = \frac{8\pi \sin 20 \text{ deg.}}{3\cdot02} = 2\cdot85.$$

Thus the aerofoil's C_L range is from 0 to 2·85.

TABLE 14

	θ (deg.)	1 χ (deg.)	2 $\frac{1}{2}e^{l_2+k}\ \frac{ds}{d\theta}$	3 . . . cos χ	4 . . . sin χ	5 x	6 y
	180	120·76	0·34202	−0·1749	0·2939	0	0
	177·5	110·32	0·30071	−0·1044	0·2820	−0·108	0·213
	175	92·72	0·30181	−0·0143	0·3015	−0·152	0·431
	172·5	82·57	0·33231	+0·0430	0·3295	−0·137	0·668
	170	75·22	0·36263	0·0925	0·3506	−0·089	0·923
	160	56·44	0·48104	0·2659	0·4009	+0·454	2·060
	150	44·83	0·59213	0·4199	0·4175	1·487	3·295
	140	36·40	0·69255	0·5574	0·4110	2·957	4·542
	130	29·42	0·77922	0·6787	0·3828	4·815	5·739
	120	23·49	0·84954	0·7791	0·3386	7·008	6·823
	110	18·11	0·90134	0·8567	0·2802	9·467	7·757
	100	13·02	0·93307	0·9091	0·2102	12·123	8·492
	90	8·01	0·94375	0·9345	0·1315	14·895	9·009
	80	2·88	0·93307	0·9319	+0·0469	17·702	9·275
	70	− 2·61	0·90134	0·9004	−0·0410	20·457	9·287
	60	− 8·79	0·84954	0·8396	−0·1298	23·075	9·029
	50	− 16·23	0·77922	0·7482	−0·2178	25·464	8·509
	40	− 26·16	0·69255	0·6216	−0·3053	27·529	7·722
	30	− 42·47	0·59213	0·4368	−0·3998	29·135	6·670
	27·5	− 49·09	0·56524	0·3701	−0·4272	29·438	6·361
	25	− 58·45	0·53772	0·2814	−0·4582	29·685	6·029
slot	22·5	− 74·28	0·50963	0·1381	−0·4906	29·846	5·673
→	20	− ∞	—	—	—	—	—
	17·5	− 74·49	1·56781	0·4193	−1·5107	6·609	5·395
	15	− 58·87	1·46563	0·7577	−1·2546	6·150	4·361
	12·5	− 49·78	1·36225	0·8796	−1·0402	5·532	3·503
	10	− 43·36	1·25787	0·9145	−0·8636	4·852	2·791
	0	− 28·44	0·83429	0·7336	−0·3973	2·330	0·964
trailing	− 10	− 19·54	0·42358	0·3992	−0·1417	0·604	0·196
→ edge	− 20	− 11·88 +168·12	0	0	0	a — 0	0 — b
	− 30	175·96	0·42358	−0·4225	+0·0298	0·629	0·084
	− 40	184·34	0·83429	−0·8319	−0·0631	2·522	+0·566
	− 50	197·15	1·21965	−1·1654	−0·3596	5·545	−0·498
	− 52·5	202·15	1·31064	−1·2139	−0·4515	6·437	−0·792
	− 55	209·04	1·39913	−1·2232	−0·6791	7·356	−1·209
	− 57·5	220·58	1·48495	−1·1278	−0·9660	8·246	−1·825
→	− 60	∞	—	—	—	—	—
slot	− 62·5	221·03	0·67559	−0·5096	−0·4435	27·223	−4·356
	− 65	209·98	0·70711	−0·6125	−0·3533	26·709	−4·655
	− 67·5	203·57	0·73728	−0·6758	−0·2948	26·314	−4·896
	− 70	199·06	0·76604	−0·7240	−0·2502	25·789	−5·100
	− 80	188·26	0·86603	−0·8570	−0·1244	23·402	−5·650
	− 90	181·85	0·93969	−0·9392	−0·0303	20·698	−5·878
	−100	177·07	0·98481	−0·9835	+0·0503	17·804	−5·845
	−110	173·01	1	−0·9926	0·1217	14·832	−5·586
	−120	169·24	0·98481	−0·9675	0·1839	11·893	−5·124
	−130	165·44	0·93969	−0·9095	0·2360	9·060	−4·493
	−140	161·31	0·86603	−0·8204	0·2775	6·457	−3·719
	−150	156·43	0·76604	−0·7021	0·3063	4·167	−2·840
	−160	149·93	0·64279	−0·5563	0·3221	2·272	−1·894
	−170	140·37	0·5	−0·3851	0·3189	0·854	−0·927
	−172·5	136·93	0·46175	−0·3373	0·3153	0·581	−0·692
	−175	132·79	0·42262	−0·2871	0·3101	0·349	−0·454
	−177·5	127·63	0·38268	−0·2336	0·3031	0·151	−0·227
	−180	120·76	0·34202	−0·1749	0·2939	0	0

$a = 36{\cdot}361$
$b = 1{\cdot}178$

APPENDIX XIV

Contraction Cone with Wall Velocity always Increasing

We take a 4 : 1 velocity ratio, so that $U = 0\cdot5$ and $V = 2\cdot0$ say. The velocity distribution is

$$\log q = \tfrac{9}{16} \log 4 (\cos \theta - \tfrac{1}{9} \cos 3\theta)\,, \quad .. \quad .. \quad .. \quad .. \quad .. \qquad \text{(XIV.1)}$$

which we compute as $q = \text{antilog}\,(0\cdot33866 \cos \theta - 0\cdot03763 \cos 3\theta)$. The corresponding value of χ is $\frac{9}{16} \log 4 (\sin \theta - \frac{1}{9} \sin 3\theta)$ which, in degrees, is $44\cdot679 \sin \theta - 4\cdot964 \sin 3\theta$. We have $\chi(\theta) = \chi(\pi - \theta)$ and $q(\theta) = \dfrac{1}{q(\pi - \theta)}$, so we only tabulate them between 0 and $\dfrac{\pi}{2}$. By (56) we want to integrate $\dfrac{\cos \chi}{q} \operatorname{cosec} \theta$ and $\dfrac{\sin \chi}{q} \operatorname{cosec} \theta$. To get the values for $\pi - \theta$, we also tabulate $q \cos \chi \operatorname{cosec} \theta$ and $q \sin \chi \operatorname{cosec} \theta$. In Table 15, columns 3, 4, 5 and 6 are integrated by Simpson's rule in columns 7, 8, 9 and 10 respectively. The values of x and y are measured from the point corresponding to $\theta = \dfrac{\pi}{2}$. To measure y from the axis, we need only express the condition that at $x = +\infty$ y is four times its value at $x = -\infty$. The final values of X and Y (measured thus and reduced to make $Y = 1$ at $X = -\infty$) are given in columns 11 and 12. The shape and velocity distribution are shown in Fig. 11.

(77090)

TABLE 15

θ (deg.)	1 χ	2 q	3 $\frac{q \cos \chi}{\sin \theta}$	4 $\frac{q \sin \chi}{\sin \theta}$	5 $\frac{\cos \chi}{q \sin \theta}$	6 $\frac{\sin \chi}{q \sin \theta}$	7 x	8 y	9 x	10 y	11 X	12 Y
90	49°38·6′	1	0·6475	0·7620	0·6475	0·7620	0	0	0	0	$-\infty$	1
80	48° 18′	1·1956	0·8076	0·9065	0·5650	0·6341					−1·9939	1·0289
70	44° 28′	1·4073	1·0688	1·0491	0·5397	0·5297	4·9467	5·4371	− 3·4472	− 3·8281	−1·5516	1·0581
60	38° 41·6′	1·6102	1·4512	1·1623	0·5628	0·4483					−1·1084	1·1184
50	31° 44·6′	1·7795	1·9755	1·2222	0·6238	0·3859	13·7958	12·3576	− 6·8619	− 6·5369	−0·8475	1·1832
40	24° 25·2′	1·8976	2·6880	1·2205	0·7465	0·3389					−0·5082	1·3347
30	17° 22·5′	1·9648	3·7503	1·1735	0·9715	0·3048	30·2736	19·6353	−11·4432	− 8·5832	−0·2553	1·5353
25	14° 5·2′	1·9824	4·5497	1·1430	1·1577	0·2908					0	1·8189
20	10° 58·9′	1·9925	5·7190	1·1098	1·4405	0·2795	44·1076	23·0629	−14·9646	− 9·4569	+0·3664	2·2216
15	8° 3·2′	1·9976	7·6420	1·0813	1·9151	0·2710					1·0218	2·7341
10	5° 16·6′	1·9995	11·4659	1·0589	2·8679	0·2649	67·9841	26·3099	−20·9490	−10·2711	2·2422	3·2732
7·5	3° 55·9′	1·9999	15·2858	1·0506	3·8218	0·2627					3·2668	3·5270
5	2° 36·6′	1·9999	22·9225	1·0449	5·7312	0·2613	91·8670	27·8864	−26·9206	−10·6654	5·0352	3·7675
											6·8041	3·8843
											∞	4

APPENDIX XV

Finite Contraction Cone with Small Adverse Velocity Gradient

The log q corresponding to (59) is

$$\frac{a}{\pi}\int_{\beta}^{\pi/2}(1-\cos(t-\beta))\left[\frac{\sin t}{\cos\theta-\cos t}+\frac{\sin t}{\cos\theta+\cos t}\right]dt \quad \ldots \quad \text{(XV.1)}$$

This is calculated to be

$$\frac{2a}{\pi}[f(\tfrac{1}{2}(\beta+\theta))+f(\tfrac{1}{2}(\theta-\beta)-f(\tfrac{1}{2}(\pi-\beta-\theta))-f(\tfrac{1}{2}(\pi+\beta-\theta))+\sec\theta\cos\beta f(\tfrac{1}{2}\pi-\theta)$$
$$+(\cos\beta\log 2-(\pi-2\beta)\sin\beta)\cos\theta]\,, \quad \ldots \quad \text{(XV.2)}$$

where $f(\theta)=\sin^2\theta\log\operatorname{cosec}\theta$. We take $\beta=1$ deg. For this it is a fair approximation to (XV.2) to omit all terms of order β^2. This reduces it to

$$\log q=\frac{2a}{\pi}[2f(\tfrac{1}{2}\theta)-2f(\tfrac{1}{2}(\pi-\theta))+\sec\theta f(\tfrac{1}{2}\pi-\theta)+(\log 2-\pi\sin\beta)\cos\theta] \ldots \quad \text{(XV.3)}$$

Now for a 4 : 1 contraction ratio we must have $q(0)/q(\pi/2)=2$, or

$\log 2 \doteq \dfrac{2a}{\pi}(\log 2-\pi\sin\beta)$, giving $a=\dfrac{\pi}{2}.\dfrac{0\cdot69315}{0\cdot63832}=1\cdot7057$. The square bracket of (XV.3) is tabulated in Table 16, column 1 and q in column 2. χ in degrees is $97\cdot73\,(1-\cos(\theta-\beta))$ in $(\beta,(\pi/2))$ and this is tabulated in column 3. q cosec cos χ, q cosec θ sin χ, $\dfrac{1}{q}$ cosec θ cos χ, $\dfrac{1}{q}$ cosec θ sin χ were tabulated in subsequent columns (not reproduced here) and integrated to give the values of x and y in columns 4–7. The values in square brackets where the integrand becomes infinite like 2 cosec θ and $\frac{1}{2}$ cosec θ respectively were obtained by using the known integral of cosec θ. The radius of the narrowest part is seen to be $28\cdot111$ in the scale of columns 4–7, and the length of contraction cone is $381\cdot974$, or $13\cdot588$ times as much. Values of X and Y (reduced with respect to the radius of the smallest part) are given in Table 17.

TABLE 16

	1	2	3	4	5	6	7
θ (deg.)	I	q	χ (deg.)	x	y	x	y
0	0·2772	2	0	[312·503]	67·974	[69·471]	16·358
5	0·2822	2·025	0·23	(203·719)	67·863	(41·714)	16·337
10	0·2924	2·079	1·20	154·031	67·352	29·853	16·208
15	0·3051	2·144	2·90	124·376	66·351	23·178	15·991
20	0·3188	2·219	5·33	102·518	64·823	18·580	15·664
25	0·3324	2·295	8·45	84·888	62·722	15·107	15·260
30	0·3447	2·368	12·26	69·945	60·023	12·358	14·755
35	0·3550	2·430	16·71	56·948	56·687	10·100	14·186
40	0·3623	2·474	21·78	45·515	52·722	8·205	13·519
45	0·3659	2·497	27·43	35·461	48·132	6·575	12·787
50	0·3652	2·492	33·61	26·696	42·989	5·173	11·952
55	0·3586	2·451	40·28	19·208	37·368	3·948	11·044
60	0·3459	2·374	47·40	13·000	31·434	2·888	10·016
65	0·3258	2·258	54·89	8·072	25·324	1·971	8·891
70	0·2967	2·100	62·70	4·388	19·278	1·203	7·612
75	0·2569	1·901	70·80	1·892	13·483	0·583	6·178
80	0·2033	1·662	79·08	+0·455	8·199	+0·139	4·506
85	0·1281	1·377	87·52	−0·095	3·609	−0·092	2·536
90	0	1	96·02	0	0	0	0

The maximum of $-\,dq/ds$, *i.e.* the maximum adverse velocity gradient, occurs at $\theta \simeq 30$ deg., *i.e.* at (2·032, 1·057), when it is 0·75. This is not very great and, it may be hoped, will not materially increase turbulence. The maximum velocity gradient on the wider end (which is of course the forward end) is much less, about a tenth of this: this is as it should be. Shape and velocity distribution are drawn in Fig. 12.

TABLE 17

X	Y
0	1
0·987	1·001
1·409	1·005
1·646	1·013
1·810	1·025
1·934	1·039
2·032	1·057
2·112	1·077
2·179	1·101
2·237	1·127
2·287	1·157
2·331	1·189
2·369	1·226
2·401	1·266
2·429	1·311
2·451	1·362
2·466	1·422
2·475	1·492
2·471	1·582
2·468	1·710
2·487	1·874
2·539	2·062
2·627	2·268
2·758	2·483
2·934	2·700
3·155	2·911
3·421	3·111
3·733	3·294
4·090	3·457
4·497	3·598
4·959	3·717
5·491	3·813
6·118	3·888
6·896	3·942
7·951	3·978
9·718	3·996
13·588	4

APPENDIX XVI

Short Contraction Cone with Small Adverse Velocity Gradient

Taking $\log q$ and χ as in (60) with $V/U = 4$, we obtain the contraction cone of Fig. 13. The velocity distribution is shown to have only a very slight adverse gradient, and this combined with the shortness of the cone makes it a very satisfactory one for practical use. Tables are omitted for this cone.

0·02227

Summary of Appendices

Appendices I, VI, VII and X (corresponding to Figs. 1, 5, 6 and 8) deal with ordinary low-drag wings. VI and VII give C_L ranges (for given thickness and point of maximum suction) well above those of any previous aerofoils that have been designed. But they suffer from the defect that the curvature at the nose is logarithmically infinite, which may influence maximum lift (though this has yet to be shown experimentally). I has a finite leading-edge radius of curvature (equal to 0·~~2207~~ chords) but suffers badly on C_L range, though with more careful design the thickness might be reduced slightly. The method of X is perhaps a more promising way out of the difficulty, but is hardly quite satisfactory in its present form.

Appendices II, IV, V, XI and XIII deal with suction wings. Boundary-layer suction enables us to obtain greater thickness and hence greater lift (and, one may add, storing capacity) without increased drag. It is also believed that it may reduce the compressibility stall by localising the shock wave at the slot, where it cannot cause separation of the boundary layer since it is all sucked away. Appendix II was chosen as an illustration of the wide possibilities of the method and perhaps cannot be taken seriously. But the other four (of thicknesses 34, 48, 30 and 41 per cent. respectively) seem to me, and to my colleagues at the N.P.L., serious practical suggestions for general future types of wing shape. In the field of cambered aerofoils XIII is probably preferable to XI, and the method of XIII should be followed up extensively to produce cambered versions of all types of aerofoil. Such cambered aerofoils should of course include cambers of all magnitudes, not just those that make the bottom of the incidence range zero.

Of the contraction cones obtained, the first two were respectively too long and with too large an adverse velocity gradient. The third, a compromise, seems likely to be very satisfactory in practice.

Finally the idea of Appendix VIII (leading-edge suction) may be noted as one which, when developed (as has been done in a forthcoming report), produces very valuable thin wings with high maximum lift for high-speed flight.

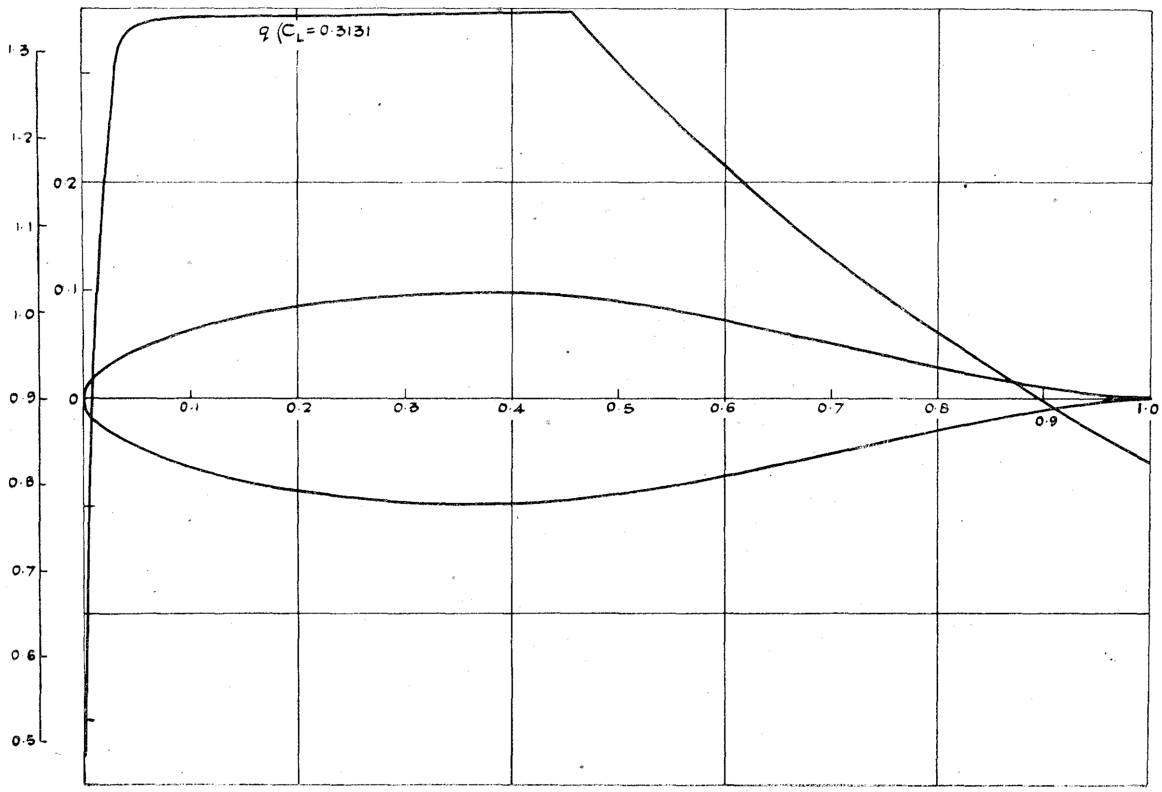

FIG. 1.—Thickness 19·6 per cent.

App. I

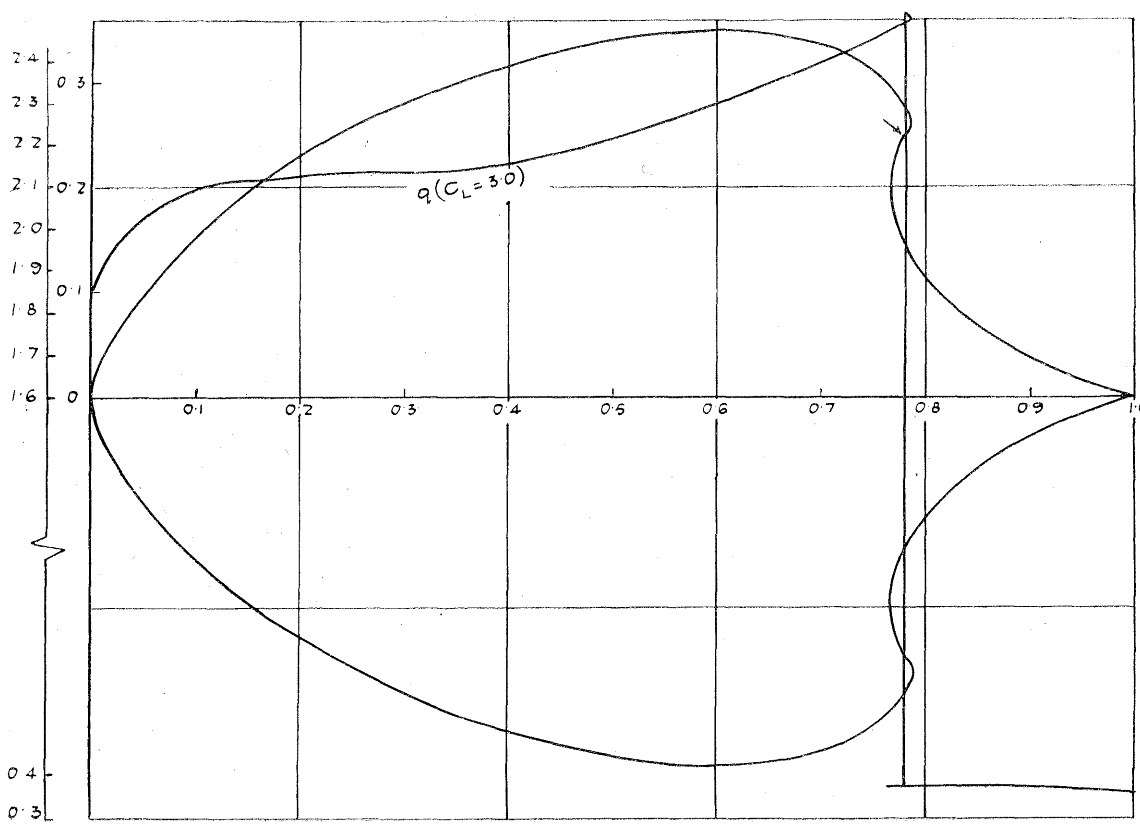

FIG. 2.—Thickness 70 per cent.

App. II

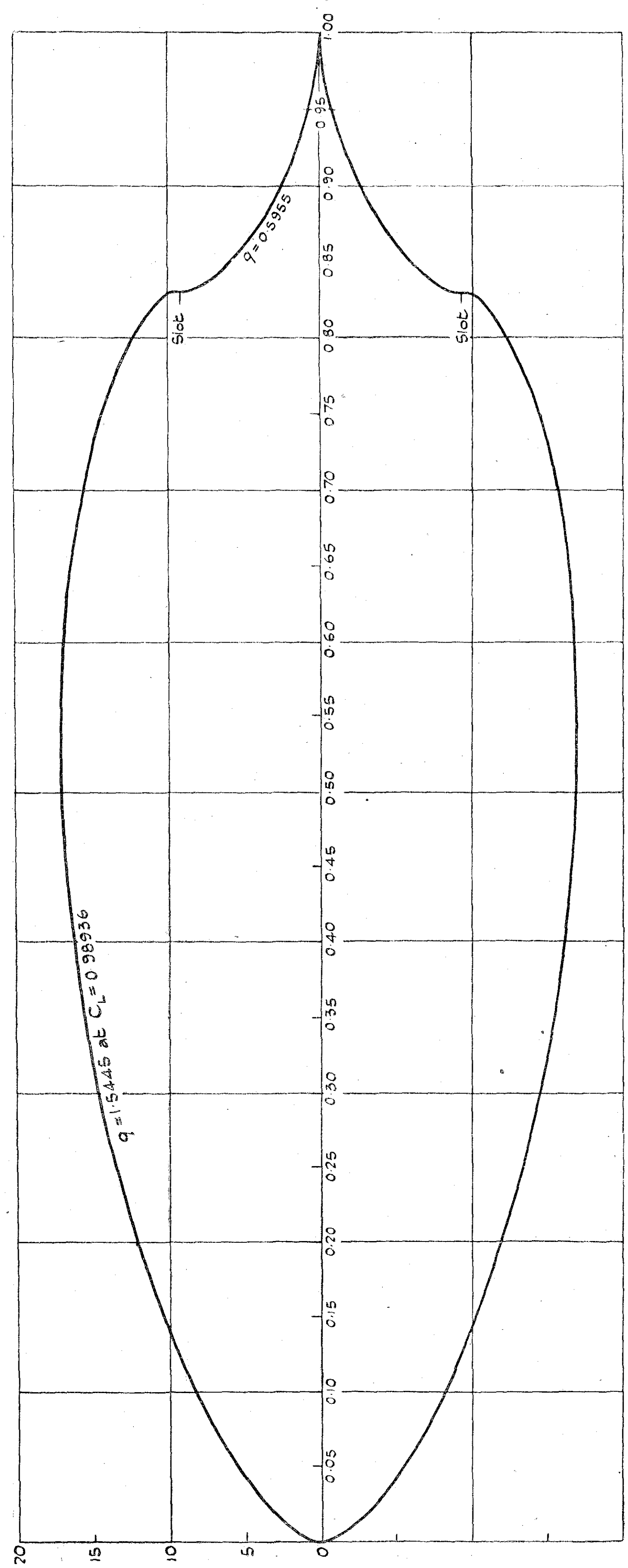

FIG. 3.— Thickness 34 per cent.

App. IV

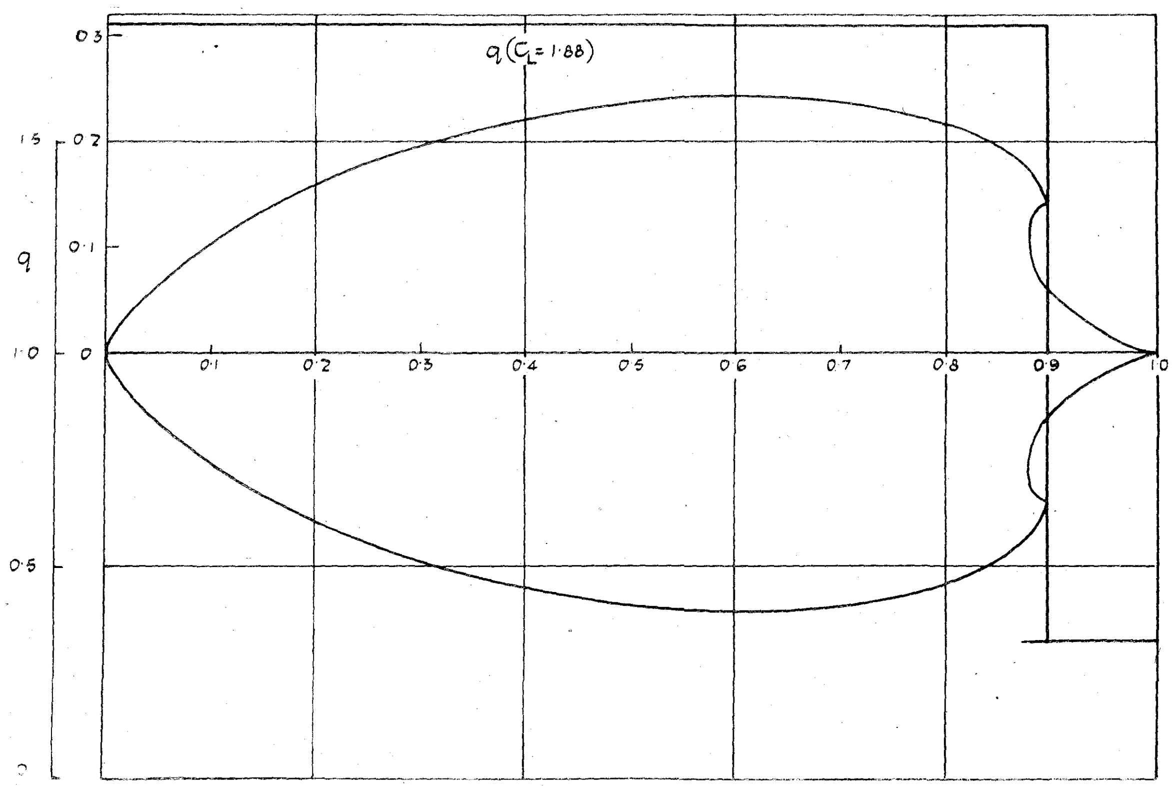

FIG. 4.—Thickness 48 per cent. App. V

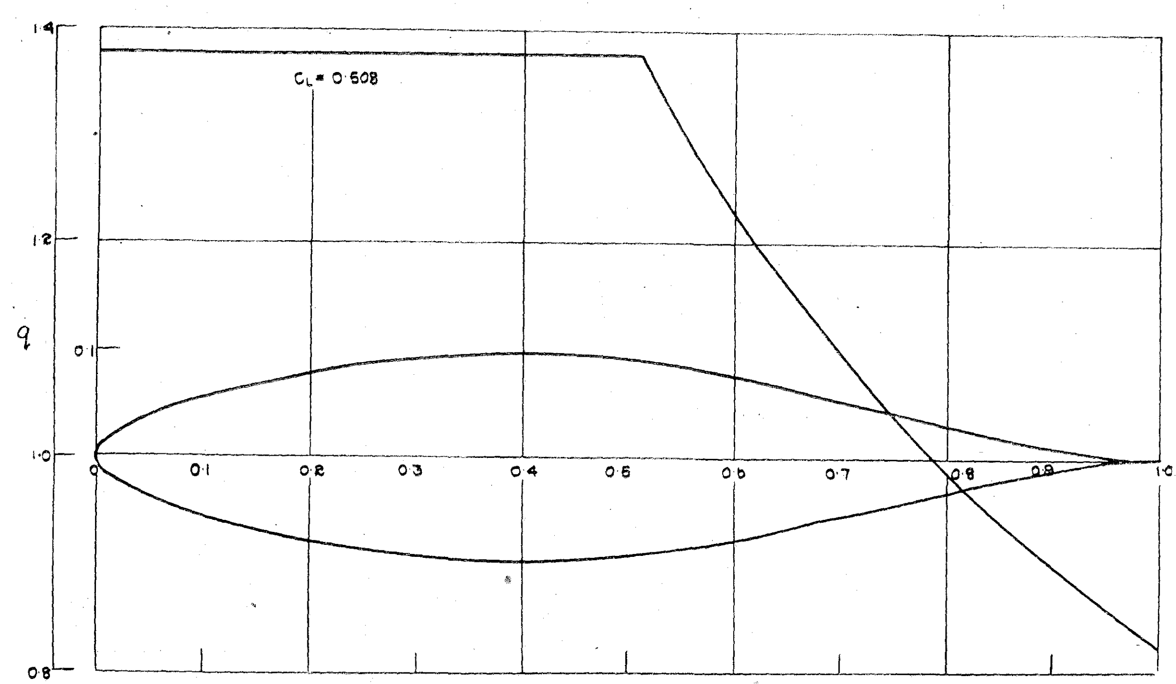

FIG. 6.—Thickness 19·2 per cent. App. VII

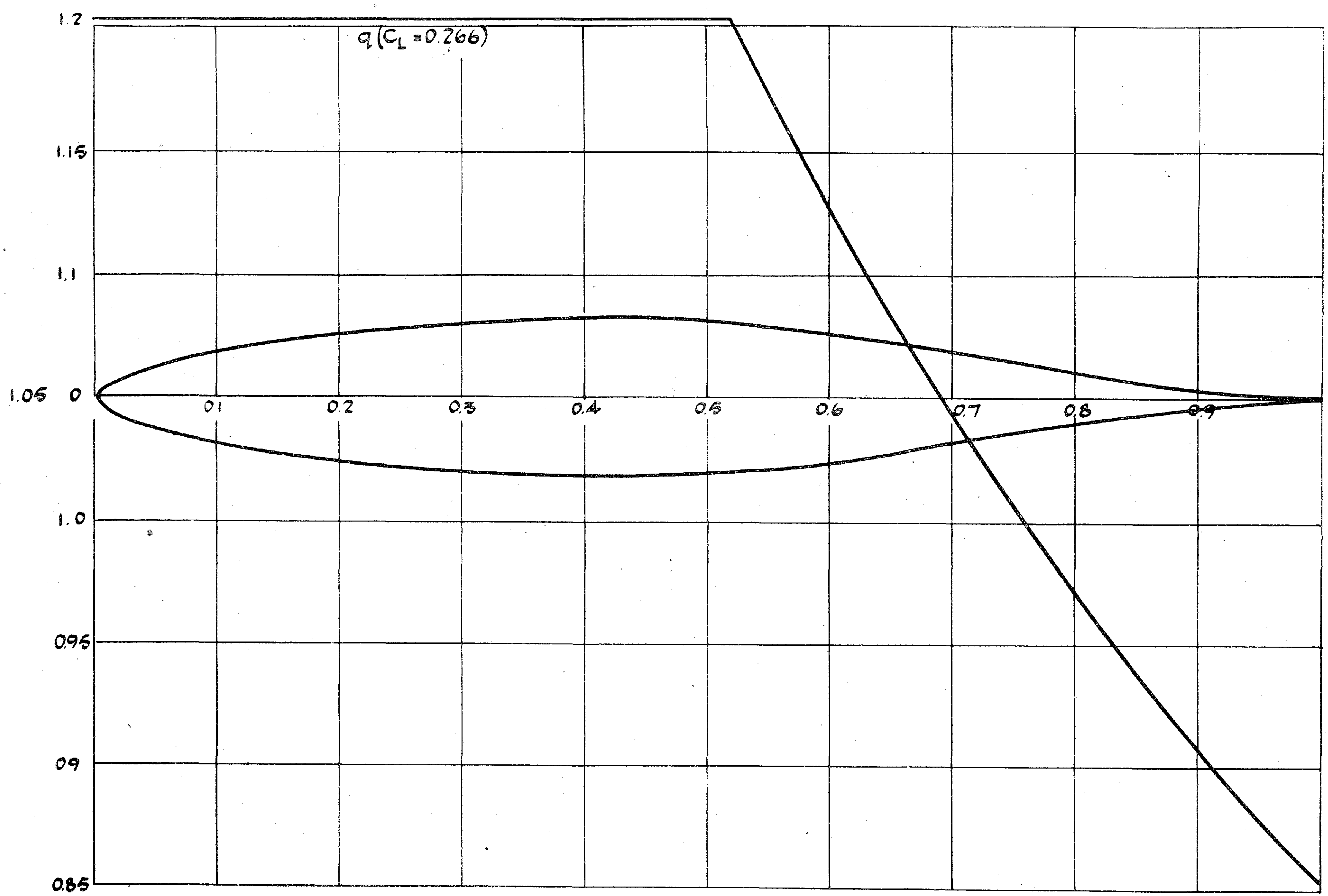

FIG. 5.—Thickness 13 per cent.

App - VI

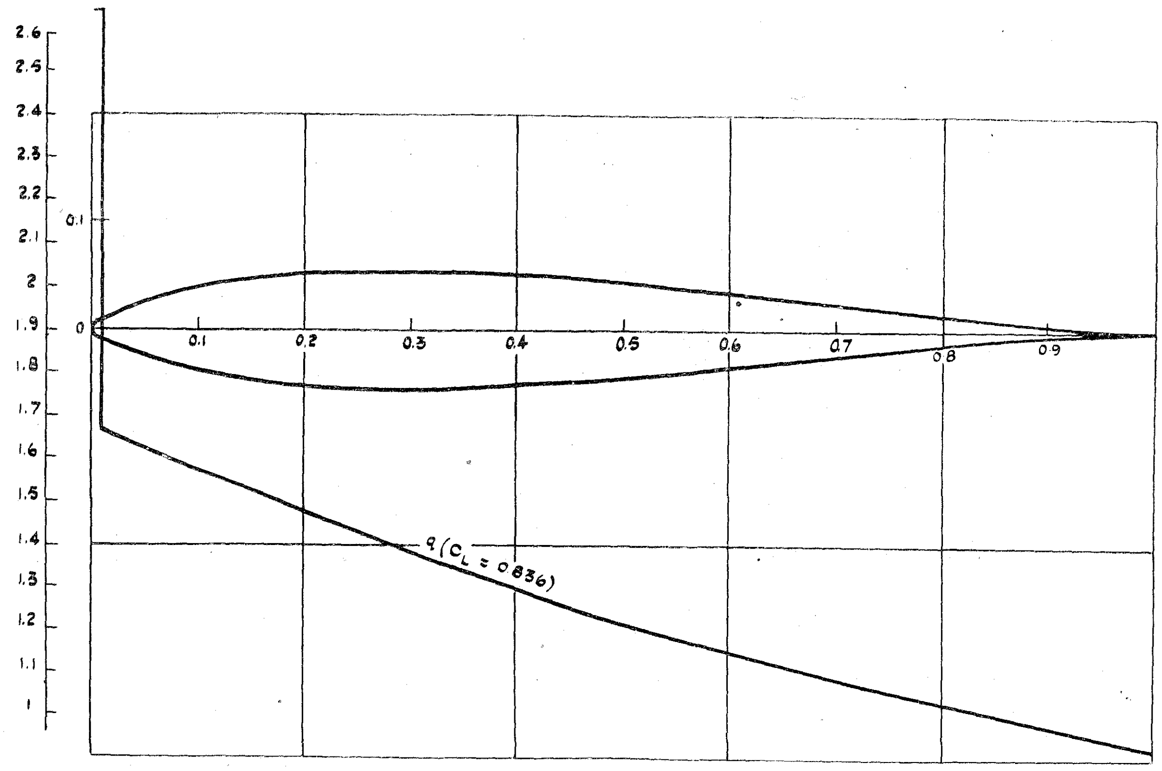

FIG. 7.—Thickness 11 per cent. App VIII

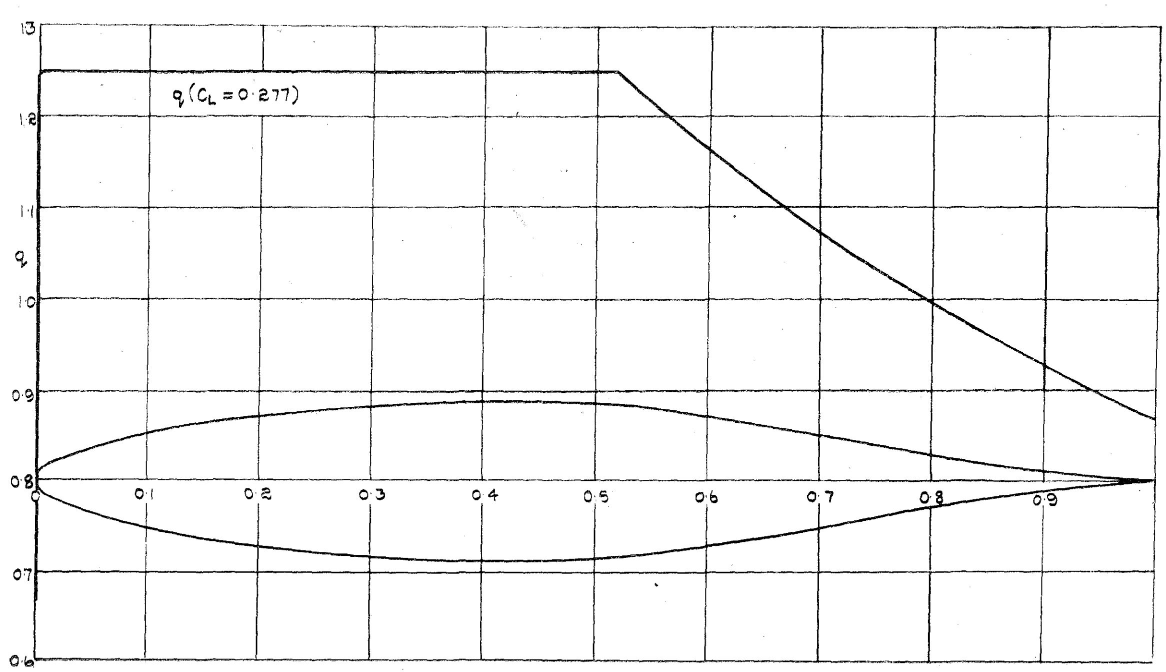

FIG. 8.—Thickness 14·1 per cent. App X

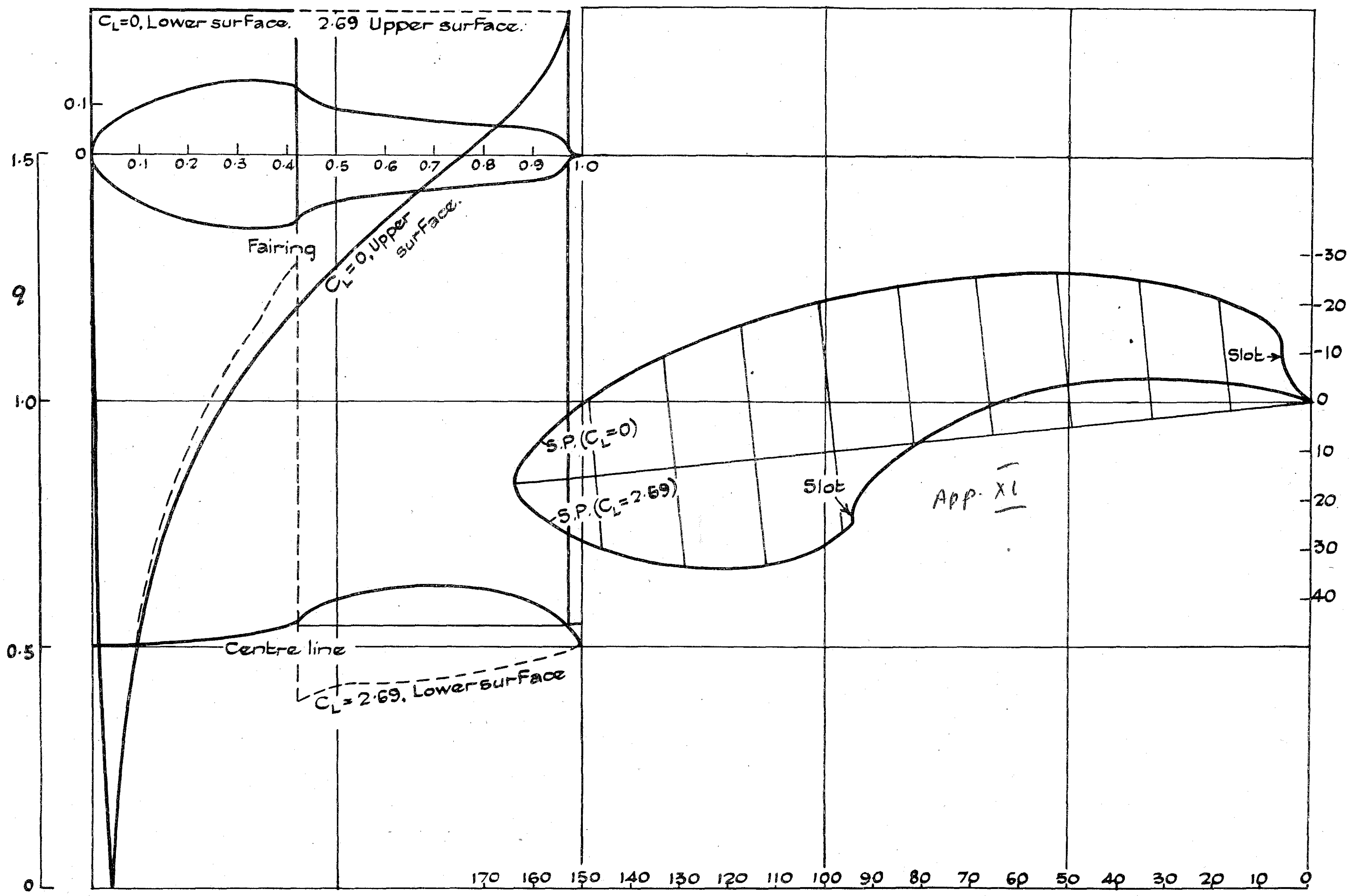

FIG. 9.—Thickness 30 per cent., C_L range from 0 to 2·69.

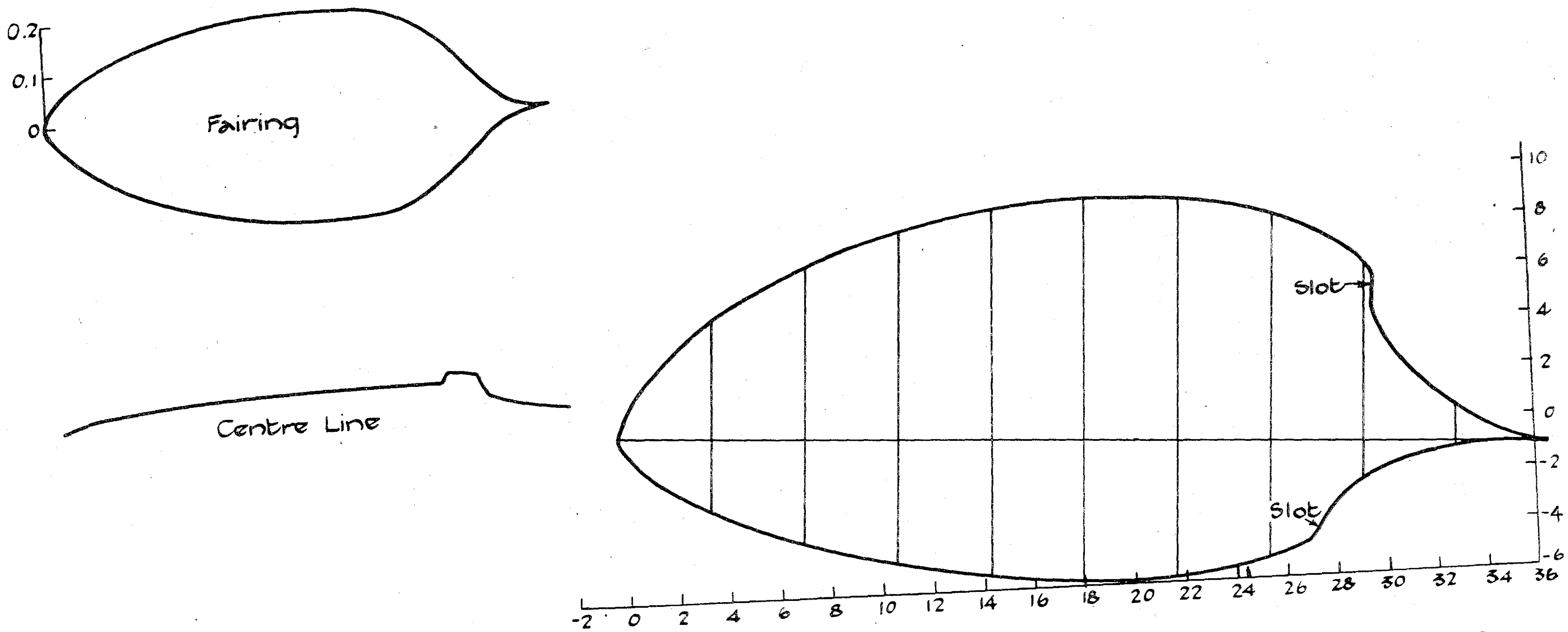

FIG. 10.—Thickness 41·2 per cent., C_L range from 0 to 2·85.

App. XIII

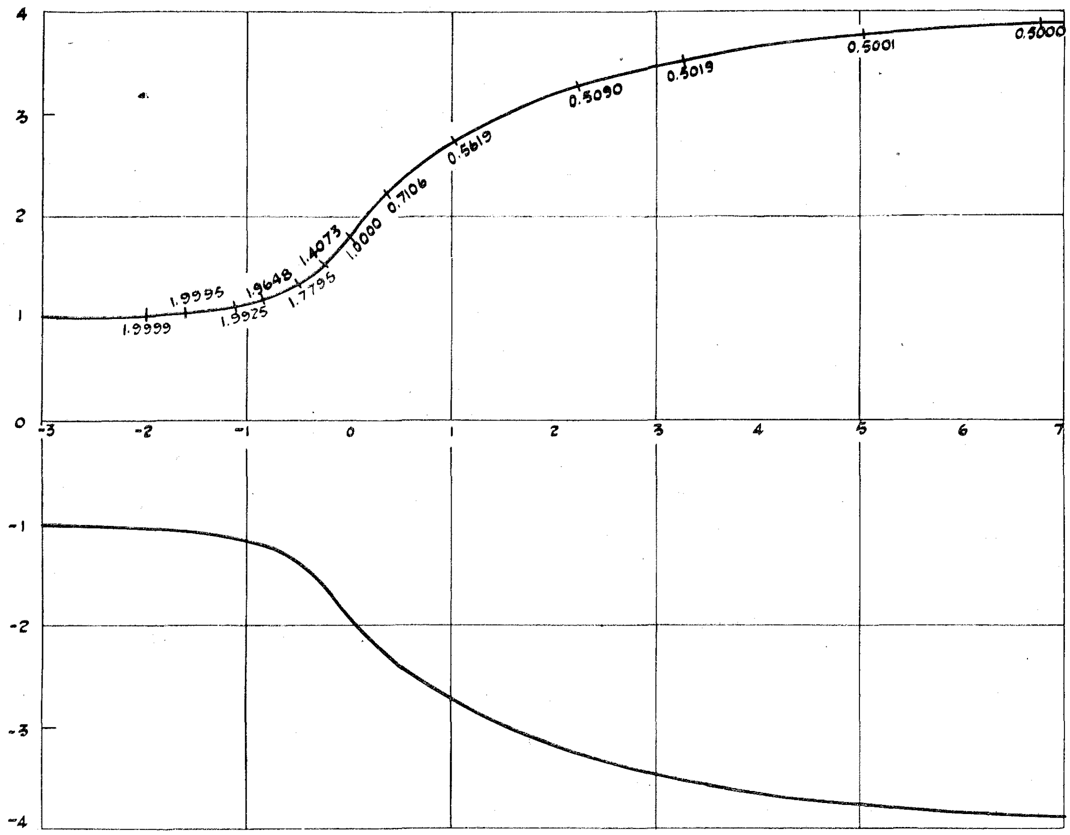

FIG. 11.—4 : 1 Contraction Cone. Velocity at Wall Shown.

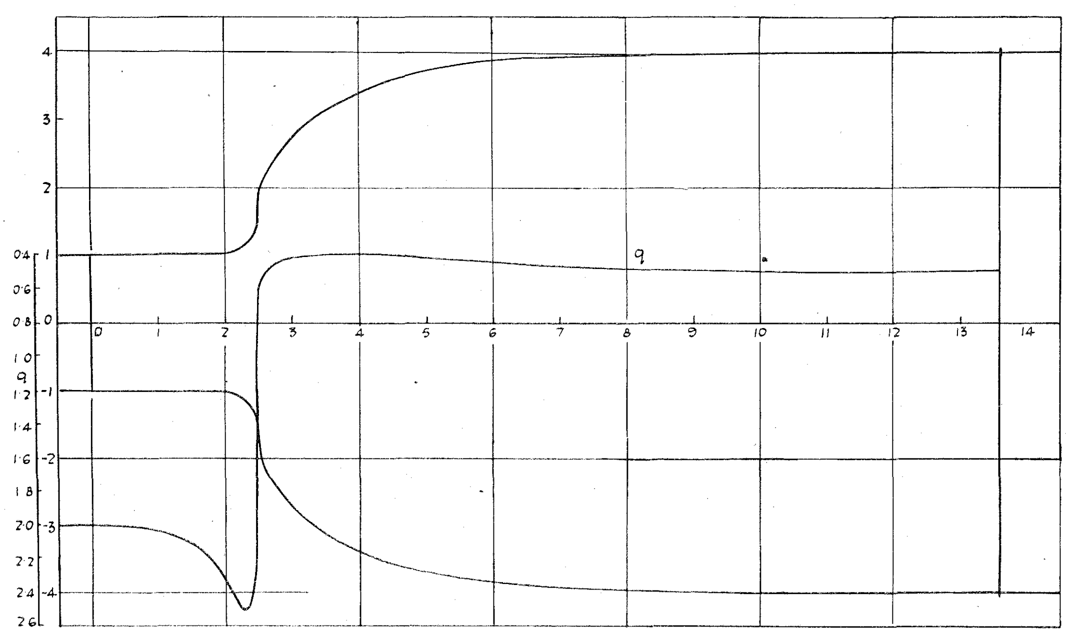

$$\text{Max}\left(-\frac{dq}{ds}\right) = 0\cdot75\,\frac{\text{Working section velocity}}{\text{Working section diameter}}\,.$$

FIG. 12.—Finite Contraction Cone (4 : 1 ratio).

770(k) Wt. 10/7116 6/47 Hw. G. 877/1

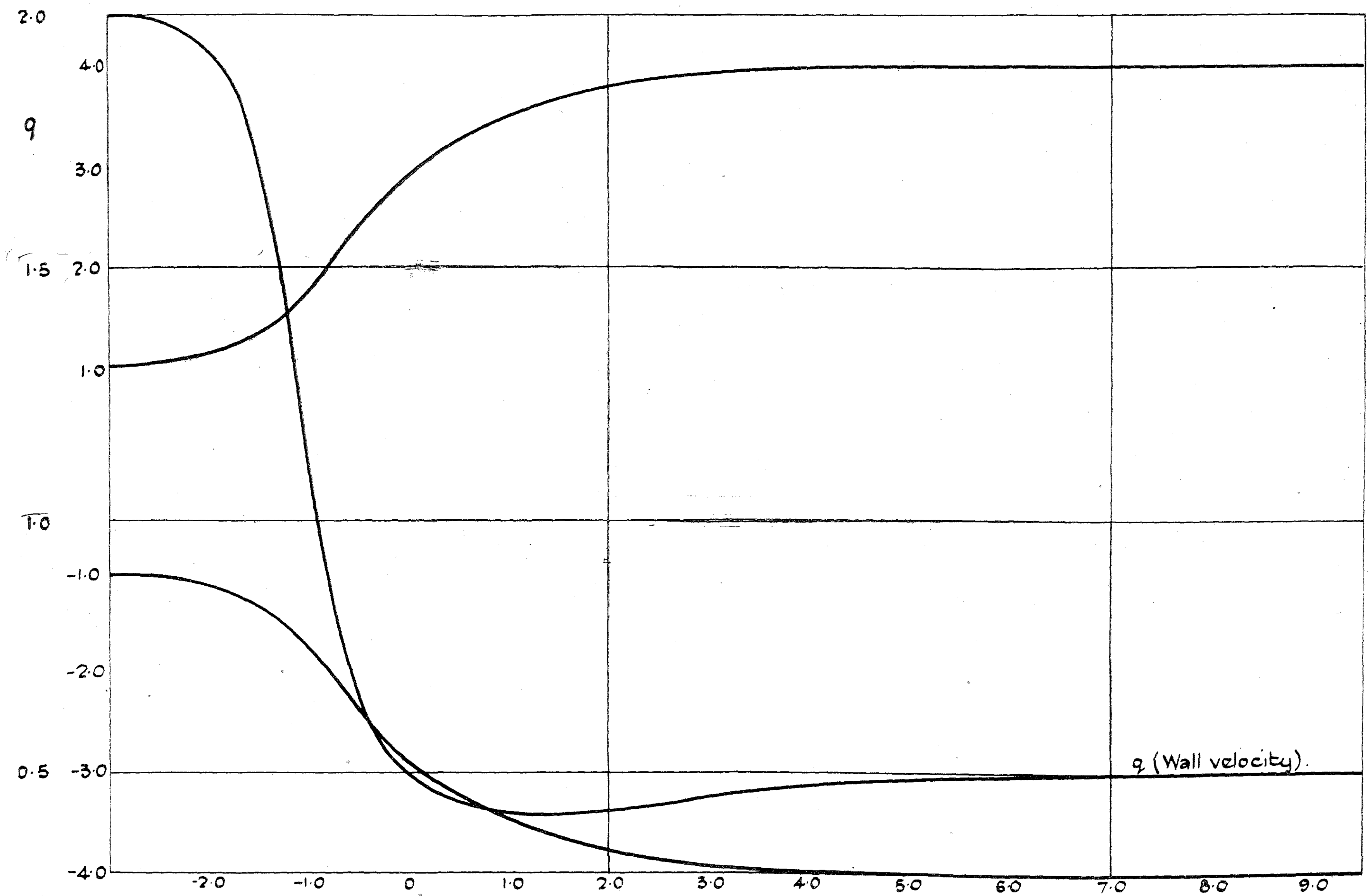

$$\text{Max}\left(-\frac{dq}{ds}\right) = 0\cdot025\ \frac{\text{Working section velocity}}{\text{Working section diameter}}.$$

FIG. 13.—4 : 1 Contraction Cone.